AD-A152 038 HIGH EFFICIENCY TRANSVERSE D C ELECTRON BEAMS(U) 1/1
RESEARCH INST OF COLORADO FORT COLLINS G COLLINS
OCT 84 RIC-247 AFOSR-TR-85-0242 AFOSR-83-0267

UNCLASSIFIED F/G 20/7 NL

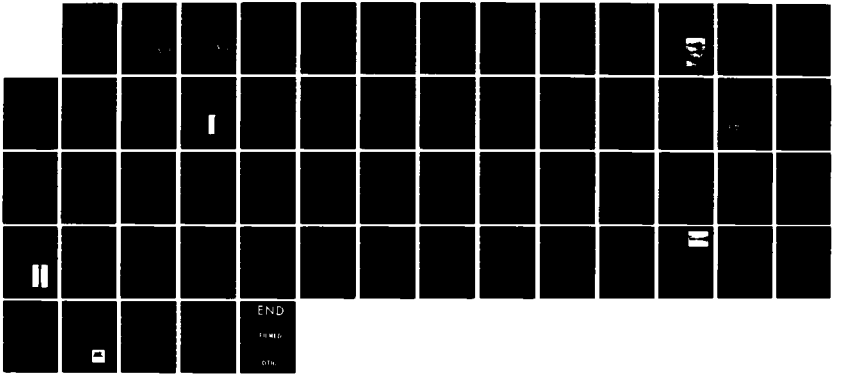

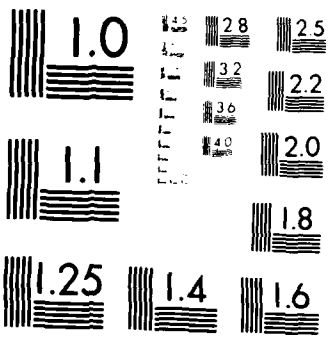

FINAL REPORT

HIGH EFFICIENCY TRANSVERSE D. C. ELECTRON BEAMS

by

George Collins, Principal Investigator

Air Force Office of Scientific Research
Grant AFOSR-83-0267
NIC #247

October, 1984

Dr. Ralph E. Kelley
Technical Project Leader

FINAL REPORT

Grant AFOSR-83-0267
RIC #247

8/1/83 - 7/31/84

UNCLASSIFIED

SECURITY CLASSIFICATION OF THIS PAGE

REPORT DOCUMENTATION PAGE

1a. REPORT SECURITY CLASSIFICATION: Unclassified	1b. RESTRICTIVE MARKINGS:
2a. SECURITY CLASSIFICATION AUTHORITY:	3. DISTRIBUTION/AVAILABILITY OF REPORT: Approved for public release; Distribution unlimited
2b. DECLASSIFICATION/DOWNGRADING SCHEDULE:	
4. PERFORMING ORGANIZATION REPORT NUMBER(S):	5. MONITORING ORGANIZATION REPORT NUMBER(S): AFOSR-TR- 85-0
6a. NAME OF PERFORMING ORGANIZATION: Research Institute of Colorado; 6b. OFFICE SYMBOL (If applicable):	7a. NAME OF MONITORING ORGANIZATION: AFOSR/NP
6c. ADDRESS (City, State and ZIP Code): Drake Creekside Two, Suite 200, 2629 Redwing Road, Fort Collins, CO 80526	7b. ADDRESS (City, State and ZIP Code): Building 410, Bolling A.F.B., DC 20332-6448
8a. NAME OF FUNDING/SPONSORING ORGANIZATION: AFOSR; 8b. OFFICE SYMBOL (If applicable): NP	9. PROCUREMENT INSTRUMENT IDENTIFICATION NUMBER: AFOSR-83-0267
8c. ADDRESS (City, State and ZIP Code): Building 410, Bolling A.F.B., DC 20332-6448	10. SOURCE OF FUNDING NOS. — PROGRAM ELEMENT NO.: 61102F; PROJECT NO.: 2301; TASK NO.: A1; WORK UNIT NO.:
11. TITLE (Include Security Classification): HIGH EFFICIENCY TRANSVERSE D.C. ELECTRON BEAMS	
12. PERSONAL AUTHOR(S):	
13a. TYPE OF REPORT: Final Scientific; 13b. TIME COVERED: FROM 8/1/83 TO 7/31/84	14. DATE OF REPORT (Yr., Mo., Day): 1984 October; 15. PAGE COUNT: 53
16. SUPPLEMENTARY NOTATION:	
17. COSATI CODES — FIELD: ; GROUP: ; SUB. GR.:	18. SUBJECT TERMS (Continue on reverse if necessary and identify by block number): High Efficiency Transverse D.C. Electron Beams,

19. ABSTRACT (Continue on reverse if necessary and identify by block number)

The proposed new sintered metal oxide-metal (e. g. Al_2O_3-Mo) cathodes have been tested. As originally predicted these cathode materials produce high current beams (1A) at multikilowatt posers in atmospheres containing a pure novel gas or a mixture of a novel gas and a metal vapor at generation efficiencies up to 75 ~~percent~~.

In contrast with other cathode materials previously used, the sintered materials allow multikilowatt electron beam operation in an oxygen free atmosphere. This is an important development in the construction of an cw electron beam excited UV laser, where no oxygen can be tolerated. These new electron guns that ~~we have~~ developed for laser excitation find also important applications in other areas of research, such as the processing of microelectronic materials, as we described in our review article, J. Appl. Phys. 56 796, (1984).

20. DISTRIBUTION/AVAILABILITY OF ABSTRACT: UNCLASSIFIED/UNLIMITED ☒ SAME AS RPT. ☐ DTIC USERS ☐	21. ABSTRACT SECURITY CLASSIFICATION: UNCLASSIFIED
22a. NAME OF RESPONSIBLE INDIVIDUAL: Dr Kelley	22b. TELEPHONE NUMBER (Include Area Code): (202) 767-4908; 22c. OFFICE SYMBOL: NP

DD FORM 1473, 83 APR EDITION OF 1 JAN 73 IS OBSOLETE.

UNCLASSIFIED SECURITY CLASSIFICATION OF THIS PAGE

This final report, "High Efficiency Transverse D.C. Electron Beams", AFOSR #83-0267, RIC #247 is approved.

George Collins
Principal Investigator

Dr. Richard T. Meyer
Chief Executive Officer

Nov. 12, 1984
Date

Dr. Richard T. Meyer, 2006 26th Roadway, Fort Collins, Colorado 80525 (303) 493-1901

FINAL REPORT

"HIGH EFFICIENCY TRANSVERSE D.C. ELECTRON BEAMS"

I. Electron Gun Research:

The proposed new sintered metal oxide-metal (e.g. Al_2O_3-Mo) cathodes have been tested. As originally predicted these cathode meterials produce high current beams (1A) at multikilowatt powers in atmospheres containing a pure noble gas or a mixture of a noble gas and a metal vapor at generation efficiencies up to 75 percent.

In contrast with other cathode materials previously used, the sintered materials allow multikilowatt electron beam operation in an oxygen-free atmosphere. This is an important development in the construction of an cw electron beam excited UV laser, where no oxygen can be tolerated. This new electron gun, which we have developed for laser excitation, also finds important applications in other areas of research, such as the processing of microelectronic materials, as we described in our review article, J. Appl. Phys. 56 796, (1984).

II. Laser Research

1) 1 Watt CW Zn Ion Laser

We have obtained 1.2 W of cw laser power on the 4911.6 and 4924.0 A transitions of Zn II by exciting a He-Zn gas mixture with a dc glow discharge electron beam. With the same excitation scheme, 0.25 W of cw laser radiation on the 6149.9 A line of Hg^+ has also been obtained. This represents an order of magnitude increase in the output power over that

previously obtained from these metal vapor laser transitions and is the first time that metal vapor ion lasers have operated cw in the visible region at a power of 1 W.

The operating efficiency also represents an order of magnitude improvement over that obtained in hollow cathode lasers. These experiments show that a cw Ag laser operating at a power between 0.1 and 1 watt at efficiencies as high as 0.5 percent should be possible. The progress towards this goal is described below. For more details on the cw zinc laser, see "1 W CW Zn Ion Laser," by J. J. Rocca, J. D. Meyer, and G. J. Collins, Appl. Phys. Lett. 43, 37, July 1983.

2) CW Atomic Fluorine Laser

We have obtained cw laser action on four transitions in the doublet system of atomic fluorine for the first time. All previously reported laser action was on a pulsed basis only. CW laser radiation was obtained when F_2 or AgF was used as a fluorine donor in an electron-beam-pumped helium plasma. A multiline output power of 200 mW was obtained. A collisional excitation reaction with an energy surplus populates the upper laser levels, causing a difference in the velocity distribution of atoms in the upper and lower laser levels. This avoids the self-termination of the laser output caused by trapping of the lower state resonant radiation observed by previous investigators.

We have also observed CW laser action on the 8446 A line of atomic oxygen exciting a $He-O_2$ mixture with a d.c. electron beam in the same experimental setup. CW laser action was also obtained when

the electron beam was used to excite pure oxygen gas. Direct current electron beams are thereby demonstrated to be a suitable method to excite cw atomic lasers. For a more detailed discussion, see "CW Laser Action in Atomic Fluorine," J. J. Rocca, J. D. Meyer, B. G. Pihlstrom, and G. J. Collins, IEEE J. of Quantum Electronics, QE-20, 625, June 1984.

Progress Towards a 1W Ultraviolet Metal Vapor Laser

3) CW Electron Beam Excited Metal Vapor Laser

In the last 6 months our efforts have concentrated in the construction of an electron beam pumped Ag II and Cu II laser with the goal of obtaining a cw ultraviolet power of 1W at efficiencies over 0.1 percent. These lasers will operate at 220 and 250 nm respectively.

To operate successfully these new devices, a metal vapor density of the order of 10^{15} cm^{-3} has to be achieved. Two laser set ups are being constructed. In one of them, the metal vapor density is produced by discharge heating in a hollow cathode discharge. In the second device, the metal vapor concentration is produced by a ceramic-molybdenum ohmic heater. Both devices should be operational by December 1984. Optimization of the laser output power and efficiency will be the subject of the research in the first months of 1985.

III. Modeling of Electron Beam Pumped CW Lasers

We have developed computer models of both cw electron beam excited noble gas argon ion lasers, currently under study at Spectra Physics, and electron beam excited He-metal vapor lasers under study at CSU.

The model calculates numerically the Boltzmann equation for electrons in an electron beam created plasma and uses it to calculate population inversion densities, laser output power, and efficiency.

The results can be summarized as follows: An Ar^+ cw laser excited transversely by a 50-100 eV electron beam is a device limited to efficiencies $<2 \times 10^{-4}$. This laser consequently has practical interest only as a low power (1.0 W device), where air cooled positive column lasers are even more inefficient.

In contrast, He-metal vapor output powers of a few watts at efficiencies as high as 0.1 percent in the visible and 0.5 percent in the UV should be possible. The results obtained experimentally with Zn^+, discussed in Section II, tend to confirm this prediction. Experimental results obtained at Spectra Physics for the transversely excited Ar^+ laser also agree well with the model. The model results and structure were presented at the "37th Gaseous Electronic Conference," in Boulder, CO in October 1984. A journal publication on the subject is currently under preparation.

JOURNAL PUBLICATIONS FOR THIS PROJECT.

1. "Studies of a glow discharge electron beam," by Zeng qi Yu, J. J. Rocca, and G. J. Collins, J. Appl. Phys. 54 (1), 131, January 1983.

2. "The energy of thermal electrons in electron beam created helium discharges," by Z. Yu, J. J. Rocca, and G. J. Collins, Phys. Lett., Vol. 96A No. 3, 125, 20 June 1983.

3. "1W Cw Zn Ion laser," by J. J. Rocca, J. D. Meyer, and G. J. Collins, Appl. Phys. Lett. 43 (1), 37, 1 July 1983.

4. "Compact Hg II laser excited by a transverse electron beam glow discharge," by J. J. Rocca, D. M. McClure, and G. J. Collins, IEEE J. Of Quantum Electronics, Vol. QE-19, No. 10, 1485, Oct. 1983.

5. "Ultraviolet ion lasers," by J. J. Rocca and G. J. Collins, Avtometriya 1 3 1984. (Invited Review Paper in Russian).

6. "Cw laser action in atomic fluorine," by J. J. Rocca, J. D. Meyer, B. G. Pihlstrom, and G. J. Collins, IEEE J. of Quantum Electronics, Vol. QE-20, No. 6, 625, June 1984.

7. "Glow-discharge-created electron beams: cathode materials, electron gun designs, and technological applications," by J. J. Rocca, J. D. Meyer, M. R. Farrell, and G. J. Collins, J. Appl. Phys. 56(3), 790, 1 Aug. 1984.

Studies of a glow discharge electron beam

Zeng qi Yu,[a] Jorge J. Rocca,[b] and George J. Collins[c]
Electrical Engineering Department, Colorado State University, Fort Collins, Colorado 80523

(Received 26 April 1982; accepted for publication 14 May 1982)

The energy spectrum of a kilovolt electron beam, generated by a helium glow discharge at pressures between 0.15 and 0.8 Torr, was measured with an electrostatic energy analyzer. An abrupt increase in the energy spread of the electron beam was observed to be coincident with an increase in the luminosity of the electron beam created plasma, and with the onset of intense microwave radiation. The relevance of these phenomena in cw electron beam pumped ion lasers is discussed.

PACS numbers: 52.80.Hc, 41.80.Dd, 52.40.Mj

I. INTRODUCTION

Under proper conditions a glow discharge may produce powerful electron beams. Glow discharge electron beams can be generated in helium at pressures from 0.1 to 2 Torr without differential pumping.[1,2] In contrast, the high-voltage operation of a hot cathode electron gun requires ambient pressures below 10^{-4} Torr. We have used glow discharge created electron beams at 1.5–3 keV and currents up to 1 amp to pump cw ion lasers. We have obtained cw laser action in both singly ionized mercury and iodine in helium-metal vapor mixtures.[3,4] Electron beam pumping is a new laser excitation scheme that could improve both the output power and efficiency of ion lasers due to the large density of energetic electrons in the active plasma medium as compared to conventional schemes.[5]

The energy spectrum of electrons emitted by a glow discharge has been measured previously[6] at discharge currents of a few milliamps with a cathode current density of up to 0.40 mA/cm^2. We have measured the electron beam energy distribution at currents between 20 and 700 mA, and helium pressures between 0.15 and 0.8 Torr using an electrostatic energy analyzer. Our measurements correspond to cathode current densities from 2 to 70 mA/cm^2. We observed that at a critical electron beam current density, dependent on pressure, a region of the electron-beam-generated plasma with unusually high luminosity was produced. The onset of this phenomena was found to be coincident with an abrupt broadening of the electron beam energy profile. We also observed that the onset of intense optical emission [illegible] was correlated with a beam-plasma interaction [illegible] frequency UHF radiation.

II. GLOW DISCHARGE CREATED ELECTRON BEAM

The electron gun consists of a cylindrical magnesium cathode 5 cm in diameter surrounded by a ceramic (Al_2O_3) shield that confines electron emission to the cathode front face. The distance between the cathode and the ceramic shield is approximately 1 mm. The front face of the cathode is [illegible] with a 9" radius of curvature to obtain a self-focused electron beam. Cathode curvature shapes the electric field in the cathode fall region so that a converging electron beam results. This electron beam, with the focus between the cathode and a target, is shown in Fig. 1(a). The cathode is water cooled to allow direct current operation at large discharge powers ($\geq$ 1 kW). The position of the anode is not important and does not influence the electron beam as long as the anode position is outside the glow discharge dark space.

Secondary electron emission from the cathode[7] occurs following bombardment of the cathode by ions which are accelerated through the cathode dark space, where practi-

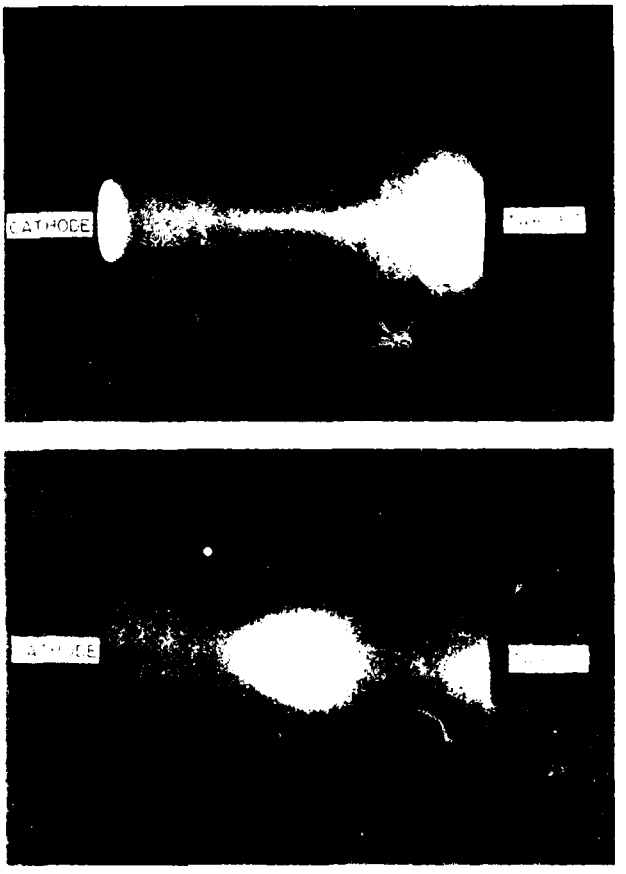

FIG. 1. (a) Self-focused electron beam discharge. (b) Electron beam discharge showing the high luminosity plasma that appears in the focal region of the electron beam in between the cathode and the target.

[a] Permanent address: Department of Physics, Fudan University, Shanghai, China.
[b] Spectra Physics Industrial Fellow.
[c] Alfred Sloan Fellow 1979–1982.

 0021-8979/83/010131-06$02.40

cally all the discharge voltage drops occur. Energetic neutrals, created by resonant charge transfer collisions[8] in the cathode fall region, also contribute to electron emission. The electrons emitted from the cathode surface are also accelerated in the dark space, in the opposite direction, to form the electron beam.

In preliminary studies with Mg cathodes, we observed that the secondary electron emission decreased by more than an order of magnitude as the native magnesium oxide was removed from the cathode surface with ion sputtering. We have determined that a large secondary electron emission from the cathode can be maintained by the addition of a small amount of oxygen (10–20 mTorr) to the discharge chamber which enables the maintenance of a magnesium oxide coating on the cathode surface. This oxide coating permits the production of the electron beam with high efficiency while at the same time reducing cathode sputtering. Using a calorimeter to measure the electron beam power directly, we found that up to 70% of the discharge power goes into the electron beam when the discharge voltage is 2.4 kV. Neglecting ionization in the dark space the electron beam current, I_e, is related to the ion current, I_+, by the relationship $I_e = \gamma I_+$, where γ is the secondary electron emission coefficient. Considering that $I = I_e + I_+$, we can state

$$I_e = \frac{\gamma}{1+\gamma} I. \tag{1}$$

Hence, from the calorimetric measurement of the electron beam power an effective secondary emission coefficient γ of 2.5 is obtained for the magnesium cathode with an oxide coating from Eq. (1).

III. ELECTRON BEAM ENERGY SPECTRUM MEASUREMENTS

The electron beam energy spectrum was measured with an electrostatic energy analyzer, using the experimental setup shown in Fig. 2. The energy analyzer chamber is connected to the electron beam glow discharge housing through a 0.05-mm-diam sampling hole. The pinhole was placed 17 cm from the cathode emitting surface. The wall dividing both chambers is made of copper and is water cooled in order to withstand the impinging electron beam which delivers several hundred watts. The electron analyzer chamber is pumped with a turbomolecular pump and the pressure is maintained below 10^{-5} Torr. Helium is flowed through the electron beam glow discharge chamber, via a needle valve, and pumped out by a rotary vacuum pump. A small amount of oxygen, accounting for a partial pressure of 10–20 m Torr in the discharge chamber, was also flowed for increased electron emission as described in Sec. II. The presence of oxygen at these partial pressures was shown to have no significant influence on the electron energy profiles.

The electron gun was mounted in a micropositioner that allows alignment of the electron beam both with the sampling hole and the entrance hole of the energy analyzer. The electrostatic energy analyzer used was a Comstock, Inc., Model AC-901 with 160° spherical sector surfaces providing an energy resolution of 0.5% with a 1-mm-diam entrance aperture to the energy analyzer.[9] Electron beam energy distributions were measured at 0.15, 0.2, 0.4, 0.6, and 0.8 Torr of helium.

Illustrative data obtained from measurements at 0.4,

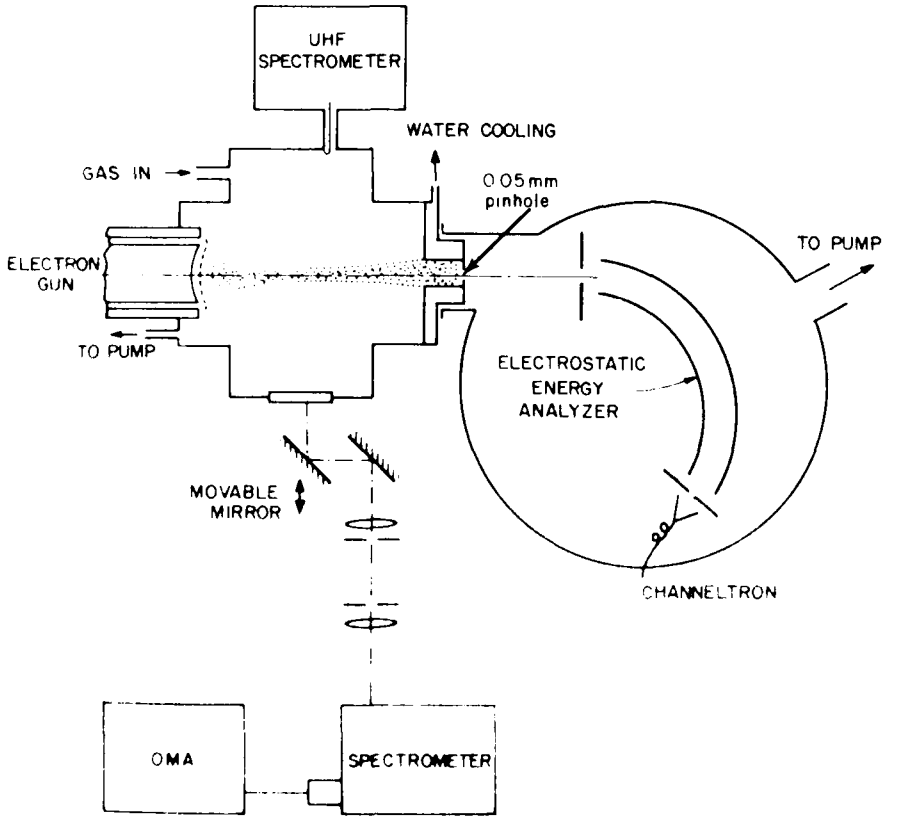

FIG. 2. Experimental setup used to study the electron beam glow discharge

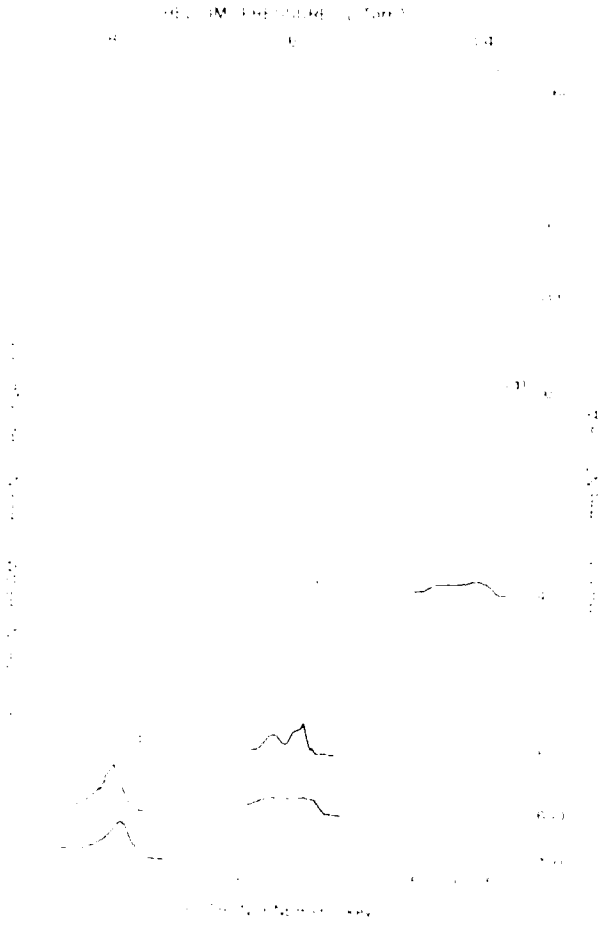

FIG. 3. Measured electron beam energy spectrums at 0.4, 0.6, and 0.8 Torr of helium are shown in three columns. The discharge current corresponding to each row is shown on the right side of the figure.

0.6, and 0.8 Torr are shown in three columns in Fig. 3 for currents between 60 and 700 mA. The individual plots show the measured energy spectrum of the electron beam at nine different discharge currents indicated on the right-hand side of Fig. 3. Note that the zero of electron beam current for each energy spectrum is indicated on the left of the figure and the energy axis at the bottom. The same relative scale was used to plot the electron beam current for every spectrum in Fig. 3. With data in this format the following trends can be observed. For all pressures the peak value of the electron beam current increases as the current is incremented, up to a critical value denoted as (a) in the series of energy spectrums of Fig. 3. Beyond this critical current, the electron beam energy profile, that up to this point was getting narrower (typically 200–300 eV full width at half-maximum) abruptly degrades into a broad profile as shown. This change in the electron beam energy spectrum is associated with the sudden appearance of a plasma region with very intense luminosity close to the focus of the electron beam. Figure 1(b) shows the electron beam glow discharge with the presence of a bright luminous plasma near the focus of the electron beam. The broad profile corresponds to the degraded electron beam energy profiles denoted in Fig. 3 by thick lines. In Fig. 1(a), the electron beam is well collimated and corresponds to the electron energy profiles in Fig. 3 denoted by narrow lines.

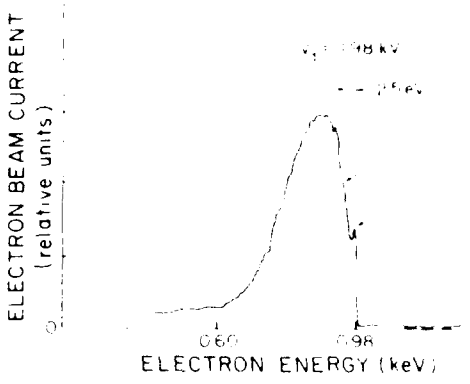

FIG. 4. Electron beam energy spectrum measured at 0.8 Torr of helium and at 0.3 A discharge current.

Figure 4 shows one illustrative electron beam energy spectrum measured at 0.8 Torr of He and at 0.3 A discharge current. This spectrum corresponds to the spectrum in the fifth row of column one in Fig. 3. Several peaks are observed in this spectrum, at intervals of approximately 25 eV, which coincides with the ionization energy of helium (24.8 eV). Beam electrons that suffered one, two, or more ionizing collisions constitute the different peaks. Elastic electron-helium collisions smooth out the distribution. The important observation to be made in Fig. 4 is that the maximum measured electron beam energy corresponds to the measured discharge voltage, V_d. This confirms that nearly all the discharge voltage drops in the cathode fall region, where the electrons are accelerated.

IV. OPTICAL MEASUREMENTS

The light emitted by the electron-beam-created glow discharge was monitored using an optical multichannel analyzer (OMA) having an intensified diode array detector of 512 elements. The optical setup shown in Fig. 2 was used. The detector was mounted on a 1/2 meter spectrometer having a diffraction grating of 280 groves per millimeter. This provided a resolution of 6 A per channel and a spectral range of nearly 3000 A. We were also able to make spatially resolved (1 mm resolution) measurements in different regions of the glow discharge, shown in Fig. 1(b) by moving one of the two parallel mirrors shown. Special attention was given to the focal region of the electron beam, in the negative glow region of the discharge, where the unusually high luminosity shown in Fig. 1(b) suddenly appears.

Most of the visible radiation from the electron beam helium discharge was observed to be from three He I spectral lines: 5015.7 A ($3p\,^1P^o \rightarrow 2s\,^1S$), 5875.6 A ($3d\,^3D \rightarrow 2p\,^3P^o$), and 6678.1 A ($3d\,^1D \rightarrow 2p\,^1P^o$). The intensity of these lines in the focal region of the electron beam as a function of discharge current is shown in Fig. 5. If single step electron excitation from the helium atom ground state is the major creation mechanism, the intensity of the 5015.7 A lines should dominate over the other two lines, since the $3\,^1P$ level has the largest electron impact excitation cross section.[7] This is the case observed at low discharge currents when the negative

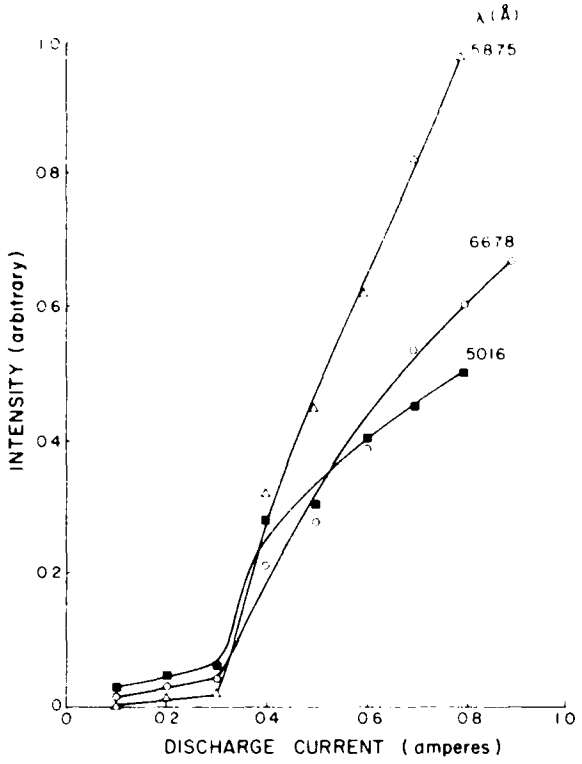

FIG. 5. Behavior of the spontaneous emissions originating from the focal region of the electron beam helium discharge. Helium pressure was 0.2 Torr.

glow, as observed by the eye, is dominantly green. In this low current range the intensity of the lines increases roughly linearly with beam current up to a critical current. Then an abrupt increase in the luminosity of this plasma region occurs, as shown in Fig. 5. When this occurs the plasma looks as shown in Fig. 1(b). Now emission from the 5875.6 line dominates, making the region of the plasma appear pink/orange to the eye. A change occurs in the electron energy distribution as shown in spectrum drawn with thick lines in Fig. 3, and direct excitation from the helium ground state by beam electrons is no longer the dominant excitation mechanism. The discharge current at which the sudden change in plasma luminosity occurs increases as the helium pressure is incremented. This is shown in Fig. 6. Below we describe the origin of the change in the electron beam energy spectrum and the correlation with the appearance of a luminous region in the beam-generated plasma.

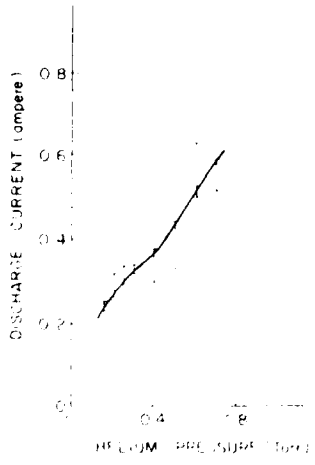

FIG. 6. Current onset of the plasma "ball of light" as a function of helium pressure. The high luminosity plasma region is observed for the conditions above the curve.

V. ULTRAHIGH FREQUENCY (UHF) GENERATION

The degradation in the electron beam energy profile and the observation of an abrupt increase in the intensity of the visible radiation emitted by the discharge previously described suggests the existence of strong beam plasma interactions.[11-13] A confirmation of the existence of plasma oscillations excited by the electron beam is the observation of an abrupt increase in the intensity of the microwave radiation generated by the discharge, in coincidence with the appearance of the optical emission phenomena described above. Figure 7 shows the *X* band UHF emission intensity as a function of the electron beam discharge current. The beam current at which the UHF radiation abruptly increases was always in coincidence with the appearance of the "ball of light" in the plasma region [shown in Fig. 1(b)] and with the pronounced degradation of the electron beam energy spectrum. Specifically, in Fig. 3 for a pressure of 0.6 Torr the onset of beam degradation occurs at 500 mA, which agrees with the current for intense UHF oscillation shown in Fig. 7. The same agreement between beam degradation and UHF threshold occurs at 0.4 A with a helium pressure of 0.4 Torr.

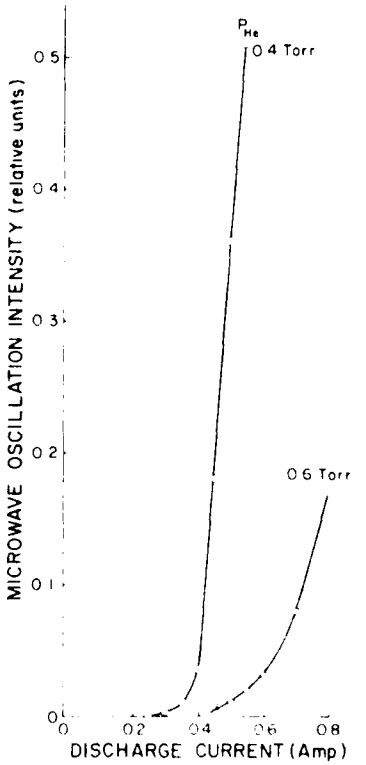

FIG. 7. Intensity of microwave radiation as a function of discharge current.

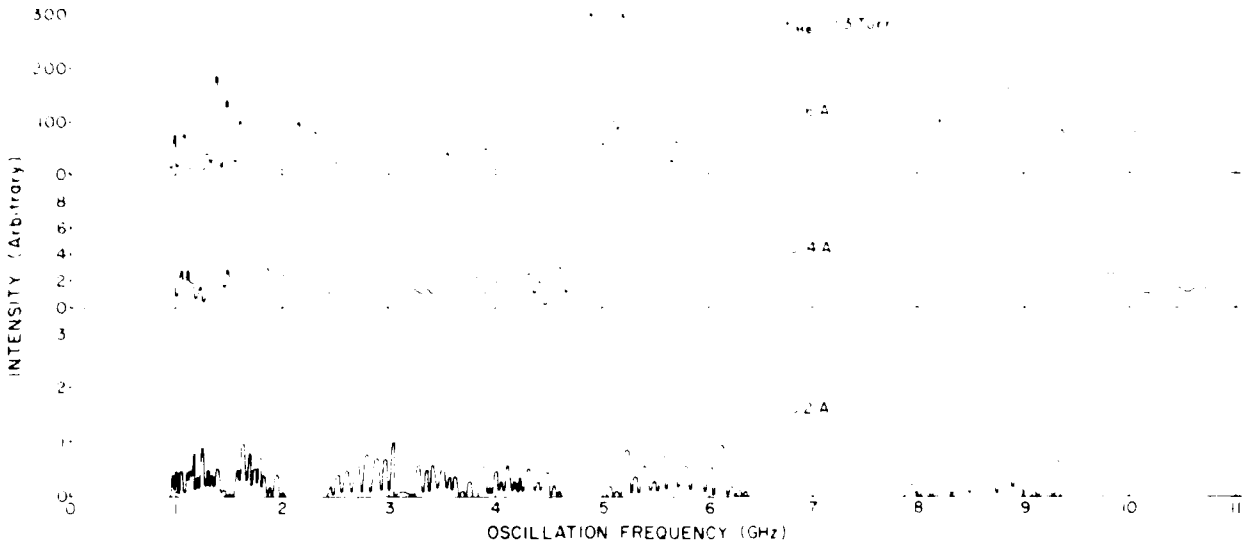

FIG. 8. Frequency spectrum of microwave signal at a pressure of 0.3 Torr and three different currents.

Figures 3 and 6 show that the current onset of these phenomena increases as the helium pressure is increased. This is in agreement with the results of Wada and Knechtli,[13] who observed that the plasma density required for energy transfer from an injected electron beam to the plasma was higher when the background gas pressure was increased. This shows that collisionless thermalization of electrons in a beam-plasma system can be inhibited, if the electron collision mean-free-path is made small enough.

The spectrum of the UHF emission between 1 and 11 GHz was measured using an UHF spectrum analyzer, and is shown for three different discharge currents at a helium pressure of 0.3 Torr, in Fig. 8. This broad spectrum is similar to the one found in previous experiments that studied the oscillations of beam-plasma discharges,[12,14] in which the dominant mode of interaction is believed to be at the plasma frequency. The plasma electrons find themselves in a rf field that accelerates them to the energy range where they can excite and ionize. This increase in the excitation rate is consistent with the observed variation of the light emission. Plasma oscillations are judged to be the mechanism that efficiently transfer energy from the electron beam into the plasma, causing the observed energy degradation of the electron beam energy profile.

VI. PLASMA OSCILLATIONS IN THE EXCITATION OF cw ION LASERS

Beam-plasma discharges, created by exciting plasma oscillations with a pulsed electron beam drifting in a longitudinal magnetic field, have been used to excite pulsed ion lasers.[14,15] In these experiments an electron beam of energy between 10 and 45 keV and current between 10 and 30 A was inserted into a plasma chamber, where the pressure ranged from 10^{-3} to 10^{-5} Torr.[15] At this low gas density the electron beam energy would be very poorly deposited into the plasma in the absence of the collective interaction between the electron beam and the plasma, that leads to intense excitation of high-frequency oscillations.

In a cw electron beam laser system, such as the one we used to obtain cw laser action in He-metal vapor mixtures[1,3] UHF oscillation could present a major disadvantage. This system is longitudinally pumped by an electron beam of approximately 3 keV. The pressure in the plasma tube is several Torr so that a beam-plasma interaction that degrades the electron energy profile in the way shown in Fig. 3 would reduce the reaching distance of the electron beam and results in a substantially shorter and nonuniform active medium.

In a transverse geometry, the range of the electron beam should be small so that the majority of the energy is deposited into the plasma and not onto the walls of the discharge chamber. Electron beam excited plasma oscillations could therefore be used to efficiently deposit the electron beam energy in the case of transverse electron beam excitation into a volume with a small cross section and long optical length. One such transverse laser excitation scheme, using glow discharge electron guns,[2] is shown in Fig. 9. The anode position is not shown since its location is not essential to the characteristics of the electron beam discharge,[2] nor will it block the optical path. The use of two cathodes allows for partial trap-

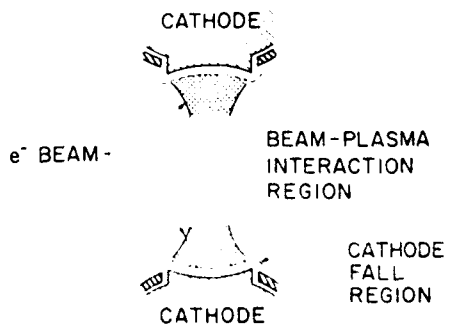

FIG. 9. Cross-sectional view of a proposed transverse electron beam pumped laser using opposing cathodes and a beam plasma interaction to achieve efficient energy deposition.

ping of the high-energy electrons. Beam electrons which reach the opposing cathode after passing through the beam-plasma region are reflected there by the electric field in the cathode fall region. Both of these effects will increase the energy deposition efficiency of the transverse electron beam.

VII. SUMMARY

The energy spectrum of a kilovolt electron beam produced by a magnesium cathode glow discharge operating in helium at pressures between 0.15 and 0.8 Torr was measured using an electrostatic energy analyzer. The maximum energy of the electrons coincide with the discharge voltage drop, V_d. The electron beam energy spectrum measured at 17 cm from the electron gun presents an energy width at half-maximum of 100–300 eV. The electron beam energy spectrum gets narrower as the discharge current is incremented up to a critical current value, at which point it abruptly degrades into a broad energy profile. This change in the electron beam energy spectrum is coincident with the sudden appearance of a plasma region with a very intense luminosity and with the emission of intense microwave radiation.

This phenomena is attributed to the generation of plasma oscillations driven by the electron beam. We suggest the use of the beam-plasma interaction as a method to efficiently deposit the electron beam energy into the plasma in a transverse electron beam discharge for the excitation of ion lasers.

ACKNOWLEDGMENTS

The authors wish to thank Dr. C. E. Patton of the physics department at CSU, and Dr. R. Hunter of NBS, Boulder, for the useful discussions, and Tom Burnell for skilled technical assistance. This work was supported by the National Science Foundation and AFOSR.

[1] J. J. Rocca, J. D. Meyer, and G. J. Collins, Phys. Lett. A **87**, 237 (1982).
[2] Z. Yu, J. J. Rocca, J. D. Meyer, and G. J. Collins, J. Appl. Phys. (to be published).
[3] J. J. Rocca, J. D. Meyer, and G. J. Collins, Appl. Phys. Lett. **40**, 300 (1982).
[4] J. D. Meyer, J. J. Rocca, Z. Yu, and G. J. Collins, IEEE J. Quantum Electron. **18**, 326 (1982).
[5] J. J. Rocca, J. D. Meyer, Z. Yu, and G. J. Collins, Presented at the Thirty-Fourth Gaseous Electronic Conference, Boston, October 1981.
[6] R. M. Chaudhri and M. M. Chadhi, Proc. VIIth Int. Conf. Ion in Gases (Belgrade) 392, 1965.
[7] G. Carter and J. S. Colligon, *Ion Bombardment of Solids* (American Elsevier, New York, 1934).
[8] W. D. Davis and T. A. Vardershee, Phys. Rev. **131**, 219 (1963).
[9] Comstock, Inc., Electrostatic Energy Analyzer Model AC-901 Manual, Oak Ridge, Tennessee.
[10] H. S. W. Massey and E. A. S. Burshop, *Electronic and Ionic Impact Phenomena, Vol. I*, (Oxford University Press, 1969). See also R. M. St. John, F. L. Miller, and C. C. Ling, Phys. Rev. A **134**, 888 (1964).
[11] D. H. Looney and S. C. Brown, Phys. Rev. **93**, 965 (1954).
[12] W. D. Getty and L. D. Smullin, J. Appl. Phys. **34**, 34 (1963).
[13] J. Y. Wada and R. C. Knechtli, Phys. Fluids **12**, 1497 (1969).
[14] Yu. U. Track, Ya. B. Fairberg, L. I. Bolotin, Ya. Ya. Bessarab, N. P. Gadetskii, Yu. N. Chernen'kii, and A. K. Berezin, JETP Lett. **6**, 371 (1967).
[15] Yu. U. Track, Ya. B. Fainberg, L. I. Bolotin, Ya. Ya. Bessarab, N. P. Gadetskii, I. I. Magda, and A. V. Sidel'nikova, Sov. Phys. JETP **35**, 886 (1972).

THE ENERGY OF THERMAL ELECTRONS IN ELECTRON BEAM CREATED HELIUM DISCHARGES *

J. YU, J.J. ROCCA, G.J. COLLINS
Electrical Engineering Department, Colorado State University, Fort Collins, CO 80523, USA

C.Y. SHIH
Physics Department, Colorado State University, Fort Collins, CO 80523, USA

Received 13 January 1983

We have measured the electron energy of the thermal group of electrons in both longitudinal and transverse electron beam created helium glow discharges. The measurement technique employs the ratio of intensities of spectral lines in the $2s\,^3S - np\,^3P$ He I series. Values of kT_e between 0.07 and 0.11 eV were obtained. These energies are typical of the beam-generated electric field free plasmas. The competitive loss of helium ions by recombination and by charge transfer in a He – He electron beam created plasma is calculated. The results are applied to the Hg^+ laser pumping scheme using a electron beam created He – He plasma.

Recently, we demonstrated that electron beam created glow discharges may be employed as a new active medium for CW ion lasers [1–4]. We have developed glow discharge electron guns for both longitudinal [5,6] and transverse [7] plasma excitation. These electron guns produce electron-beam currents up to 1 A at energies between 1 and 10 keV.

Fig. 1 shows the calculated electron energy distribution in the electron beam generated helium plasma obtained by solving the Boltzmann equation in the electric field free negative glow region [8]. Although the ionization is due to collisions of gas atoms with high- and intermediate-energy electrons, the most numerous group of electrons in the negative glow has near thermal energy (see fig. 1). This is because the

* Work supported by the National Science Foundation and AFOSR.

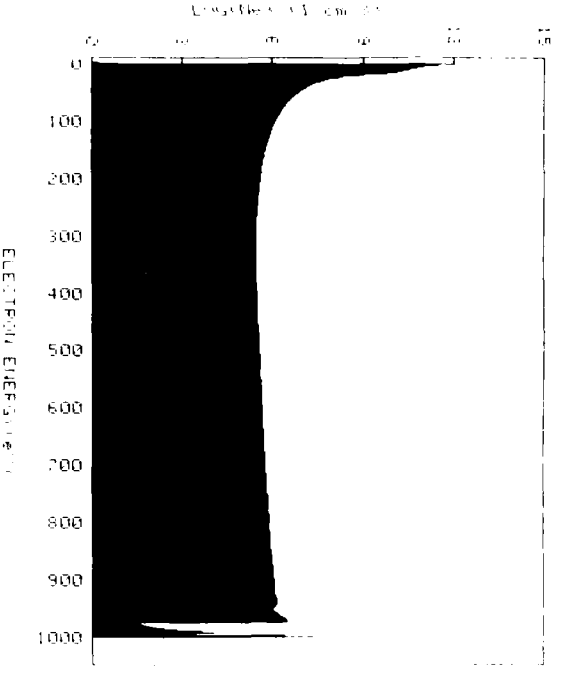

Fig. 1. Calculated electron energy distribution for helium plasma excited by a 1 keV electron beam. He density 6×10^{16} cm^{-3}.

differential cross section for the production of secondary electrons in ionizing electron–atom collisions peaks at zero energy [9]. Moreover, each beam electron can create numerous secondary electrons. These secondary electrons gain energy via superelastic collisions with excited atoms, elastic collisions with beam electrons or as a result of three-body electron–ion recombination and are thermalized by elastic collisions in the field-free negative glow region.

We have measured the electron temperature of the thermal energy group of electrons in the negative glow of both longitudinal and transverse glow discharges using the ratio of spectral intensities of the $2s\,^3S$ – $np\,^3P$ He I series.

Knowledge of the temperature of this thermal electron group is necessary to determine if the plasma is diffusion or recombination dominated [10], since collisionally assisted (three-body) electron–ion recombination is proportional to $T_e^{-4.5}$ [11]. In a charge transfer ion laser electron recombination represents a loss of buffer gas ions, thereby limiting output power and efficiency. Also, if the plasma is to be used as laser active medium these low-energy electrons will play an important role in the electron de-excitation of the laser levels [12].

The longitudinally excited electron-beam plasma was created using a glow discharge electron gun similar to the one described in ref. [6] and having a LaB_6 cathode 3.2 cm in diameter. The electron gun was introduced into a stainless-steel vacuum chamber having suprasil quartz windows for optical measurements. The metal chamber was grounded and served as the anode of the glow discharge. The line intensity measurements took place approximately 10 cm from the cathode emitting surface, far from the cathode dark space and well into the field-free negative glow region.

The transverse electron-beam discharge was established in the same vacuum chamber by replacing the electron gun described above by two transverse electron guns similar to the ones described in ref. [7]. They were positioned parallel facing each other as indicated in fig. 1 of ref. [7] with the distance between the cathode emitting surfaces of 3 cm. The cathodes were slotless, 5 cm long by 1.2 cm wide with a radius of curvature of 1.5 cm. Again, line intensity measurements were made in the negative glow, in the central portion of the discharge. We also have measured the electron temperature in a longitudinal electron-beam He plasma confined by a magnetic field. In this case the e⁻ beam created plasma arrangement was similar to the one we used to obtain laser action in various He–metal vapor mixtures, described in detail in refs. [1,2]. The only difference being the use of two electron guns, one at each end of the electromagnet, to increase plasma uniformity.

The spontaneous emission from the electron beam excited plasma was collected through a suprasil window and focused into the slit of a 1 m SPEX spectrometer by a quartz lens. We used an RCA C31034 Peltier cooled photomultiplier. The spectral response of the entire optical detection system was measured using a tungsten ribbon lamp calibrated at N.B.S. so that the measurements of relative intensities were properly corrected. The ratio of intensities I, of the lines of the $2s\,^3S$ – $np\,^3P$ He I series, assuming the levels are in local thermodynamic equilibrium (LTE) is related to kT_e by:

$$kT_e = \Delta E(n', n) \times \{\ln[(\lambda')^3 (n')^3 I(n' \to 2)/\lambda^3 n^3 I(n \to 2)]\}^{-1}, \quad (1)$$

where $\Delta E(n', n)$ is the difference of energy between levels n and n', λ' and λ are the wavelengths of the radiation originating from the n' and n levels respectively. This equation for kT_e is particularly sensitive to measurement errors of relative intensities for high values of n and n'. A remedy is to extend the range of measurements over a large number of Rydberg levels. A plot of $\ln(1/\lambda^3 n^3 I)$ versus $E(n)$ where $E(n)$ is the energy level n, yields the average electron temperature from the slope of a line connecting the data points.

Griem [13] has formulated an approximate electron density criterion for a hydrogenic level n to be within 10% LTE with the neighboring level $n + 1$

$$n_e \geqslant (7.4 \times 10^{18}/n^{17/2})(kT_e/13.6)^{1/2} \times \exp(\Delta E_{(n,n+1)}/kT_e). \quad (2)$$

Notice that kT_e is in eV. For an electron temperature of 0.1 eV and $n = 8$, eq. (2) requires an electron density in excess of 2.1×10^{10} cm^{-3}. Under the discharge condition of these experiments the electron density in the negative glow of the electron-beam discharge is judged to be always $>10^{11}$ cm^{-3}. Consequently all the levels with $n \geqslant 8$ should be in LTE and the plots of the $2s\,^3S$ – $np\,^3P$ helium series are expected to give the temperature of the thermal electrons in the electron beam discharge.

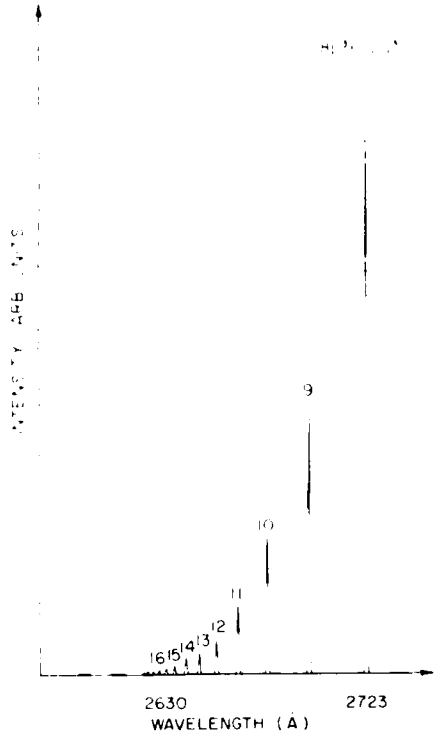

Fig. 2. $2s\,^3S \rightarrow np\,^3P$ He I series spectrum in a He plasma longitudinally excited by a 0.1 A/cm^2, 2 keV electron beam. Helium pressure 2 Torr.

A scan of the $2s\,^3S \rightarrow np\,^3P$ helium series for $n \geqslant 8$ taken at 2 Torr of helium at an electron gun voltage of 2 kV and a current of 75 mA is shown in fig. 2. Graphs of $\ln(1/\lambda^3 n^3 I)$ versus $E(n)$ for the longitudinal glow discharges are shown in fig. 3 for different discharge conditions. The data for each condition were fit to a straight line using a weighted least-squares-fit routine. The relative errors in the determination of the slopes, taken as one standard deviation, were between 15 and 30%. The standard deviations of kT_e, corresponding to a set of four spectral recordings repeated at the same discharge conditions, were between 4 and 13%. At helium pressures between 1 and 4 Torr, currents between 0.1 and 0.6 A and electron energies between 0.75 and 5.3 keV, the longitudinal discharges had values of kT_e for the thermal electrons between 0.075 and 0.105 eV. Measurements done in the transverse discharge at pressures between 1 and 3 Torr, currents between 0.05 and 0.5 A and voltages between 0.6 and 1 keV give similar electron energy values for

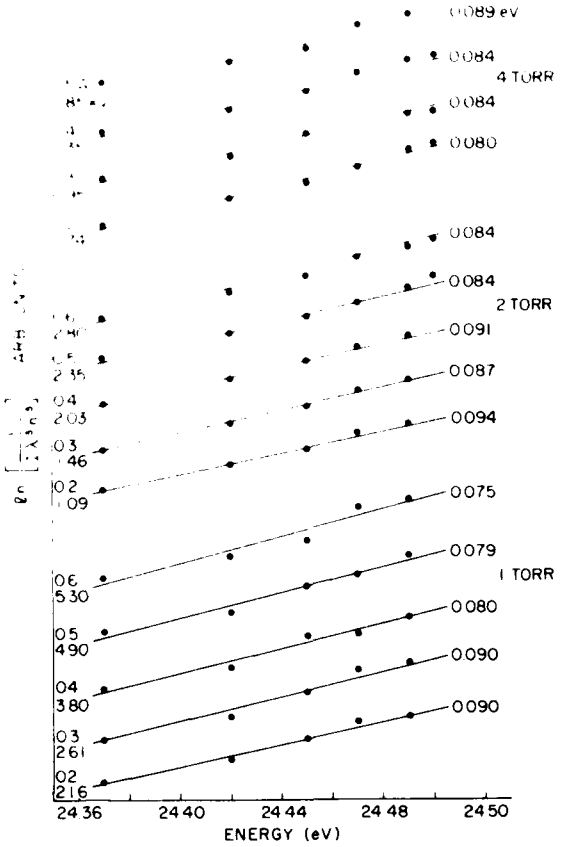

Fig. 3. Semilogarithmic plots of the line intensities of the $2s\,^3S \rightarrow np\,^3P$ He I series in a helium plasma excited by a longitudinal electron beam. Helium pressure, electron beam current and voltage are indicated for each plot on the left. The corresponding values of kT_e are indicated at the right of each plot.

the thermal electrons between 0.066 and 0.96 eV. Variations of kT_e as a function of current and pressure in the range mentioned above are within the error range of the measurements. Measurements done in the electron beam plasma confined by a 2.7 kG axial magnetic field at pressures between 2 and 4 Torr, electron beam energies between 1.2 and 3 kV and at a discharge current of 0.25 A gave electron energies between 0.090 and 0.101 eV. For a few discharge conditions we also independently measured the electron temperature using the $2s\,^1S \rightarrow np\,^1P$ He I series obtaining, as expected, good agreement with the results obtained using the $2s\,^3S \rightarrow np\,^3P$ series.

The electron temperatures measured are in good

agreement with previous measurements ($kT_e = 0.094$ eV) by Persson in the negative glow of a brush cathode discharge operating at 1 Torr of helium at a current of 150 mA [10]. Moreover, the electron temperatures measured in the negative glow of hollow cathode discharges have similar values. Warner [14] measured values of kT_e for the thermal electrons between 0.068 and 0.1 eV in a planar hollow cathode discharge operating at pressures of 8 and 4 Torr. McNeil [15] measured electron energies between 0.07 and 0.15 eV in a cylindrical hollow cathode discharge operating at pressures between 7 and 16 Torr of He. All the above glow discharges are electron-beam generated and essentially uniform in the negative glow. The most numerous charged species in the negative glow of this discharge are thermal electrons, created predominantly at zero electric field ionization processes. These electrons gain energy from superelastic collisions, elastic collisions with energetic electrons and three-body recombination processes. However, the fact that there is no electric field in the negative glow and the large number of elastic collisions keeps the electron temperature thermal.

Knowing the value of the electron temperature of the numerous thermal electrons the importance of electron recombination as a loss mechanism of ions in this electron beam created plasma can be calculated. The quantitative values of the various creation and loss mechanisms of ground-state buffer gas ions is important in charge-transfer electron-beam pump lasers. In particular we will consider the losses of He^+ in a He–Hg electron-beam pumped laser plasma. We assume that the loss mechanisms for helium ions are: thermal charge-transfer collisions with Hg atoms; collisionally assisted three-body recombination; radiative electron recombination; and diffusion to the walls. In an electron-beam laser plasma of the kind used in ref. [1], with mercury vapor density, Hg, between 1×10^{15} and 1×10^{16} and $kT_e = 0.1$ eV the last two processes are negligibly small compared with the first two.

Consequently the fraction of ions loss by three-body electron recombination, F_R, is:

$$F_R = \frac{A(T_e/300)^{-4.3} N_e^2}{K[\mathrm{Hg}] + A(T_e/300)^{-4.3} N_e^2},$$

where $A = 7.1 \times 10^{-20}$ cm^6/s [11] and $K = v^* \sigma$, is the charge-transfer rate constant, where $\sigma = 1.4 \times 10^{14}$ cm^2 is the total velocity-averaged cross section [16] for

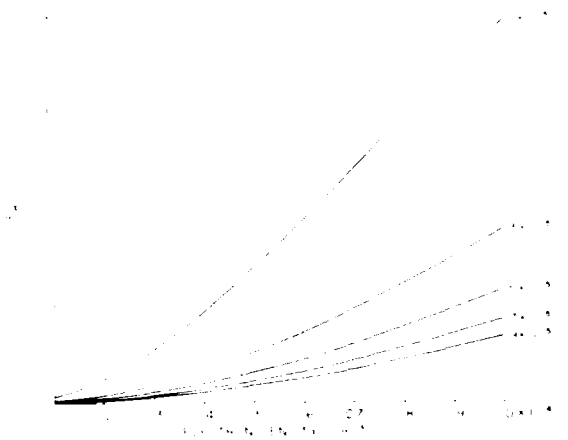

Fig. 4. Fraction of helium ions loss by recombination in a He–Hg plasma with $kT_e = 0.1$ eV as a function of electron density for the different Hg concentrations indicated at the right of the plot.

the charge-transfer reaction:

$$He^+(^2S_{1/2}) + Hg(^1S_0) \rightarrow He(^1S_0) + Hg^+(7p\,^2P) + \Delta E.$$

Fig. 4 shows the fraction of ions lost by collisionally assisted (three-body) electron recombination as a function of the electron density, for a plasma with $kT_e = 0.1$ eV, for various Hg concentrations. Electron densities up to 1×10^{14} cm^{-3} are considered. Larger electron densities are not of great interest in the case of a cw Hg^+ laser operating at 6149.9 Å because the upper laser level would be strongly depopulated by superelastic electron collisions. The atomic temperature was chosen to be 1000 K, since there cannot be a large temperature difference between the electron gas and the parent gas in a beam-generated plasma [10]. For Hg concentrations $\geq 3 \times 10^{15}$ cm^{-3} electron recombination losses of He^+ are small ($<20\%$) for electron densities below 10^{14} cm^{-3}. If the Hg concentration is decreased recombination will be an increasingly important loss mechanism of He^+ ions and the efficiency of the laser would decrease. However, it is important to notice that the Hg vapor concentration cannot be arbitrarily increased since Hg has a total ionization cross section peak value more than 10 times larger than He and the amount of electron-beam power loss in electron-impact ionization and excitation of Hg^+ would also limit the efficiency of a charge-transfer pumped He–Hg^+ laser. The conclusions of fig. 4 can

also be applied to other He–metal vapor ion lasers. Since the thermal charge-transfer cross sections between He^+ and Hg is the largest measured, the relative importance of electron recombination as a loss mechanism of He^+ is larger in other systems, and can be the main loss channel for He^+ if the metal vapor concentration is low ($< 5 \times 10^{14}$ cm^{-3}) when the device is operated at high electron densities.

In summary, we have measured the electron temperature of the numerous low-energy electrons in both longitudinal and transverse electron beam created helium glow discharges using line intensity ratio of the $2s\,^3S - np\,^3P$ He I series. The measured values of kT_e in both discharges were similar and lie between 0.07 and 0.11 eV. These low electron energies are typical of electric field free plasmas created by electron-beam excitation. At high electron densities and low metal vapor concentrations three-body recombination competes with charge transfer as the main loss channel of buffer gas ions in cw electron-beam pumped metal vapor lasers.

References

[1] J.J. Rocca, J.D. Meyer and G.J. Collins, Appl. Phys. Lett. 40 (1982) 300.
[2] J.J. Rocca, J.D. Meyer and G.J. Collins, Phys. Lett. 90A (1982) 358.
[3] J.J. Rocca, J.D. Meyer and G.J. Collins, IEEE J. Quantum Electron. 18 (1982) 1052.
[4] J.D. Meyer, J.J. Rocca, Z. Yu and G.J. Collins, IEEE J. Quantum Electron. 18 (1982) 326.
[5] J.J. Rocca, J. Meyer and G.J. Collins, Phys. Lett. 87A (1982) 237.
[6] J.J. Rocca, J. Meyer, Z. Yu, M. Farrell and G.J. Collins, Appl. Phys. Lett. 41 (1982) 811.
[7] Z. Yu, J.J. Rocca, J. Meyer and G.J. Collins, J. Appl. Phys. 53 (1982) 4704.
[8] G. Fetzer, J.J. Rocca and G.J. Collins, unpublished.
[9] L.R. Peterson, Phys. Rev. 187 (1965) 105.
[10] K.B. Persson, J. Appl. Phys. 36 (1965) 3086.
[11] C.B. Collins, A.S. Hicks, W.F. Wells and R. Burton, Phys. Rev. A6 (1972) 1545.
[12] J.M. Green, G.J. Collins and C.E. Webb, J. Phys. B6 (1973) 1545;
J.M. Green and C.E. Webb, J. Phys. B8 (1975) 1484.
[13] H.R. Griem, Phys. Rev. 131 (1963) 1170.
[14] B. Warner, Ph.D. dissertation, University of Colorado (1979).
[15] J.R. McNeil, Ph.D. dissertation, Colorado State University (1977).
[16] V.S. Aleinkov and V.V. Ushakov, Opt. Spectrosc. (USSR) 33 (1972) 116;
K. Kano, T. Shay and G.J. Collins, Appl. Phys. Lett. 27 (1975) 610.

1-W cw Zn ion laser

J. J. Rocca, J. D. Meyer, and G. J. Collins
Department of Electrical Engineering, Colorado State University, Fort Collins, Colorado 80523

(Received 28 March 1983; accepted for publication 19 April 1983)

We have obtained 1.2 W of cw laser power on the 4911.6- and 4924.0-A transitions of Zn II by exciting a He-Zn gas mixture with a dc glow discharge electron beam. In addition, 0.25-W output power has been obtained on the 6149.9-Å line of Hg^+ using the same excitation scheme. The combination of electron beam ionization of rare gas atoms and subsequent charge transfer excitation to metal ion levels is shown to have the potential of significantly increasing the efficiency of ion lasers. cw multiwatt visible and ultraviolet ion lasers operating at efficiencies $\sim 10^{-3}$ appear feasible using this excitation scheme.

PACS numbers: 42.55.Hq, 42.60.By

We have obtained 1.2 W of cw laser power on the 4911.6- and 4924.0-A transitions of Zn II by exciting a He-Zn gas mixture with a dc glow discharge electron beam. With the same excitation scheme 0.25 W of cw laser radiation on the 6149.9-A line of Hg^+ has also been obtained. This represents an order of magnitude increase in the output power previously obtained from these metal vapor laser transitions[1,2] and is the first time that metal vapor ion lasers have operated cw in the visible region at a power of 1 W.

The laser designs used to obtain these results were similar to those employed previously,[1,2] the main difference being the use of two glow discharge electron guns, one at each end of the plasma tube, as shown in Fig. 1. These glow discharge electron guns produce well collimated dc electron beams at energies between 1 and 6 keV and at currents up to 1 A. They have been described in a previous publication.[3] The use of two electron guns doubles the available electron beam power and also increases the uniformity of the electron beam created plasma.

In the laser setup of Fig. 1(a), the two 50-cm-long elec-

 0003-6951/83/130037-03$01.00

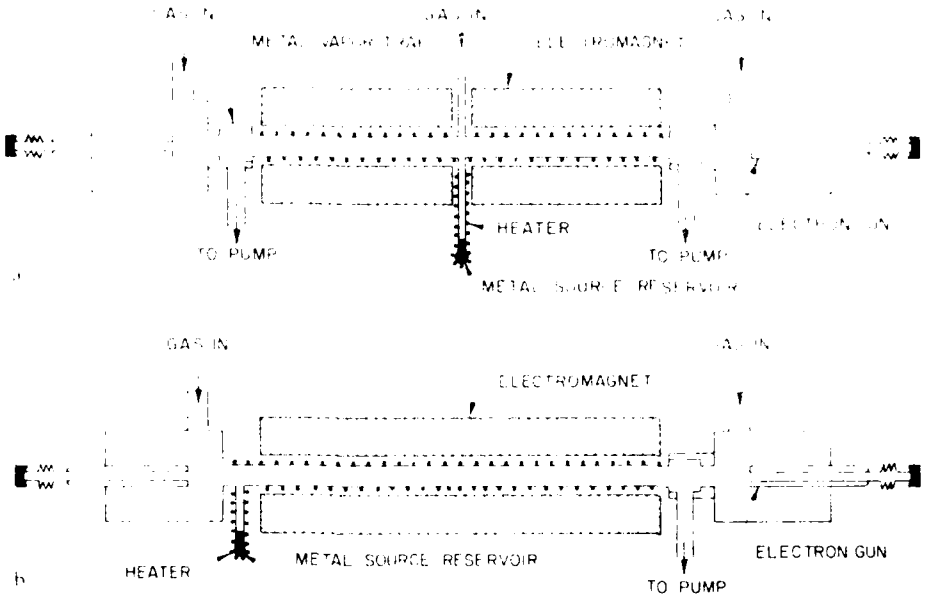

FIG. 1. Schematic diagram of the dual electron beam laser setup used in the (a) He-Hg and (b) He-Zn experiments, respectively.

tromagnets that help to confine the electron beams are separated from each other by approximately 2 cm to allow the introduction of both metal vapor and helium into the middle of the plasma tube. Both ends of the plasma tube are connected to a vacuum pump, allowing for continuous gas flow.

Using this experimental setup and internally mounted 2-m radius of curvature mirrors, we obtained 0.25 W of cw laser power on the 6149.9-Å transition of Hg II. The variation of laser output with electron beam discharge current and voltage is shown in Fig. 2. The laser output power increases linearly with current and no saturation was observed up to the maximum current investigated. The output coupler in this case had 94% reflectivity at 6150 Å. The optimum operating conditions were 1.5 Torr of He, a Hg source reservoir temperature of 130 °C, and a magnetic field of 3.2 kG.

Placing the metal vapor source reservoir in the middle of the plasma tube helped to provide a more uniform metal vapor distribution; however, the reduction of the magnetic field in this region, owing to the separation of the electromagnets, caused part of the electron beam to collide with the plasma tube walls. To reduce electron beam power loss in the Zn II laser experiment we used the setup shown in Fig. 1(b). In this scheme the metal vapor source reservoir was at one end of the plasma tube and the vacuum pump connection at the other end. High purity helium was introduced into the electron gun chamber at the reservoir side to assist in the distribution of Zn vapor. Helium was also introduced into the opposite gun chamber to permit the control of the pressure for optimum operation of the electron guns. The glow discharge electron guns used in this experiment had aluminum cathodes, just as the ones described in Ref. 3, but had an 8.5-mm-diam optical path through the axis to allow better use of the active volume and to diminish diffraction losses. The optical cavity consisted of two 4-m radius of curvature internally mounted mirrors. Reflectivities were $R_1 > 99.8\%$ and $R_2 = 93.5\%$ at 4920 Å. Using this laser setup we obtained 1.2 W of cw laser power on the 4911.6- and 4924.0-Å transitions of Zn II. This output power was obtained at a discharge current of 1.7 A and a total discharge input power of 3.5 kW. The optimum helium pressure in the plasma tube was 3 Torr and the magnetic field for maximum output was 2.9 kG. This output power is 30 times larger than the highest cw power obtained with hollow cathode devices[7] and also represents a 18 fold improvement over our previously reported value obtained with electron beam excitation.[2] The efficiency is 0.034% and is over eight times greater than that obtained in hollow cathode lasers.[7]

We consider that even larger improvements in the output power and operating efficiency of electron beam pumped ion lasers is possible by optimizing the optical cavity to make

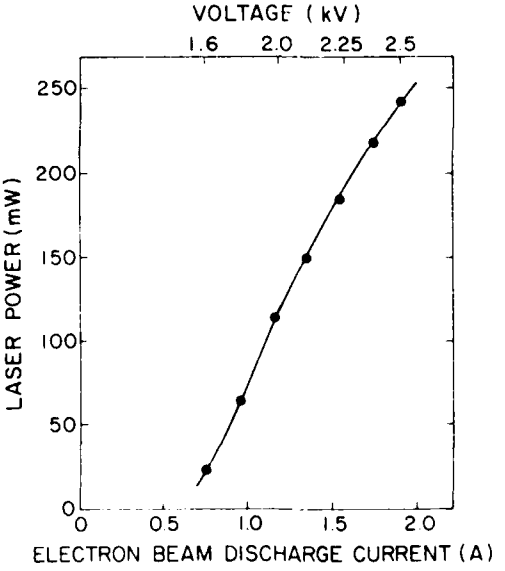

FIG. 2. Laser output power of the 6149.9-Å Hg II transition as a function of electron beam discharge current and voltage. Average helium pressure in the active medium was 1.5 Torr. Magnetic field 3.2 kG. Hg reservoir temperature was 130 °C.

better use of the active volume, by improving the efficiency with which the electron beam power is deposited into the gas, and by using proper gas to pump metal vapor. The simplified calculations presented below give an estimate of the maximum possible efficiency with which electron beam pumped charge transfer lasers can operate. In a first approximation, we can estimate the laser efficiency E_l as shown in Eq. (1):

$$E_l = D_e \cdot q \cdot Br \cdot E_o \tag{1}$$

where D_e is the efficiency with which we deposit the discharge power into the upper laser level, q the quantum efficiency, Br the branching ratio, and E_o the optical extraction efficiency.

In an electron beam excited noble gas-metal vapor mixture, the laser upper level is mainly populated by thermal charge transfer collisions of noble gas ions with ground state metal vapor atoms. The noble gas ions are created dominantly by direct electron beam ionization of noble gas atoms. We can generate electron beams with an efficiency g_e between 50% and 80% using glow discharge electron guns.[3] An electron beam of energy ~ 0.5 keV impinging on a He gas target deposits 60% of its power into the creation of ions.[8] However, only a portion of that power I_e will be deposited into the production of helium ions when an electron beam impinges on a helium-metal vapor mixture. In the case of a 10 to 1 partial pressure ratio of helium to metal vapor, we would expect roughly half of the power to be deposited into helium ions if the ionization cross-section ratio of metal atoms to helium atoms was 10 to 1.[9] Consequently, we expect that the fraction I_e of the electron beam power to be used in the creation of helium ions will equal 30%. Only a fraction of these ions will pump upper laser levels via charge transfer. The noble gas ions are lost by diffusion to the walls, electron recombination, and charge transfer collisions with ground state metal vapor atoms. Thermal charge transfer collisions have a large cross section (130 Å^2 in the case of He$^+$-Hg collisions).[10] Therefore, at metal vapor concentrations $\sim 10^{15}$ cm^{-3} and electron densities below 10^{14} cm^{-3} the charge transfer loss channel dominates, and the fraction F of noble gas ions lost by pumping upper laser levels can be $F \sim 0.8$. In summary, the overall efficiency D_e with which the discharge power is deposited in the laser upper level is then

$$D_e = g_e \cdot I_e \cdot F \sim 0.15. \tag{2}$$

The quantum efficiencies for visible metal vapor laser transitions ($h\nu \sim 2.4$ eV) excited by He$^+$ ions are roughly 10%. Then, considering $q = 0.1$ and assuming $Br \cdot E_o = 0.2$ we estimate from Eq. (1) the maximum laser efficiency is $\sim 3 \times 10^{-3}$ which is still considerably higher than the efficiencies we have obtained up to date. For ultraviolet transitions ($h\nu \sim 8$ eV) in helium metal vapor systems the quantum efficiency $q \sim 0.2$ and in principle, according to Eq. (1), efficiencies in the vicinity of 0.6% could be obtained in an electron beam excited charge transfer system. Although the above calculations are only a crude estimate, it is clear that the possibility of high efficiency is based on three important points summarized below. The first point is that the majority of the discharge power (50% – 80%) goes into the creation of beam electrons; secondly, helium ions are efficiently created by these energetic beam electrons; finally, charge transfer reactions can selectively and efficiently deposit the energy stored in the rare gas ions into the laser upper level. For a more accurate estimate of the maximum possible efficiency of electron beam pumped charge transfer ion lasers, an elaborate model of the electron beam created plasma is required. We are presently working on a computer model in which the electron energy distribution is calculated by numerically solving the Boltzmann equation for electrons. The distribution is then used to calculate the excitation and ionization rates necessary to determine the population in the laser levels and subsequently laser output power and operating efficiency.

In summary, we have obtained 1.2 W of cw laser power on the blue lines of Zn II exciting a He-Zn mixture with an electron beam. cw multiwatt visible and ultraviolet ion lasers operating at efficiencies $> 10^{-3}$ seem feasible using this new excitation scheme.

This work was supported by the National Science Foundation.

[1] J. J. Rocca, J. D. Meyer, and G. J. Collins, Appl. Phys. Lett. **40**, 300 (1982).
[2] J. J. Rocca, J. D. Meyer, and G. J. Collins, IEEE J. Quantum Electron. **QE-18**, 1052 (1982).
[3] J. J. Rocca, J. D. Meyer, Z. Yu, M. Farrell, and G. J. Collins, Appl. Phys. Lett. **41**, 811 (1982).
[4] J. J. Rocca, J. D. Meyer, and G. J. Collins, Opt. Commun. **42**, 125 (1982).
[5] J. D. Meyer, J. J. Rocca, Z. Yu, and G. J. Collins, IEEE J. Quantum Electron. **QE-18**, 326 (1982).
[6] J. J. Rocca, J. D. Meyer, and G. J. Collins, Phys. Lett. A **90**, 358 (1982).
[7] J. Piper and P. Gill, J. Phys. D **8**, 127 (1975).
[8] B. Warner, Ph.D. thesis, University of Colorado, Boulder, Colorado, 1979.
[9] W. Lotz, Z. Phys. **232**, 101 (1970); H. S. Massey, E. H. Burhop, and H. B. Gilbody, *Electronic and Ionic Impact Phenomena* (Oxford University, Oxford, England, 1971), Vol. 1.
[10] K. Kano, T. Shay, and G. J. Collins, Appl. Phys. Lett. **27**, 610 (1975); V. S. Aleinkov and V. V. Ushakov, Opt. Spectrosc. **33**, 116, 1972.

Compact Hg II Laser Excited by a Transverse Electron Beam Glow Discharge

JORGE J. ROCCA, DAVID M. MC CLURE, AND GEORGE J. COLLINS

Abstract—CW laser action at an output power of 6 mW has been obtained on the 6149.5 Å transition of Hg II, using a 10 cm long transverse electron beam glow discharge. Beam energies are typically 1 keV. Laser tube design, discharge characteristics, and laser output power are reported.

We have obtained CW laser action on the 6149.5 Å transition of Hg II using a 10 cm long transverse electron beam excited glow discharge. We previously reported the generation of CW laser radiation in several singly ionized species in He-metal vapor mixtures using longitudinal electron beam excitation [1]-[5]. In this excitation scheme a glow discharge electron gun [6] produces an electron beam with an energy between 1 and 5 keV that is guided by an axial magnetic field to generate a laser active medium 50-100 cm long. In the transverse excitation scheme we describe below the magnetic field is not needed to ensure efficient deposition of the electron beam energy into the gas mixture. Rather, electrostatic fields confine and partially trap the beam electrons. This allows for the compact laser geometry shown schematically in Figs. 1 and 2(a).

A new cathode material is used in our glow discharge electron gun. It is a sintered mixture of molybdenum and magnesium oxide particles (10 μm diameter) in certain proportions

Manuscript received March [illegible], 1983; revised May 13, 1983. This work was supported by the National Science Foundation and the AFOSR. [illegible] Engineering, Colorado State University, Fort Collins, CO 80523. [illegible] D. M. McClure [illegible] New York, NY.

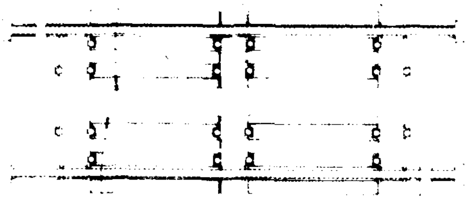

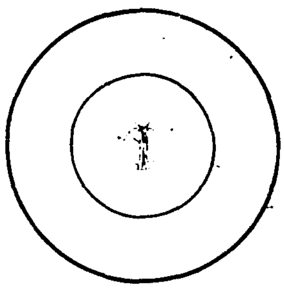

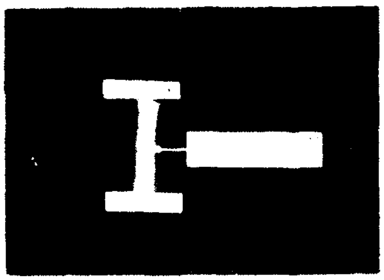

[illegible]

[illegible] gas [illegible] vapor-helium gas mixture with [illegible] addition of oxygen [illegible] cathode [illegible].

[illegible] water-cooled [illegible]. Two [illegible] were separated [illegible] as shown in Fig. 1. Each cathode was [illegible] through a [illegible] also separated from the [illegible] spacers. O-rings were used [illegible] between [illegible]. The stainless steel end [illegible] support a slotted [illegible] which acts as the [illegible] anode. The anode [illegible] approximately 0.5 [illegible] from the cathode and has two sets of opposite slots 0.5 cm wide and 5 cm long as shown in Fig. 2(a), through which the electron beam passes.

The [illegible] also covers the regions between different [illegible] and consequently protects the O-ring seals from the [illegible] discharge. The 0.5 mm distance between the electrodes under operating conditions (pressures between 1 and 6 torr) is less than the mean free path for an ionizing electron collision. For an electron with an energy near the peak value of the total cross section (120 eV) for ionization of helium ($\sigma = 3.7 \times 10^{-17}$ cm^2), the corresponding mean free path is 5 mm at a helium pressure of 6 torr and a gas temperature of 1000°C. Higher electron energies and lower pressures have even larger mean free paths for ionization. Consequently, there is not sufficient ionization in the annular interelectrode region to establish a stable discharge. In this way, a constricted glow discharge with a length of 10 cm is created. The electron beam is produced by acceleration in the cathode dark space of the electrons emitted following cathode bombardment by ions and fast neutrals. Practically all the discharge voltage V_c drops in this cathode fall region, creating an electron beam of energy approximately equal to $e \cdot V_c$. The concave cathode geometry focuses the electron beam towards the axis of the discharge volume. The beam electrons lose part of their energy in exciting and ionizing collision as they travel towards the opposite cathode surface. The beam electrons are then reflected by the electric field in the opposite dark space [8]. The opposing concave cathode surfaces allow for both the trapping [8] and focusing of the beam electrons, and consequently efficient deposition of beam energy into the gas mixture occurs. The electron beam, electrostatically trapped in this way, creates a bright plasma with the clear boundaries as shown in Fig. 2(b). Transverse high voltage glow discharges have been obtained in the past [9], [10] by similar techniques but with lower [illegible] cathode materials and without allowing for electrostatic trapping of the beam electrons.

Mercury [illegible] was introduced into the discharge tube by [illegible] located in one of the stainless steel end [illegible]. Helium was introduced at the same end of the discharge [illegible] SCCM [illegible]. The optical cavity was [illegible] using two [illegible] dielectric [illegible] of [illegible].

[illegible] glow [illegible] discharges at

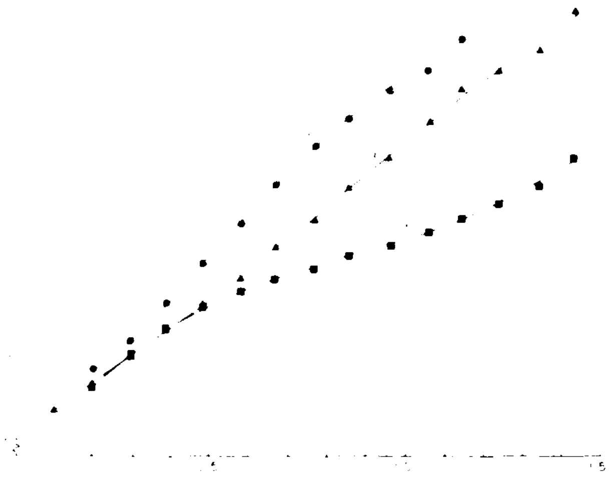

Fig. 3. I-V characteristics of the transverse electron beam glow discharge in helium using two cathode segments.

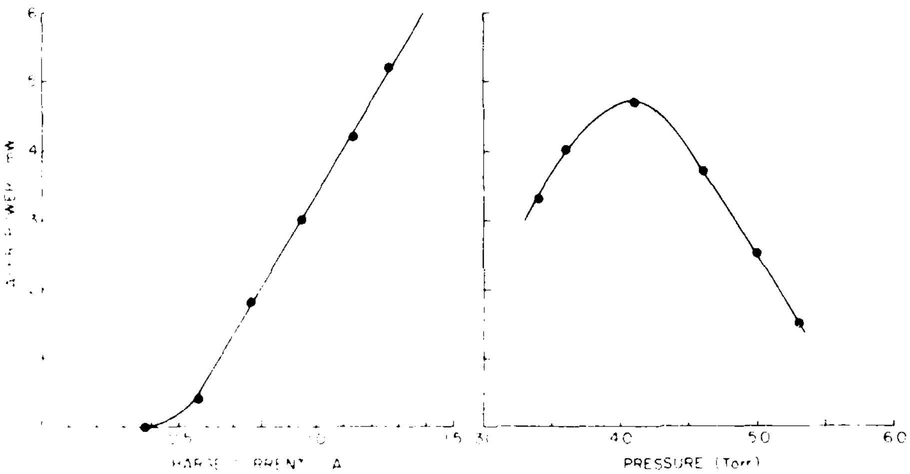

Fig. 4. (a) Laser output power as a function of discharge current. Helium pressure was 4 torr. The reservoir temperature was 180°C. (b) Laser output power as a function of helium pressure for a discharge current of 1.5 A. Temperature of the Hg reservoir was 180°C.

currents over 1 A and at a voltage of 1 kV have been obtained using two cathode segments each having an effective discharge length of 5 cm. The laser output power versus discharge current is shown in Fig. 4(a) for a helium pressure of 4 torr. The laser output power increases linearly with current and no saturation was observed up to the maximum discharge current investigated. A CW laser output power of 6 mW was obtained using an optimized output coupler of 99.8 percent reflectivity at [illegible] A. Fig. 4(b) shows the variation of the laser output power as a function of helium pressure for a discharge current of 1.5 A. The dominant excitation mechanism is proposed to be charge transfer excitation of the Hg II $7p\,^2P_{3/2}$ level from the helium ion ground state He II $1s\,^2S_{1/2}$ [11]. The [illegible] of modular construction can be extended adding more cathode segments to obtain larger laser power.

Recently we have also obtained CW laser action in the 6149.5 A transition of Hg II using a 10 cm long transverse electron beam glow discharge to excite a He-Hg mixture.

Acknowledgment

The authors wish to thank D. A. Perkins for his assistance in the experiments.

References

[1] J. J. Rocca, J. D. Meyer, and G. J. Collins, "Electron beam pumped CW He-ion laser," *Appl. Phys. Lett.*, vol. 40, pp. 300–302, 1982.
[2] —, "CW laser oscillations in Cd II in an electron beam created plasma," *Phys. Lett.*, vol. 90A, pp. 358–360, July 1982.
[3] —, "Electron beam pumped CW Se II laser," *Opt. Commun.*, vol. 42, pp. 125–127, June 1982.
[4] J. D. Meyer, J. J. Rocca, Z. Yu, and G. J. Collins, "CW iodine laser excited by an electron beam," *IEEE J. Quantum Electron.*, vol. QE-18, pp. 326–327, Mar. 1982.
[5] J. J. Rocca, J. D. Meyer, and G. J. Collins, "Zn II-As II laser tran-

sitions excited by an electron beam," *IEEE J. Quantum Electron.*, vol. QE-18, pp. 1052-1054, July 1982.
[6] J. J. Rocca, J. D. Meyer, Z. Yu, M. Farrell, and G. J. Collins, "Multi-kilowatt electron beams for pumping CW ion lasers," *Appl. Phys. Lett.*, vol. 41, pp. 811-813, Nov. 1982.
[7] J. J. Rocca, J. Meyer, M. R. Farrell and G. J. Collins, "Glow discharge created electron beams: Cathode materials, electron gun designs and applications," unpublished.
[8] Z. Yu, J. J. Rocca, J. Meyer, and G. J. Collins, "Transverse electron guns for plasma excitation," *J. Appl. Phys.*, vol. 53, pp. 4704-4710, July 1982.
[9] K. Rozsa, M. Janossy, J. Bergou, and L. Csillag, [illegible] CW hollow cathode with internal anode [illegible] *Commun.*, vol. 23, pp. [illegible]
[10] T. Iuima, "New type hollow cathode discharge tube with [illegible] variable voltage," *[illegible] J. Appl. Ph[illegible]*, vol. [illegible], pp. 1476-1477.
[11] H. Kano, T. Shay, and G. J. Collins, "A second look at the excitation mechanism of the He-Hg[illegible] laser," *Appl. Phys. Lett.*, vol. 27, pp. 610-612, Dec. 1975.

АКАДЕМИЯ НАУК СССР
СИБИРСКОЕ ОТДЕЛЕНИЕ

АВТОМЕТРИЯ

(Отдельный оттиск)

1

ИЗДАТЕЛЬСТВО «НАУКА»
СИБИРСКОЕ ОТДЕЛЕНИЕ
Новосибирск · 1984

АКАДЕМИЯ НАУК СССР
СИБИРСКОЕ ОТДЕЛЕНИЕ
АВТОМЕТРИЯ

№ 1 1984

ФИЗИКА ОПТИЧЕСКИХ КВАНТОВЫХ ГЕНЕРАТОРОВ

УДК 621.378.3

ДЖ. ДЖ. РОККА, Г. ДЖ. КОЛЛИНЗ
(Колорадо, США)

УЛЬТРАФИОЛЕТОВЫЕ ИОННЫЕ ЛАЗЕРЫ

Введение. В настоящее время ионные лазеры являются наиболее мощными источниками когерентного излучения в ультрафиолетовой (УФ) области спектра, работающими в непрерывном режиме. В этой области спектра описано более ста лазерных переходов ионов с самой короткой длиной волны 224,2 нм на переходе AgII. На рис. 1 даны длины волн и мощности наиболее существенных переходов УФ ионных лазеров. Приведены мощности, достигнутые в непрерывном и квазинепрерывном режимах или в режиме длинных импульсов. Многократно ионизованные атомы благородных газов обеспечивают самую высокую мощность непрерывной генерации, например 61 Вт, при одновременной генерации длин волн 351,1 и 363,8 нм линий ArIII. Более низкий пороговый ток и более короткая длина волны генерации получены на переходах однократно ионизованных паров металлов, возбуждаемых в разрядах с полым катодом. Генерация ионного лазера в УФ-области на рекомбинирующей плазме наблюдалась только в импульсном режиме. Лазеры на многократно ионизованных атомах благородного газа генерируют и вакуумное ультрафиолетовое (ВУФ) излучение, но в настоящее время — только в импульсном режиме.

Ниже будет дан обзор работ по ионным лазерам на инертном газе с разрядом в положительном столбе, с полым катодом на ионах металла, импульсным рекомбинационным ионным лазерам и лазерам на многократно ионизованных атомах благородного газа в вакуумном ультрафиолетовом диапазоне. Недавно продемонстрировано использование

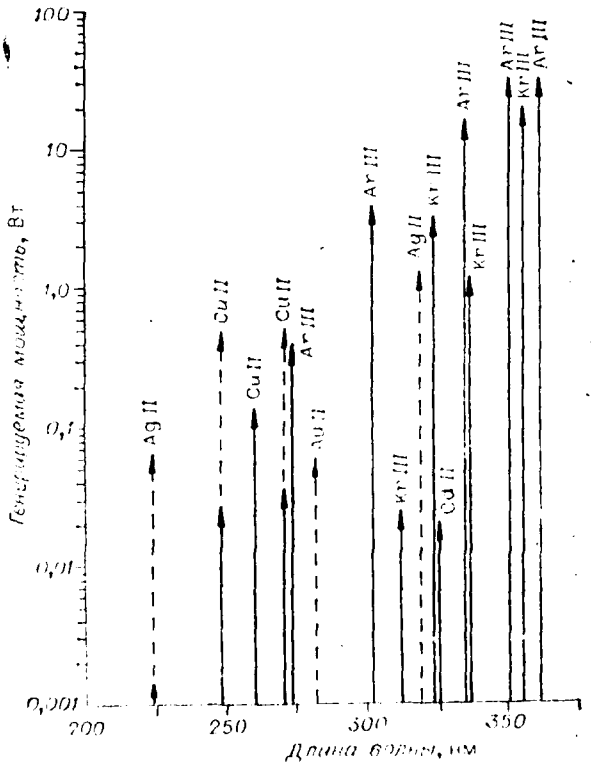

Рис. 1. Наиболее сильные линии ионных УФ-лазеров непрерывного и квазинепрерывного действия:
сплошная линия — непрерывная мощность, штриховая — квазинепрерывная.

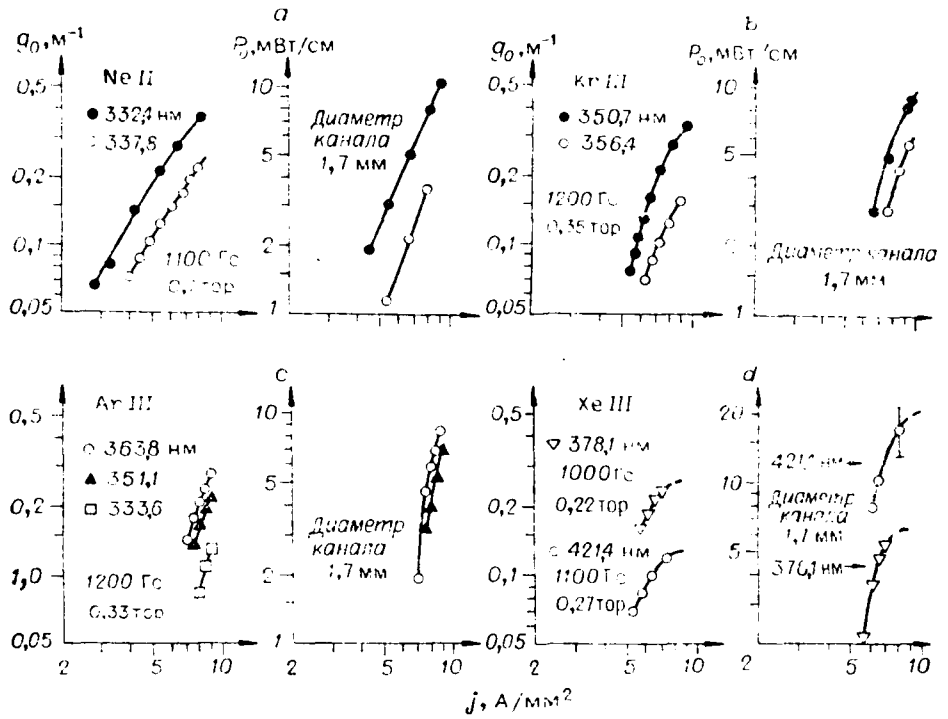

Рис. 2. Коэффициент усиления слабого сигнала и выходная мощность ионного УФ-лазера как функция разрядного тока:
a — NeII, *b* — KrIII, *c* — ArIII, *d* — XeIII [2].

электронного пучка постоянного тока для возбуждения ионного лазера непрерывного действия. Этот новый механизм возбуждения позволяет получить более высокую эффективность и короткую (ВУФ) длину волны, поэтому мы также обсудим эту новую схему возбуждения для ионных лазеров непрерывного действия.

Ультрафиолетовые ионные лазеры на инертном газе. Впервые непрерывное лазерное УФ-излучение было получено Паананеном [1] в 1966 г. Он зарегистрировал излучение лазера на XeII (332,4 и 337,8 нм), ArIII (351,1 нм) и KrIII (350,7 нм) при токе от 45 до 85 А в разрядной трубке с внутренним диаметром 3,5 мм, эффективная длина которой 56 см. Паананен получил мощность лазера в непрерывном режиме 0,3 Вт, 30 и 13 мВт для переходов KrIII, XeII и ArIII соответственно. В 1968 г. Федли [2] провел подробное исследование лазерного УФ-излучения ионизованных газов Xe, Ar, Kr и Xe, измерил коэффициент усиления и мощность сильнейших линий излучения лазера, в котором использовалась секционированная графитовая трубка длиной 34 см с внутренним диаметром 1,7 мм. Эти результаты приведены на рис. 2.

Бансе и другие [3] получили мощность лазера непрерывного действия свыше 1 Вт при одновременной генерации на переходах ArIII (351,1 и 363,8 нм) и KrIII (350,7 нм) в трубке из плавленого кварца с внутренним диаметром 12 мм. Латимер [4], а также Бриджес и Мерсер [5] сообщили о мощности непрерывного лазера ~1,7 и 2,3 Вт для линий ArIII соответственно при использовании разрядных трубок из вольфрамовых дисков с малым внутренним диаметром (4 и 2,3 мм). На рис. 3 представлены результаты, полученные Бриджесом и Мерсером. Они сообщили об эффективности порядка $1 \cdot 10^{-3}$. Выходные мощности лазеров в этих экспериментах и основные характеристики разрядных трубок аналогичны серийным разрядным трубкам непрерывных ионных лазеров, которые применяются в настоящее время.

В 1976 г. Тио и другие [6] достигли значительно больших выходных мощностей лазеров с разрядной трубкой из вольфрамовых дисков с внутренним диаметром 12 мм и длиной 15 см. Они получили суммарную мощность 16 Вт на линиях ArIII при разрядном токе 485 А; 55% мощности было найдено на линии 363,8 нм, а остальная — на переходе 351,1 нм. Кроме того, они сообщили о лазерах непрерывного действия с мощностью порядка 7; 1,8 и 0,15 Вт на УФ-переходах KrIII (350,7 и 350,4 нм), XeIII (378,1 и 374,6 нм) и NeII (332,4 нм). И, наконец, Лючи и другие [7] в 1977 г. сообщили о самой высокой в настоящее время мощности непрерывного УФ-лазера, которую получили, используя секционированную металлическую разрядную трубку с внутренним диаметром 12 мм, и достигли на переходах ArIII (351,1 и 363,8 нм) мощности 61 Вт.

Таблица 1

Ультрафиолетовые УФ-лазерные переходы в непрерывном режиме. Измеренная мощность УФ-лазера при максимальном токе источника питания i 480 А (диаметр разряда 12 мм, длина разряда 1,7 м, давление газа 1,25 тор для Ar; 1,3 тор для Kr [7])

Ион	Длина волны, нм	Мощность, Вт	Коэффициент отражения выходного зеркала, %	Относительный вклад, %
ArIII	363,7 351,1	61	98	50 50
ArIII	335,8 334,4 333,6	17	97,5	25 45 30
ArIII	305,4 302,4 300,2	3,8	99	5 40 55
ArIII	275,4	0,4	98,5	100
KrIII	356,4 350,7	19	98	30 70
KrIII	337,4 323,9 312,4	4,5	97,5	25 70 5

В табл. 1 и на рис. 4 приведены результаты, полученные Лючи и другими для ArIII и KrIII. Выходная мощность увеличивалась без насыщения до максимально возможного разрядного тока ~480 А, это указывает на то, что для большинства УФ-линий возможны бо́льшие выходные мощности при бо́льших плотностях разрядного тока.

При работе с импульсным разрядом [8] (τ 0,2 0,3 мкс[1] [illegible] дался рост максимальной мощности при увеличении плотности разрядного тока j до величины, которая на порядок больше, чем в экспериментах Лючи и других. В частности, для линии ArIII 351,1 нм мощность в импульсном режиме составляла 1 кВт (j ~ 7200 А·см$^{-2}$, B 0,3 см$^{-2}$·[illegible]

Ионные лазеры на парах металла. He–Cd$^+$-лазер. Силваст [9] и независимо Голдсборо [10] получили генерацию в непрерывном режиме в CdII на линии λ = 325,0 нм. Силваст зарегистрировал мощность 0,5 мВт на смеси He—Cd в разрядной трубке диаметром 4 мм и длиной [illegible] Голдсборо [11] получил мощность 20 мВт в трубке диаметром [illegible] и длиной 143 см при токе ~110 мА и давлении гелия 3,4 тор.

Силваст [12], следуя Веббу, предложил реакцию Пеннинга

$$He^*(2s^3S_1) + Cd \rightarrow He + Cd^+(5s\ ^2D) + e + \Delta$$

для возбуждения верхних лазерных уровней $5s^2D$ перехода [illegible] нм и 141,6 нм и быстрый радиационный распад по хорошо разрешенным УФ-переходам в основное состояние иона как процесс девозбуждения нижних лазерных уровней $5p^2P$. Эксперименты Колиншо [13], Вебба [14], Ширера и Надовани [15] и Силваста [16] подтверждают эту схему возбуждения. Однако дело в том, что была также получена генерация лазера (при гораздо меньшей мощности) в Ne—Cd, Ar—Cd и Ne—Cd смесях [17]. Это усложняет простую картину, в которой процесс Пеннинга является единственным механизмом возбуждения.

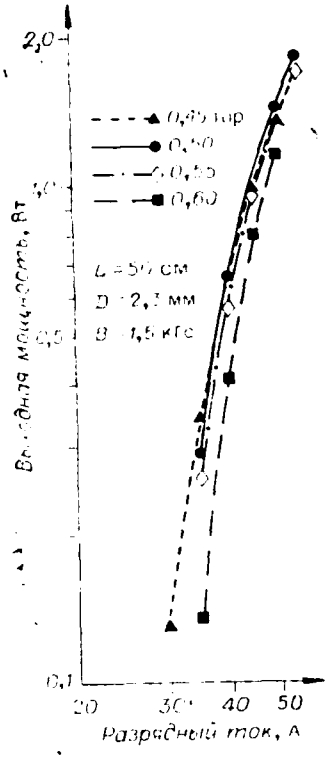

Рис. 3. Выходная мощность ультрафиолетового ArII-лазера (на линиях 351,1 и 363,8 нм) с трубкой из дисков.

(На рисунке даны параметры трубки [51].)

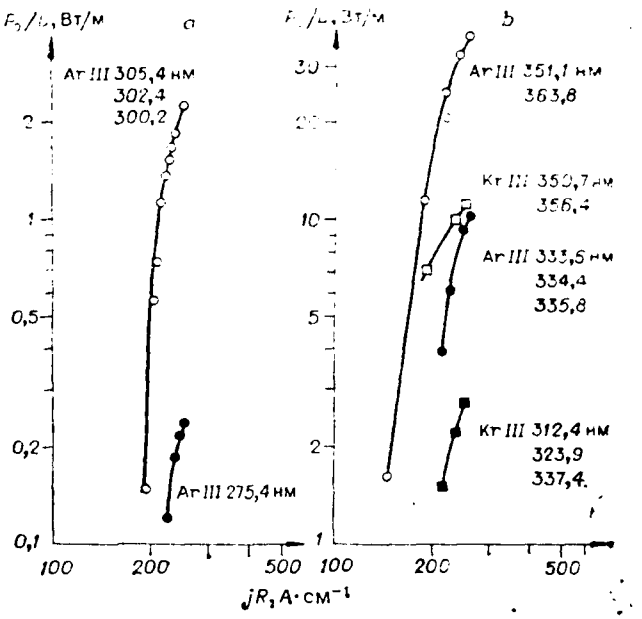

Рис. 4. Зависимость выходной мощности УФ-лазера P_2 на единицу длины разряда от произведения плотности тока на радиус трубки:

а — длина волны <310 нм, диаметр разряда 12 мм, давление газа оптимизировано для каждого значения тока [7]; *b* — длина волны >310 нм [7].

Ванг и Зигман [17] отметили увеличение мощности лазера при уменьшении давления инертного газа; механизмом возбуждения для таких экспериментальных условий является непосредственное столкновение электрона с атомом кадмия в основном состоянии. В. С. Алейников и В. В. Ушаков [18] измерили большое поперечное сечение ($1{,}5 \cdot 10^{-16}$ см$^{-2}$) для этого процесса.

Совсем недавно группа ученых из Нагойского университета изучила механизмы возбуждения He—Cd^+-лазера путем моделирования и экспериментально [19, 20], а также заселенность верхнего уровня перехода в CdII на $\lambda = 441{,}6$ нм $5s^2\,{}^2D_{5/2}$. Предполагается, что расчеты должны быть верны и для верхнего уровня $5s^2\,{}^2D_{3/2}$ линии 325,0 нм. Установлено, что модель будет соответствовать экспериментальным данным только в том случае, если учесть обе реакции — и Пеннинга, и ступенчатое возбуждение электронами из основного состояния Cd(II). Авторы [20] доказали, что основным механизмом возбуждения при плотности тока в несколько миллиампер является процесс Пеннинга по реакции 1 и что процесс ступенчатого возбуждения электронным ударом преобладает при более высокой плотности тока.

Лазеры на однократно ионизованных атомах паров металлов в ультрафиолетовой области. Разряды в положительном столбе — не очень хорошая активная среда для ионных лазеров на парах металлов, так как температура электронов очень быстро уменьшается при увеличении давления паров металла. Это убедительно показали Гото и другие [21] методом двойного зонда в условиях разряда, типичных для He—Cd^+-лазера. Их результаты представлены на рис. 5. Вследствие указанной выше причины плотность паров металла и температуру электронов нельзя оптимизировать независимо. Уменьшение температуры электронов вызывает также снижение скорости ионизации, что является недостатком для большинства ионных лазеров на парах металлов. Схемы возбуждения

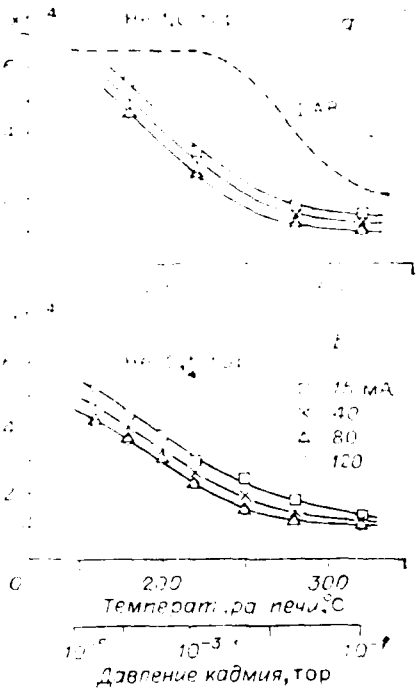

Рис. 5. Температура электронов как функция давления кадмия (температуры печи) *в типичных условиях He — Cd⁺ разряда.* Штриховой линией показан результат, вычисленный по теории Доргеля и других [21]

электрическим разрядом, в которых нет этого недостатка, описаны в следующих разделах.

Ионные лазеры с полым катодом на парах металлов. Разряд в полом катоде имеет более подходящие характеристики для генерации лазера на смеси инертных газов с парами металлов. Разряд, заполняющий полый катод, является в основном отрицательным, поддерживаемым электронами пучка высокой энергии [22]. В результате бомбардировки поверхности катода ионами, быстрыми нейтральными частицами и фотонами эмиттируются вторичные электроны, которые затем ускоряются в темной катодной области и формируют электронный пучок с энергией 300—400 эВ. Эти быстрые электроны могут эффективно ионизовать атомы в разряде, создавая подходящую активную среду для ионных лазеров. На рис. 6 показано распределение энергии электронов, выведенное из уравнения Больцмана для электронов в He—Hg-разряде в полом катоде [23]. Основные характеристики этого распределения хорошо согласуются с измерениями Гилла и Вебба, выполненными при использовании электростатического анализатора энергии [24]. Электроны в пучке, попадающие в отрицательный разряд при энергии, близкой к eV_c, где V_c — напряжение в разряде, теряют энергию вследствие неупругих и упругих столкновений. Большинство вторичных электронов, возникших во время

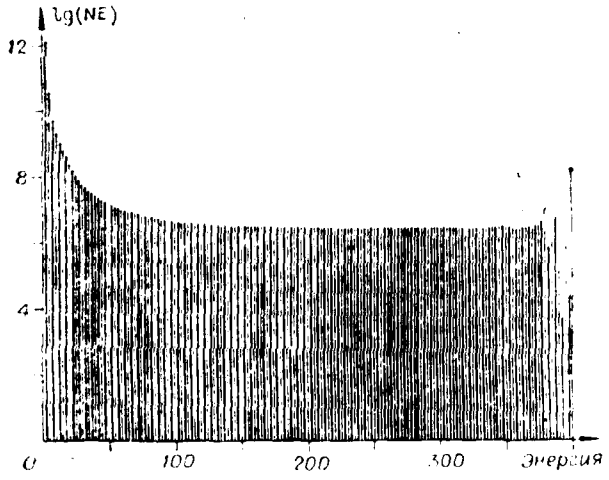

Рис. 6. Распределение энергии электронов в He — Hg-разряде с полым катодом диаметром 0,3 см, длиной 50 см, вычисленное по уравнению Больцмана для электронов:

разрядный ток 10 А, плотность He $1{,}2 \cdot 10^{17}$ см$^{-3}$, плотность Hg $3 \cdot 10^{15}$ см$^{-3}$ [23].

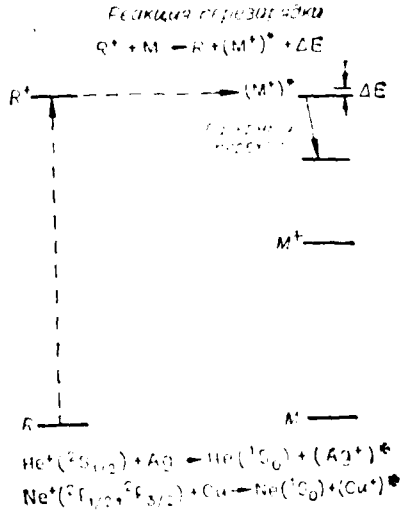

Рис. 7. Схема реакции перезарядки.

ионизующих столкновений, образуются при низкой энергии [25], в результате чего получается распределение, показанное на рис. 6.

Поскольку поле в отрицательном разряде, поддерживаемом электронами пучка, мало, то он будет менее чувствителен к наличию паров металла, которые распыляются с катода, по сравнению с положительным столбом. Это является преимуществом, так как позволяет лучше оптимизировать концентрацию паров металла без резкого уменьшения энергии электронов и скорости ионизации. Более того, как впервые указали Виллет [26] и Карабут [27], материал самого катода может распыляться в разряде, в результате чего получаются атомы металла в основном состоянии. Таким образом можно испарять нелетучие металлы без использования печи и саморазогревающихся разрядов. Это существенное практическое преимущество; впервые оно было реализовано в лазере Сциллагом и другими [28] в щелевом полом катоде Шубеля [29].

Верхние лазерные уровни для многих переходов паров металлов в разрядах с полым катодом заселяются в результате реакций перезарядки, которые схематически представлены на рис. 7 и записываются как

$$R^+ + M \rightarrow R + (M^+)^* + \Delta E, \qquad (1)$$

где R, R^+ и M — атомы и ионы буферного газа и атомы металла соответственно; $(M^+)^*$ — ионы металла в возбужденном состоянии, с которого происходит лазерная генерация, а ΔE — разность энергий между R^+ и $(M^+)^*$ в реакции (1). Дуффендак с соавторами [30–36], а также Такахаши [37] исследовали различные смеси металлов и благородных газов, в которых происходило возбуждение ионных уровней вследствие перезарядки. Применение разрядов с полым катодом для создания инверсии заселенностей было мало распространено до тех пор, пока Фаулз с сотрудниками из университета Юта не продемонстрировал впервые, что перезарядка [38—40] может привести к селективному возбуждению верхних лазерных уровней в устройствах с положительным столбом разряда. Несколько лет спустя, используя возбуждение в разряде с полым катодом, Карабут [27], Сугавара [41], Шубель [42] и Пенсен [43] получили лазерную генерацию на смесях $He—Cd^+$ и $He—Zn^+$.

Впервые об инверсии заселенности в случае только катодного распыления сообщили Сциллаг и другие в 1974 г. [28] при генерации CuII-лазера на 780,8 нм. Верхний лазерный уровень CuII селективно заселялся реакциями перезарядки между ионами гелия и атомами меди, находившимися в основном состоянии и полученными путем распыления. Позднее в [44—46] было сообщено об ультрафиолетовых лазерных переходах в CuII, AgII и AuII. В табл. 2 даны длины волн этих переходов, обозначение уровней, выходные мощности лазера и пороговый ток.

Металлы, указанные выше, наиболее пригодны для использования в лазерах с полым катодом, поскольку все они хорошо распыляются при бомбардировке ионами с энергией ~300 эВ [47]. Следовательно, путем распыления можно получить плотность паров металла в разряде, большую или равную 10^{15} см$^{-3}$ [48]. Кроме того, уровни ионов металла, энергия которых соответствует энергии ионов инертного газа в основном состоянии, заселяются реакциями перезарядки [30–36]. Совокупность этих факторов обеспечивает нужную инверсию заселенностей. Ниже рассмотрим лазеры с полым катодом и характеристики наиболее важных УФ лазеров с полым катодом: $Ne—Cu^+$, $He—Ag^+$ и $He—Au^+$.

Геометрия лазеров с полым катодом. Лазерная генерация была получена с разнообразными геометриями полого катода. На рис. 8 представлены различные конфигурации поперечного возбуждения. В. П. Чеботаев [49] и Смит [50] впервые использовали разряд в полом катоде с двойным возбуждением (на рис. 6 не показано) в $He—Xe$-лазере на 1,5 мкм. Впоследствии Байер [51], Видер [52], Карабут [27], Сугавара [41], Шубель [42], Пенсен [43], Шпер [53], Сциллаг [28], а также Айхлер и другие [54] применили разряд с полым катодом для возбуждения лазеров на ионах металлов. Большинство работ по изучению лазеров

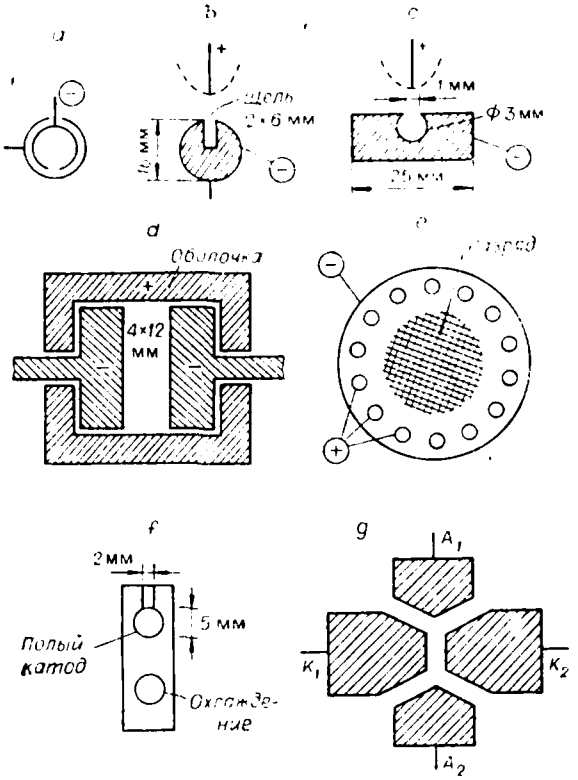

Рис. 8. Конфигурации лазера с полым катодом с поперечным возбуждением:

типа Шубели (*a*), прямоугольный щелевой полый катод (*b*), круглая щель (*c*), типа волновода (*d*), полый анод или затрудненный разряд (*e*), желобковый полый катод (*f*) и прямоугольный полый катод (*g*). K_1 и K_2 — катоды, A_1 и A_2 — аноды.

выполнено со щелевым полым катодом Шубеля с поперечным возбуждением [29] (см. рис. 6, *b*, *c*).

На рис. 9 показаны типичные графики вольтамперных характеристик для серебряных, медных и алюминиевых щелевых полых катодов с различными смесями буферных газов. Следует отметить, что требования к вольтамперным характеристикам почти такие же, что и в случае серийного лазера на ионах инертного газа. Однако полное динамическое сопротивление разряда с полым катодом будет всегда положительным и низким (<20Ω), что, учитывая низкий уровень напряжения пробоя, уменьшает нестабильности в цепи разряда. Все конфигурации электродов, представленные на рис. 7, будут работать в режиме полого катода только в том случае, если области отрицательного свечения от противоположных поверхностей катода сольются или перекроются.

Ne—Cu⁺-лазеры. В разрядах с полым катодом в смеси Ne—Cu⁺ уровни $3d^9 5s$ CuII заселены реакциями перезарядки между атомами меди и ионами инертного газа в основном состоянии. В табл. 2 даны самые сильные переходы CuII. На рис. 10 демонстрируется селективность схе-

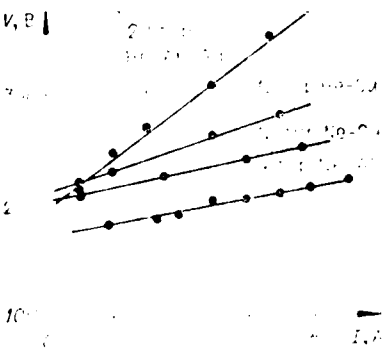

Рис. 9. Вольтамперные характеристики разрядов в полом катоде, выполненном из материалов: Ag, Cu и Al.

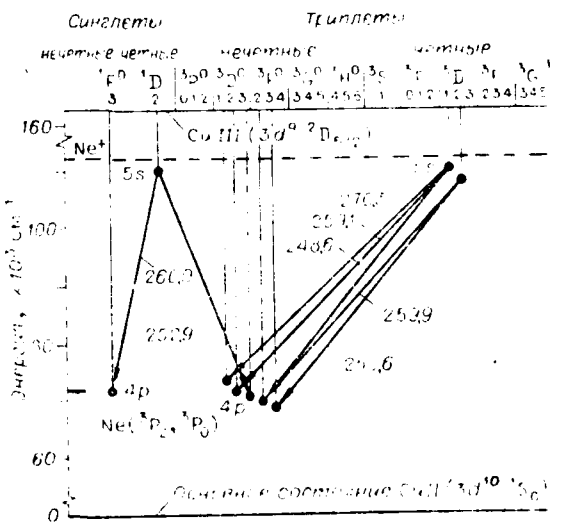

Рис. 10. Схема термов CuII с указанием отдельных лазерных переходов (сплошные линии).

Длина волны дана в нанометрах.

Таблица 2

Коэффициенты усиления слабого сигнала и выходные мощности лазеров на некоторых УФ-переходах Ag^+, Cu^+ и Au^+ [60, 80]

Длина волны, нм		Измеренный полный коэффициент усиления $g_0 - L_i$, %*,**	Коэффициент усиления на 1 м $g_0 2l$, $\%\,м^{-1}$	Мощность лазера**
318,1	Ag^+	5,3	3,8	1,3 Вт
270,3	Cu^+	5,1	3,6	0,5 Вт
260,0	Cu^+	3,2	2,3	0,25 Вт
252,9	Cu^+	2,6	1,9	
248,6	Cu^+	12,2	8,3	0,5 Вт
224,3	Ag^+	—	—	65,0 мВт
282,2	AuII	—	—	
291,8	AuII	—	—	600 мВт ***

* Коэффициенты усиления слабых сигналов при прохождении активной среды в прямом и обратном направлениях за вычетом собственных потерь в резонаторе для катода $l = 0{,}75$ м.

**, Длительность импульса 120 мкс, частота повторений 40 Гц, амплитуда тока 100 А.

*** Получена при частоте повторения 40 Гц и длительности 25 мкс.

мы возбуждения при перезарядке для Ne—Cu^+, обусловленная совпадением энергии ионов инертного газа и верхних лазерных уровней для характерных лазерных переходов, например 248,6 нм. Наблюдались семь лазерных УФ-переходов в CuII с уровней $3d^9 5s$ с длинами волн от 248,6 до 270,3 нм [44]. Интегральная мощность лазера на линиях 259,9; 260,0 и 270,3 нм составляла 350 мВт, а при работе лазера на одной линии (248,6 нм) была получена мощность 500 мВт. В случае Ne—Cu^+-лазера использовался только неон, другие буферные газы не добавлялись, чтобы не увеличивать распыление. Оптимальное давление неона составляло 12 тор. Лушвиц и другие [55] сообщили об увеличении длительности импульса излучения УФ-лазера за счет добавки 0,1% аргона к буферному газу (неону). Для линий лазера 259,1 и 260,0 нм была получена средняя выходная мощность 60 мВт (полное пропускание зеркала 2%).

Позднее Джейн [56] добился увеличения мощности УФ-излучения до 800 мВт на всех линиях. Разряд возбуждался в полом катоде желобкового типа длиной 25 см (см. рис. 8, *f*) импульсами длительностью 40 мкс при пиковом токе 40 А и частоте повторения 250 Гц. Распределение выходной мощности лазера по линиям 248,6; 252,9; 259,1 и 259,9—260,0 нм составляло 0,23; 0,11; 0,37; 0,29. Самая высокая мощность непрерывной генерации (200 мВт) достигнута Айхлером и другими [57]. Разряд возбуждался в щелевом полом катоде размером 2×6 мм (см. рис. 8, *b*) при токе 70 А с характерной пульсацией трехполупериодного выпрямления. Коэффициент усиления оценивался как 5% $м^{-1}$, и использовалось выходное зеркало с оптимальным пропусканием 3,6%. Айхлер с соавторами также сообщили о квазинепрерывной пиковой выходной мощности 0,9 Вт при возбуждении выпрямленным однополупериодным током 50 Гц. На рис. 11 показана разница между мощностью генерации в непрерывном режиме и средней мощностью при однополупериодном выпрямлении как функция от разрядного тока.

He—Ag^+-лазер. Конфигурации $4d^9nx$ и $4d^9 5s^2$ иона AgII возбуждаются в разрядах He—Ag и Ne—Ag соответственно. На рис. 12 представлены отдельные лазерные переходы и указано на совпадение верхних лазерных уровней и уровней гелия. В эту диаграмму также включены видимые и инфракрасные лазерные переходы AgII.

Излучение с длиной волны 224 нм на лазерном переходе $5d^1S_0 - 5p^1P_1^0$, полученное впервые Мак Нейлом и другими [45], является са-

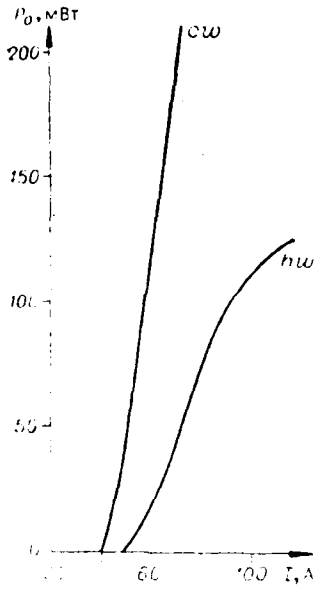

Рис. 11. Выходные мощности УФ-лазера на CuII как функция разрядного тока полого катода в непрерывном режиме (*cw*) и при возбуждении током после однополупериодного выпрямления (*hw*) [57].

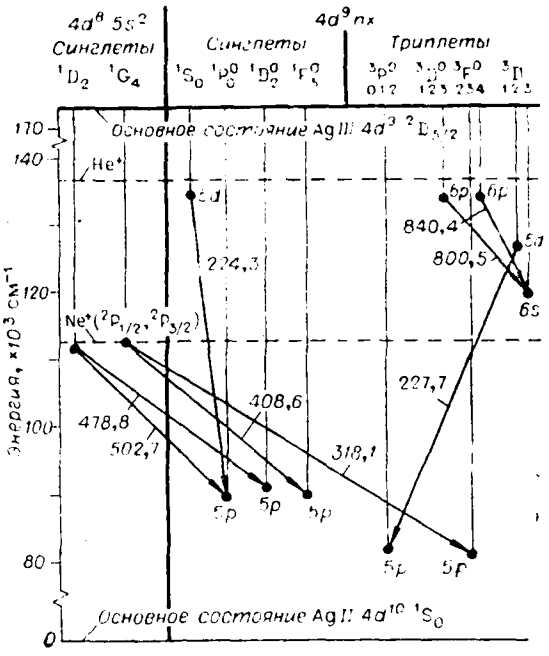

Рис. 12. Схема термов AgII.
Указаны отдельные лазерные переходы (сплошные линии) и энергии относительно основного состояния ионов неона и гелия. Длина волны дана в нанометрах.

мым коротковолновым непрерывным лазерным излучением, описанным в литературе. Порог для этого перехода составляет всего 2 А, а пиковая выходная мощность — 50 мВт при среднем значении 1 мВт [58]. Оптимальное давление He — 20 тор и Ag — 0,2 тор. На рис. 13 показано изменение выходной мощности при вариации пропускания зеркала на линии 224 нм в прямоугольном щелевом катоде длиной 25 см при импульсе тока 40 А. Значение ненасыщенного коэффициента усиления порядка 25%/м соответствует экспериментальным данным. Наиболее сильный лазерный переход AgII, согласно экспериментам Варнера и других [59], а также Соланки и других [60], на 318 нм, $4d^85s^2\,^1G_4 - 4d^9\,5p^3\,F_3^0$, дает пиковую выходную мощность на одной линии 1,3 Вт. Этот переход возбуждается при столкновениях с переносом заряда с Ne^+. Однако в экспериментах, проведенных Джейном и Ньютоном [56], установлено, что этот переход значительно слабее, чем линия 224 нм, а измеренный коэффициент усиления на $\lambda = 318$ нм — 5%/м.

He—Au$^+$-лазер. На рис. 14 показаны шесть ультрафиолетовых лазерных переходов AuII, которые наблюдались при возбуждении разряда в гелии в золотом полом катоде. Следует отметить, что все лазерные переходы AuII начинаются с энергетических уровней, близкорасположенных к основному состоянию ионов гелия. Пороговые токи для лазерных переходов $\lambda = 280$ нм составляли всего 3 А, или почти в 20 раз меньше, чем пороговые токи для лазерных УФ-переходов в лазерах на ионах инертных газов. В диапазоне 250 ÷ 290 нм наблюдалась выходная мощность на всех линиях 125 [46] и 600 мВт [58]. Джейн и Ньютон [56] получили непрерывную лазерную генерацию для щелевого катода длиной всего лишь 5 см на линии 282 нм. При длине катода 2,5 см достигалась генерация в квазинепрерывном режиме с импульсами тока длительностью 300 мкс.

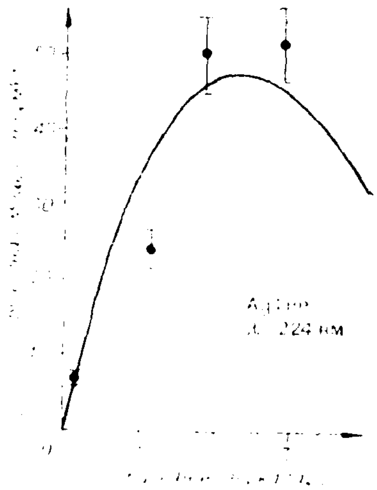

Рис. 13. Зависимость выходной мощности от пропускания зеркала для линии $\lambda = 224$ нм AgII в He—Ag лазере с полым катодом. Сплошная линия соответствует коэффициенту усиления [illegible], параметру насыщения S [illegible] Вт и [illegible] потерям резонатора 0,7 [illegible].

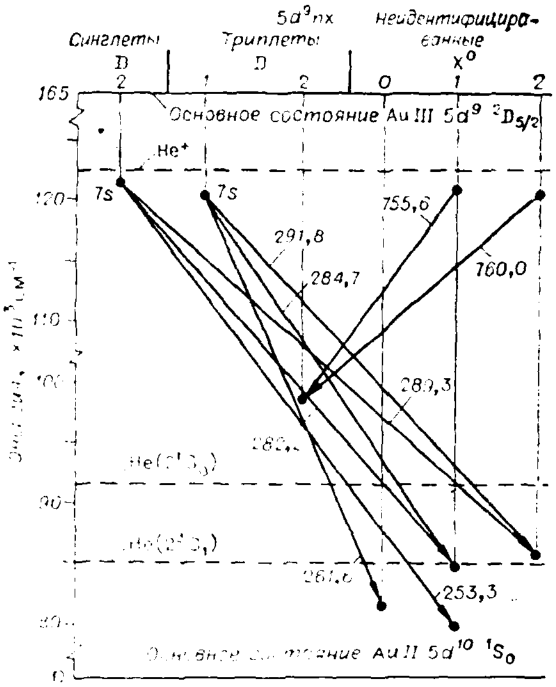

Рис. 14. Схема термов AuII с указанием отдельных лазерных переходов (сплошные линии) и энергии от основного состояния ионов гелия. Длина волн дана в нанометрах.

ВУФ-излучение сильноионизованных благородных газов. Как сообщалось выше, наиболее коротковолновое непрерывное излучение на ионных лазерных переходах (224,3 нм на AgII) получено в He—Ag-разрядах с полым катодом. Однократно ионизованные благородные газы служат наиболее мощным источником непрерывного видимого лазерного излучения. Непрерывное УФ-лазерное излучение в благородных газах в основном получают на дважды ионизованных атомах. Марлинг продемонстрировал лазерную генерацию в ВУФ-области на высокоионизованных благородных газах в импульсном режиме (200 нс) [61]. При смещении в сторону более коротких длин волн и высокозарядных ионов требуется более высокая плотность тока. Для получения лазерной генерации в области длин волн ниже 200 нм Марлинг использовал возбуждение импульсным электрическим разрядом с длительностью импульса 500 нс и пиковой плотностью тока до 14 000 А/см² в з-нитче продольного разряда. В табл. 3 приведены результаты для ВУФ-лазеров, использующих высокоионизованные благородные газы. Наиболее мощное излучение

Таблица 3

ВУФ-излучение ионных лазеров на инертных газах [61]

Измеренная длина волны в вакууме, нм(± 0,003 нм)	Ион	Порог **, А/см²	Относительная интенсивность***	Измеренная длина волны в вакууме, нм(± 0,003 нм)	Ион	Порог **, А/см²	Относительная интенсивность***
206,530 *	NeIV?	4 000	~ 50	196,808	KrIV	8000	~ 4
202,219 *	NeIV	4 500	~ 50	195,027	KrIV	7000	440
184,343	ArV?	11 000	~ 10	183,243	KrV?	9600	10
219,192 *	KrIV	6 200	600	175,641	KrIV	7800	1000
205,108 *	KrIV	7 500	3	231,536 *	NeIV?	3000	1400

* Длина волны в воздухе. Эти линии взяты для сравнения из [8].
** Порог при давлении, соответствующем максимальной мощности. При более низком давлении порог может достигать половины этой величины.
*** Интенсивность при плотности разрядного тока 11 000 А/см². Для переходов из [8] интенсивности даны в ваттах.

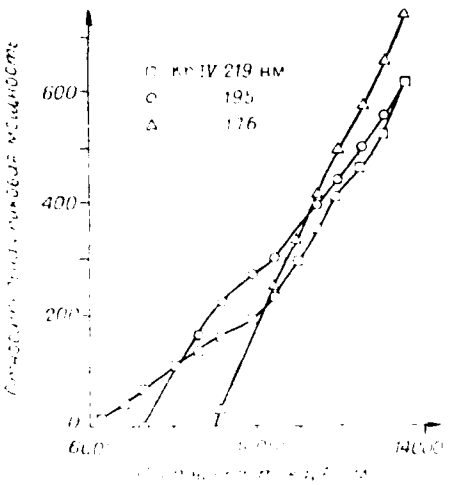

Рис. 15. Относительная пиковая мощность KrIV-лазера на переходах 176, 195 и 219 нм при изменении максимальной плотности тока возбуждения от 6000 до 14 000 А/см². Насыщение отсутствует [64].

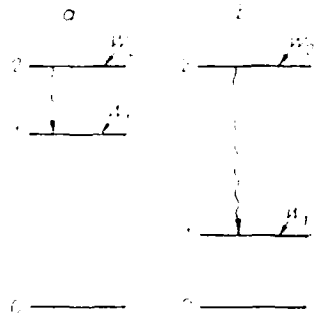

Рис. 16. Схемы уровней.
(W_1 и W_2 представляют скорости возбуждения термов в рекомбинирующей плазме.)

(0,1—1 кВт) зарегистрировано на линиях 195,0 и 175,6 нм KrIV. На рис. 15 показана относительная пиковая мощность на этих лазерных переходах как функция тока разряда. Отметим, что насыщение в данном случае отсутствует. С помощью того же метода возбуждения Марлинг нашел множество новых лазерных переходов на многозарядных ионах в области 200—250 нм [8].

Резюмируя, можно сказать, что лазерная генерация в ВУФ-области получена на нескольких высокоионизованных атомах. Однако сделать это удалось лишь при возбуждении коротким импульсом (500 нс), так как требовалась плотность тока порядка 10^5 А.

Рекомбинационные ионные лазеры. В 1963 г. Л. И. Гудзенко и *Л. А. Шелепин предположили*, что инверсия заселенностей может создаваться при рекомбинации плазмы [62]. Таким способом можно эффективно использовать энергию, накопленную в ионах плазмы для эффективного возбуждения лазерных переходов. По этому принципу возбуждения было получено излучение на нескольких УФ-лазерных переходах. В 1976 г. В. В. Жуков и др. [63] использовали экспериментальные данные о рекомбинационных лазерах, полученные за годы, прошедшие после предложения Л. И. Гудзенко и Л. А. Шелепина, для более точной формулировки требований к условиям разряда и распределению атомных и ионных активных уровней, чтобы инверсия населенностей достигалась в период рекомбинации плазмы. В. В. Жуков и другие определили общий критерий существования инверсии населенностей, который в случае больших промежутков между уровнями, в предположении, что каждая группа состоит из одного уровня, будет

$$g_1(A_1 + F_1 n_e)/g_2(A_2 + F_2 n_e) > W_1/W_2, \qquad (2)$$

где g_i, A_i, F_i, W_i — статистический вес, вероятность перехода, скорость девозбуждения электронами и полная скорость возбуждения верхнего ($i = 2$) и нижнего ($i = 1$) уровней. Авторы [63] проанализировали случаи радиационного и столкновительного режимов, как описано ниже. При низкой плотности электронов можно пренебречь членами $F_i n_e$, и инверсия устанавливается благодаря оптическим переходам. В этом случае обычно необходимо проверять, чтобы промежуток между верхним и нижним уровнями был значительно меньше промежутка между нижним и основным уровнями, поскольку такое распределение уровней дает нужное соотношение между вероятностями оптических переходов. Такие системы уровней показаны на рис. 16, *а*. Однако инверсия исчезает, когда n_e и, следовательно, скорость возбуждения при рекомбинации достаточно увеличиваются, так как в этом случае члены $F_i n_e$ и $F_2 n_e$ преобладают

и их значения возрастают при уменьшении расстояния между уровнями. При таком распределении уровней достижение высоких коэффициентов усиления и выходных мощностей в рекомбинационном режиме маловероятно, поскольку девозбуждение электронами накладывает ограничение на величину инверсии. Тем не менее, если система уровней имеет структуру, показанную на рис. 16, *b*, то девозбуждение электронами может благоприятствовать инверсии населенности. Инверсию нельзя создать путем оптических переходов, поскольку $A_{21} > A_{10}$ (благодаря тому, что $\Delta E_{21} > \Delta E_{10}$). Соотношение вероятностей переходов становится приемлемым в результате девозбуждения электронами, потому что в этом случае $F_1 n_e > F_2 n_e$. На переходах со структурой, показанной на рис. 16, *b*, при эффективном девозбуждении электронами инверсия населенностей может быть создана при высоких плотности плазмы и рекомбинационной скорости возбуждения, так что вынужденное излучение будет интенсивным, а коэффициент усиления — высоким.

Сотрудники Ростовского университета сформулировали общие требования, которые надо выполнить для достижения инверсии населенностей в рекомбинационно-столкновительных условиях, следующим образом [62]:

1) верхний лазерный уровень должен быть одним из самых низких в высшей группе близкорасположенных уровней;

2) нижний лазерный уровень должен быть одним из самых высоких в нижней группе близкорасположенных уровней;

3) разрешены переходы между уровнями;

4) плотность электронов достаточно высока, так что вероятность столкновительных переходов внутри групп превышает вероятность оптических переходов;

5) температура электронов должна быть максимально низкой.

Такие условия выполняются для перехода с $\lambda = 373{,}7$ нм в CaII в послесвечении разряда в He—Ca. В. В. Жуков и другие [64] получили среднюю выходную мощность 0,5 Вт на этой линии с помощью импульсов возбуждения с током 300 А длительностью 150 нс при частоте повторения 5 кГц в разрядной трубке диаметром 11 мм и длиной 50 см. Длительность лазерных импульсов составляла несколько микросекунд. Силваст и другие тоже получили генерацию в УФ-области в рекомбинирующей плазме в InII на длине волны 298,3 и 300,8 нм [65]. В этом эксперименте лазерная генерация была получена, когда серия сгустков плазмы испаренного металла, образованной высоковольтным импульсом в зазорах между рядом электродов, выполненных из генерирующего элемента, могла расширяться или рекомбинировать [66]. Длительность лазерных импульсов также была порядка нескольких микросекунд. Силваст и другие наблюдали генерацию лазера на переходе в AgII (ИК-диапазон) и аналогичных переходах CdIII (видимый) и InIV и продемонстрировали, что для получения генерации в рекомбинационных лазерах на более коротких длинах волн можно использовать концепцию изоэлектронной последовательности [65].

До настоящего времени в литературе нет сообщений о рекомбинационном лазере непрерывного действия в УФ-области. Причина заключается в трудности получения плазмы с высокой скоростью ионизации и низкой температурой электронов, в которой не происходит значительного возбуждения нижнего лазерного уровня из основного состояния при столкновениях с электронами. Однако Вуд и Силваст [67] сообщили только о квазинепрерывной (длительностью 1 с) генерации лазера в ИК-области на переходах CdI 1,40; 1,43; 1,44 и 1,64 мкм. Этот результат получен в дуге между двумя кадмиевыми электродами, где быстро протекал газ He для создания расширяющей плазмы.

Последние достижения и перспективы. Как было сообщено в предыдущем разделе, распределение электронов по энергии в разрядах с полым катодом имеет высокоэнергетичную составляющую (300—500 эВ). Эти высокоэнергетичные электроны могут легко ионизировать ионы бу-

ферного газа, которые заселяют верхние лазерные уровни путем реакций с тепловым переносом заряда. Схема с переносом заряда в разряде с полым катодом успешно применялась для получения лазерной генерации с низким пороговым током более чем на 10 переходах с длинами волн меньше 300 нм. Однако получение высокоэнергетичных электронов в обычном разряде с полым катодом малоэффективно.

В разряде с полым холодным катодом (ПХК) электроны в основном образуются при бомбардировке ионами поверхности катода. Затем эти электроны ускоряются благодаря катодному падению напряжения и формируются в электронный пучок. В пренебрежении ионизацией в темном пространстве ток электронного пучка, I_e связан с ионным током I_+ соотношением

$$I_e = \gamma I_+, \tag{3}$$

где γ — коэффициент вторичной эмиссии электронов. Полагая, что полный ток $I = I_e + I_+$, получаем

$$I_e = (\gamma/(1+\gamma))I. \tag{4}$$

Отсюда следует, что эффективность генерации электронного пучка R_e будет

$$R_e = I_e/I = \gamma/(1+\gamma). \tag{5}$$

При энергии налетающих на катод ионов 200—300 эВ большинство материалов имеет $\gamma \cong 0{,}1$. Следует также отметить, что большинство ионов не налетает на катод с полной энергией катодного падения eV_c, так как они претерпевают столкновения с перезарядкой. При значении $\gamma = 0{,}1$ эффективность генерации электронного пучка из (5) составляет $\eta = 0{,}09$. Недавно Рокка и другие [69] предложили и осуществили [70—74] новый способ возбуждения ионных лазеров непрерывного действия с помощью электронных пучков постоянного тока. С этой целью они разработали электронные пушки на тлеющем разряде [75—78], которые создают хорошо коллимированные электронные пучки с энергиями от 1 до 10 кэВ и током до 1,2 А. Электронные пушки на тлеющем разряде работают в гелии при давлении до 3 тор без дифференциальной откачки. Эффективность генерации электронного пучка достигала 80%. Эти результаты на порядок величины превосходят характеристики разряда с полым катодом. На рис. 17 представлена фотография свечения электронного пучка током 0,5 А, полученного с помощью электронной пушки на тлеющем разряде. С помощью лазерной установки, показанной на рис. 18, сотрудники Государственного университета в Колорадо осуществили генерацию в лазере непрерывного действия более чем на 30 переходах в инфракрасной и видимой областях спектра 7 различных однократно ионизованных атомов: Hg, I, Cd, Se, As, Zn и Kr. В лазерной установке (см. рис. 18) пучок электронов, образованный с помощью электронной пушки на тлеющем разряде, дополняется аксиальным

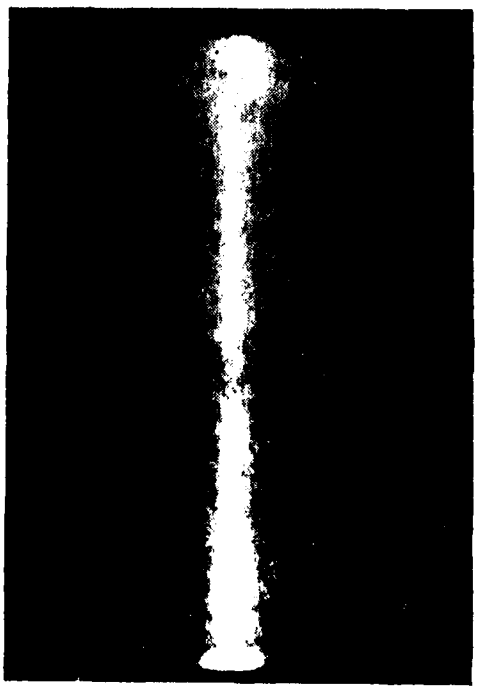

Рис. 17. Излучение от электронного пучка 0,5 А, полученного от электронной пушки на тлеющем разряде.

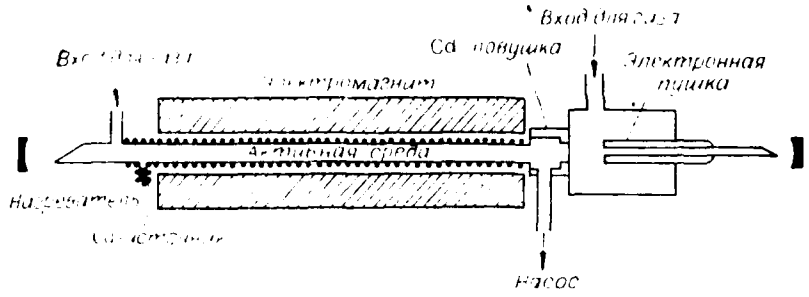

Рис. 18. Схема ионного лазера на Cd с накачкой электронным пучком [74].

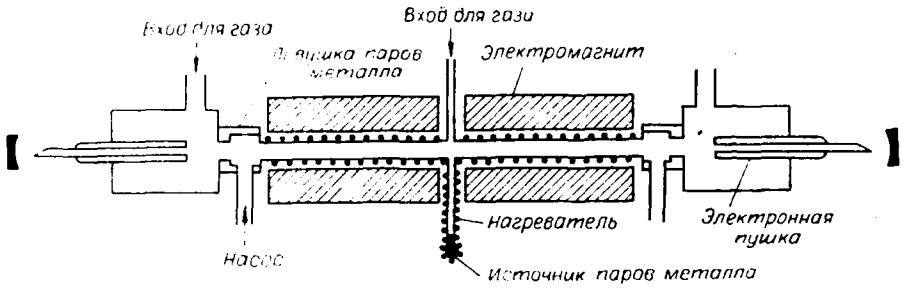

Рис. 19. Ионный лазер на парах металла, возбуждаемый двумя электронными пучками [79].

магнитным полем для эффективного поглощения мощности электронного пучка в газе. Электронные пушки обладают уникальной особенностью обеспечивать свободный оптический путь вдоль оси. Это дает возможность согласовать электронный пучок, полученный в плазменном объеме, с соответствующим объемом оптического резонатора. Конфигурация лазера на рис. 19 аналогична конфигурации на рис. 18, но в этом случае использованы две противоположно направленные пушки, что позволяет увеличить мощность электронного пучка, поглощенную в единице объема, а также дает более однородную плазму. На данной установке Рокка и другие получили мощность непрерывного лазера 1,2 Вт на переходах ZnII с $\lambda = 491{,}2$ и 492,4 нм, возбуждая He—Zn-смесь, и мощность 0,25 Вт на переходе HgII с $\lambda = 614{,}9$ нм в случае He—Hg-смеси [79]. Эта мощность более чем на порядок выше мощностей, полученных с помощью лазеров с полым катодом или в положительном столбе. Рокка с сотрудниками также впервые получили непрерывную лазерную генерацию в видимом диапазоне мощностью >1 Вт на ионах паров металла. На рис. 20 показано изменение мощности лазера на 614,9 нм при изменении параметров разряда, в котором генерируется электронный пучок.

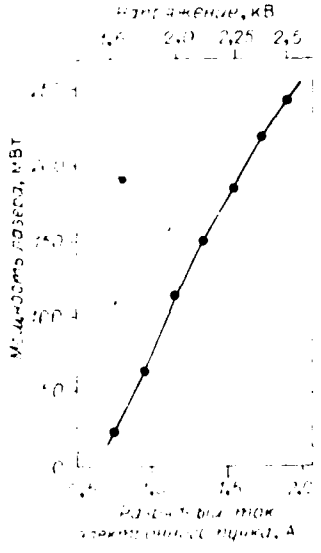

Рис. 20. Выходная мощность лазера на переходе 614,9 нм HgII как функция разрядного тока и напряжения в генераторе электронного пучка:
среднее давление гелия в активной среде 1,5 тор, магнитное поле 3,2 кГс, температура резервуара с Hg 120°C [79].

До сих пор мы стремились продемонстрировать преимущества этой новой схемы возбуждения в системах с перезарядкой, работающих в видимом диапазоне спектра. Можно ожидать, что подобные преимущества будут реализованы и для УФ-перехода, в системах типа Ne—Cu и He—Ag это составит одну из целей будущей работы.

С помощью систем с перезарядкой при возбуждении электронным пучком можно создать высокоэффективные непрерывные УФ-лазеры при условии, что:

а) большая часть мощности разряда (до 80%) идет на образование электронов пучка высокой энергии;

б) электроны пучка эффективно создают ионы благородного газа;

в) большая часть энергии, накопленной в ионах инертного газа, может селективно передаваться на верхние лазерные уровни посредством тепловой перезарядки с очень большим поперечным сечением ($>10^{-15}$ см^2);

г) системы типа $Ne—Cu^+$ и $He—Ag^+$ имеют большую квантовую эффективность (24 и 20% соответственно) для переходов в области спектра $\lambda \approx 250{,}0$ нм.

Упрощенный расчет показывает, что для систем с перезарядкой при непрерывной накачке электронным пучком ожидается эффективность порядка 1%.

Заключение. Двухзарядные ионы инертного газа являются в настоящее время наиболее мощным источником когерентного излучения в ультрафиолетовой области спектра. При одновременной генерации на двух линиях ArIII 351,1 и 363,8 нм достигнута выходная непрерывная мощность 61 Вт. Получена лазерная генерация в ВУФ-области на многозарядных ионах инертного газа, но лишь в импульсном режиме. Использование разряда в полом катоде в смеси паров металла и инертного газа позволило расширить спектральный диапазон, в котором получена непрерывная генерация, в коротковолновую сторону и понизить пороговый ток. Верхние лазерные уровни ионов металла в этих лазерах селективно возбуждались в реакциях перезарядки с ионами инертного газа. В настоящее время самой коротковолновой линией непрерывного ультрафиолетового лазера является $\lambda = 224{,}2$ нм AgII-лазера, найденная в смеси He—Ag в разряде с распыляющимся полым катодом.

Генерация в УФ-области может быть получена также на ионах в рекомбинирующей плазме, но в настоящее время только в импульсном режиме. Применение электронного пучка постоянного тока позволяет увеличить более чем на порядок максимальную выходную мощность в лазерах на парах металла с перезарядкой. Ожидается, что этот новый механизм возбуждения даст возможность увеличить мощность и эффективность ультрафиолетовых ионных лазеров на парах металла и расширить их диапазон до вакуумного ультрафиолета.

ЛИТЕРАТУРА

1. **Paananen R.**— Appl. Phys. Lett., 1966, vol. 9, p. 3—4.
2. **Fendler J. R., Jr.**— IEEE J. Quant. Electron., 1968, vol. QE-4, p. 627.
3. **Banse K., Herzimger G., Schäfer G., Seelig W.**— Phys. Lett., 1968, vol. A27, p. 682.
4. **Latimer I. D.**— Appl. Phys. Lett., 1968, vol. 13, p. 333.
5. **Bridges W. B., Mercer G. N.** Ultraviolet ion laser. Rep ECOM 0229F, Hughes Res. Lab., Malibu, California, 1969 (unpublished). Available from N. T. I. S., Assession Number AD 861927.
6. **Tio T. K., Luo H. H., Lin S. C.**— Appl. Phys. Lett., 1976, vol. 29, p. 795.
7. **Lüthi H. R., Seelig W., Steinger J.**— Appl. Phys. Lett., 1977, vol. 31, p. 670.
8. **Marling J. B.**— IEEE J. Quant. Electron., 1975, vol. QE-11, p. 822.
9. **Silfvast W. T.**— Appl. Phys. Lett., 1969, vol. 15, p. 23.
10. **Goldsborough J. P.**— IEEE J. Quant. Electron., 1969, vol. QE-5, p. 133.
11. **Goldsborough J. P.** Appl. Phys. Lett., 1969, vol. 15, p. 159.
12. **Silfvast W. T.** Appl. Phys. Lett., 1968, vol. 13, p. 169.
13. **Collins G. J., Jensen R. C., Bennett W. R., Jr.**— Appl. Phys. Lett., 1971, vol. 19, p. 125.
14. **Webb C. E., Turner-Smith A. R., Green J. M.**— J. Phys. B, 1970, vol. 3, p. 4135.
15. **Schaerer L. D., Padovani F. A.**— J. Chem. Phys., 1970, vol. 52, p. 1618.
16. **Silfvast W. T.** - Phys. Rev. Lett., 1971, vol. 27, p. 1489.
17. **Wang S. C., Siegman A. E.**— Appl. Phys. Lett., 1973, vol. 2, p. 143.
18. **Алейников В. С., Ушаков В. В.** — Опт. и спектр., 1970, т. 29, с. 211.
19. **Mori M., Murayama M., Goto T., Hattoni S.**— IEEE J. Quant. Electron., 1978, vol. QE-14, p. 427.

20. **Goto T., Hane K., Hattori S.**— J. Phys. D: Appl. Phys., 1981, vol. 14, p. 587.
21. **Goto T., Kawahara A., Collins G. J., Hattori S.**— J. Appl. Phys., 1971, vol. 42, p. 3816.
22. **Willett C. S.** *Introduction to gas lasers: population inversion mechanisms.*— Oxford: Pergamon Press, 1974.
23. **Fetzer G., Rocca J. J., Collins G. J.**— Fort Collins, Colorado: Colorado State University (unpublished).
24. **Gill P., Webb C. E.**— J. Phys. D., 1977, vol. 10, p. 299.
25. **Peterson L. R.**— Phys. Rev., 1965, vol. 187, p. 105.
26. **Heavenes O. S., Willett C. S.**— Z. Ang. Math. Phys., 1965, vol. 16, p. 87—88.
27. **Карабут Е. К., Михалевский В. С., Папкин В. Ф., Сэм М. Ф.**— ЖТФ, 1970, т. 14, с. 1447—1448.
28. **Csillag L., Janossy M., Rosa V., Salamon T.**— Phys. Lett. A, 1974, vol. 50, p. 13—14.
29. **Schuebel W. K.**— IEEE J. Quant. Electron., 1970, QE-6, p. 574—575.
30. **Duffendack O. S., Smith H. L.**— Nature, 1927, vol. 119, p. 743—744.
31. **Duffendack O. S., Black J. G.**— Science, 1927, vol. 66, p. 401—402.
32. **Duffendack O. S., Black J. G.**— Phys. Rev., 1929, vol. 34, p. 35—43.
33. **Duffendack O. S., Henshaw C., Goyer M.**— Phys. Rev., 1929, vol. 34, p. 1132—1137.
34. **Duffendack O. S., Thomson K.**— Phys. Rev., 1933, vol. 43, p. 106—111.
35. **Manley J. H., Duffendack O. S.**— Phys. Rev., 1935, vol. 47, p. 56—61.
36. **Duffendack O. S., Gran W. H.**— Phys. Rev., 1937, vol. 51, p. 804—809.
37. **Takahashi Y.**— *Ann. Phys.*, 1929, vol. 3, p. 49—57.
38. **Fowles G. R., Jensen R. C.**— Proc. IEEE, 1964, vol. 52, p. 851—852.
39. **Fowles G. R., Silfvast W. T.**— Appl. Phys. Lett., 1965, vol. 6, p. 236—237.
40. **Silfvast W. T., Fowles G. R., Hopkins B. D.**— Appl. Phys. Lett., 1966, vol. 8, p. 318—319.
41. **Sugawara Y., Tokiwa Y.**— Jap. J. Appl. Phys., 1970, vol. 9, p. 588—589.
42. **Schuebel W. K.**— Appl. Phys. Lett., 1970, vol. 16, p. 470—472.
43. **Jensen R. C., Collins G. J., Bennett W. R., Jr.**— Appl. Phys. Lett., 1971, vol. 18, p. 50.
44. **McNeil J. R., Collins G. J., Persson K. B., Franzen D. L.**— Appl. Phys. Lett., 1975, vol. 27, p. 595.
45. **McNeil J. R., Johnson W. L., Collins G. J., Persson K. B.**— Appl. Phys. Lett., 1976, vol. 29, p. 172. For a discussion of unidentified Ag II lines see: **Reid R. D., Gerstenberger D. C., McNeil J. R., Collins G. J.**— J. Appl. Phys. Lett., 1977, vol. 48, p. 3994.
46. **Reid R. D., McNeil J. R., Collins G. J.**— Appl. Phys. Lett., 1976, vol. 29, p. 666.
47. **Laegrid N., Wehner G. K.**— J. Appl. Phys., 1961, vol. 32, p. 365—369.
48. **De Hoog F. J., McNeil J. R., Collins G. J., Persson K. B.** Discharge studies of the Ne—Cu *laser.*— *J. Appl. Phys., 1977, vol. 48, p. 3701—3704.*
49. **Чеботаев В. П.** Об одном режиме работы оптического квантового генератора на смеси гелий — неон.— Радиотехника и электроника, 1965, т. 10, с. 372—374.
50. **Smith J.** Optical maser action in the negative glow region of a cold cathode glow discharge.— J. Appl. Phys., 1964, vol. 35, p. 723—724.
51. **Byer R. B., Bell W. E., Hodges E., Bloom A. L.** Laser emission in ionized mercury: Isotope shift, linewidth and precise wavelength.— JOSA, 1965, vol. 55, p. 1598—1602.
52. **Weider H., Myers R. A., Fischer C. L., Powell C. G., Columbo J.** Fabrication of wide bore hollow cathode Hg+ lasers.— Rev. Sci. Instrum., 1967, vol. 38i, p. 1538—1540.
53. **Piper J. A., Webb C. E.** A hollow cathode system for CW helium — metal vapor laser system.— J. Phys. D, 1973, vol. 6, p. 400—407.
54. **Eichler H. J., Wittwer W.**— J. Appl. Phys., 1980, vol. 51, p. 80—83; **Eichler H. J., Koch H. J., Salk J., Schafer G.**— IEEE J. Quant. Electron., 1979, vol. QE-15, p. 908—912; **Eichler H. J., Koch H., Paffenholz J., Salk J., Skrobol C.**— J. Phys., 1979, vol. 7, p. 379—380.
55. **Auschwitz B., Eichler H. J., Wittwer W.**— Appl. Phys. Lett., 1980, vol. 36, p. 805.
56. **Jain K., Newton S. A.**— Appl. Phys. B, 1981, vol. 26, p. 43.
57. **Eichler H., Koch H., Molt R., Qiu J. L.**— Appl. Phys. B, 1981, vol. 26, p. 49.
58. **Jain K.**— Appl. Phys. Lett., 1979, vol. 34, p. 398; IEEE J. Quant. Electron., 1980, vol. QE-16, p. 120.
59. **Warner B. E., Gerstenberger D. C., Reid R. D., McNeil J. R., Solanki R., Persson K. B., Collins G. J.**— IEEE J. Quant. Electron., 1978, vol. QE-14, p. 568.
60. **Solanki R., Fairbank W. M., Jr., Collins G. J.**— IEEE J. Quant. Electron., 1980, vol. QE-16, p. 1292.
61. **Marling J. B., Lang D. B.**— Appl. Phys. Lett., 1977, vol. 31, p. 181.
62. **Гудзенко Л. И., Шелепин Л. А.**— ЖЭТФ, 1964, т. 18, с. 998.
63. **Жуков В. В., Латуш Е. Л., Михалевский В. С., Сэм М. Ф.**— Квантовая электроника, 1977, т. 4, с. 1249.
64. **Жуков В. В., Кучеров В. С., Латуш Е. Л., Сэм М. Ф.**— Квантовая электроника, 1977, т. 4, с. 1257.
65. **Silfvast W. T., Szeto L. H., Wood O. R., II.**— Appl. Phys. Lett., [illegible], p. 212.
66. **Silfvast W. T., Szeto L. H., Wood O. R., II.**— Appl. Phys. Lett., 1980, vol. 36, p. [illegible]
67. **Silfvast W. T., Wood O. R., II, Macklin J. J.**— Appl. Phys. Lett., 1983, vol. 42, p. [illegible]
68. **Carter G., Colligon J. S.** Ion bombardment of solids.— N. Y., Elsevier, 1968.
69. **Rocca J. J., Meyer J. D., Collins G. J.**— Phys. Lett., 198[illegible], vol. 87A, p. 237; Roc-

ca J. J., Meyer J. D., Yu Z., Collins G. J. Electron beam excitation of CW lasers.— In: 34th Gaseous Electronic Conference. Boston, Massachusetts, October 1981.
70. Rocca J. J., Meyer J. D., Collins G. J. Zn II and CW laser transitions excited by an electron beam. - IEEE J. Quant. Electron., 1982, vol. QE-18, p. 1052.
71. Rocca J. J., Meyer J. D., Collins G. J. Electron beam pumped CW Se II laser.— Opt. Comm., 1982, vol. 42, p. 125.
72. Rocca J. J., Meyer J. D., Collins G. J. Electron beam pumped CW Hg ion laser.— Appl. Phys. Lett., 1982, vol. 40, p. 300.
73. Meyer J. D., Rocca J. J., Yu Z., Collins G. J. CW iodine ion lasers excited by an electron beam. - IEEE J. Quant. Electron., 1982, vol. QE-18, p. 326.
74. Rocca J. J., Meyer J. D., Collins G. J. CW laser oscillations in Cd II in an electron beam created plasma.— Phys. Lett., 1982, vol. 90A, p. 358.
75. Rocca J. J., Meyer J. D., Collins G. J. Hollow cathode electron guns for the excitation of CW lasers.— Phys. Lett., 1982, vol. 87A, p. 237.
76. Rocca J. J., Meyer J. D., Yu Z., Farrell M., Collins G. J. Multikilowatt electron beams for pumping CW ion lasers.— Appl. Phys. Lett., 1982, vol. 41, p. 811.
77. Yu Z., Rocca J. J., Meyer J. D., Collins G. J. Transverse electron guns for plasma excitation — J. Appl. Phys., 1982, vol. 53, p. 4704.
78. Yu Z., Rocca J. J., Collins G. J. Studies of a glow discharge electron beam.— J. Appl. Phys., 1983, vol. 54, p. 131.
79. Rocca J. J., Meyer J. D., Collins G. J. 1 watt CW Zn II laser (to be published).
80. Gerstenberger D. C., Solanki R., Collins G. J.— IEEE J. Quant. Electron., 1980, vol. QE-16, p. 8202.

Поступила в редакцию 28 апреля 1983 г.

УДК 621.378.3

И. Г. ИВАНОВ

(Ростов на Дону)

ИОННЫЕ ЛАЗЕРЫ НА ПАРАХ МЕТАЛЛОВ С ПОПЕРЕЧНЫМИ ТИПАМИ РАЗРЯДА

Введение. В данном обзоре рассматриваются лазеры, относящиеся к бурно развивающемуся в последние годы подклассу обширного класса газоразрядных лазеров на парах металлов [1]. Использование продольного (тлеющего или дугового) разряда для возбуждения переходов в атомарных ионах позволило значительно расширить набор длин волн, генерируемых лазерами на парах металлов в видимой, ультрафиолетовой и ближней инфракрасной областях спектра в импульсном и, что особенно важно, в непрерывном режимах излучения. Однако ограниченность числа эффективных и пригодных для практики лазеров с продольным разрядом стимулировала поиск других более эффективных способов возбуждения и новых ионных переходов. Результатом таких работ и явилось создание лазеров с поперечными типами разряда — разрядом в полом катоде (РПК) и поперечным высокочастотным разрядом (ПВЧР). Возбуждение активной среды (как правило, смеси буферного инертного газа и паров металла) осуществляется в таком лазере в электрическом поле, направление которого перпендикулярно оптической оси лазера, и происходит для лазеров с РПК в слабоионизованной плазме отрицательного свечения, а для лазеров с ПВЧР в области, по свойствам близкой к отрицательному свечению (ОС). Последнее и определяет сходство характеристик этих двух типов разряда и выходных параметров лазеров, их использующих.

Впервые генерация в лазере с РПК получена на атомарных переходах в ионе Ar^+ [2], однако затем было установлено, что поперечный разряд более эффективен именно для ионных переходов. К настоящему времени генерация в лазерах с РПК и ПВЧР наблюдалась более чем для 260 линиях 21 иона. Первыми металлами, чьи пары использовались в лазерах, были Hg, Cd и Zn [3—11], затем число металлов достигло

18, а число лазерных переходов в них — 239 и было найдено, что возбуждение в ОС наиболее эффективно происходит для тех ионных переходов паров металлов, верхние уровни которых заселяются ударами 2-го рода при столкновениях атомов металла с ионами или возбужденными атомами инертного газа (реакции перезарядки и пеннинг-процесс соответственно).

Исследования ионных лазеров на парах металлов с поперечным разрядом существенно расширили набор длин волн излучения газоразрядных лазеров в наиболее важных для практики областях спектра — видимой и УФ, с мощностью излучения на отдельных линиях до 1 Вт в непрерывном и импульсно-периодическом режимах; привели к созданию сравнительно простых по конструкции непрерывных лазеров милливаттного уровня мощности генерации на УФ-линиях в диапазоне длин волн 0,22—0,32 мкм. Кроме того, в лазере данного типа получено излучение трех основных цветов — синего, зеленого и красного, дающих белый свет. Излучая на линиях атомарных ионов, эти лазеры обладают узкими линиями генерации (порядка 10^3—10^9 Гц), а также имеют весьма низкий уровень шумов излучения, связанный с возбуждением их активных сред в ОС разряда [12, 13].

Ниже приведены основные результаты исследований лазеров с РПК и ПВЧР, работающих как в непрерывном и квазинепрерывном режимах, так и в режиме возбуждения микросекундными импульсами; рассмотрены особенности возбуждения и способы создания паров металла; описаны конструкции активных элементов лазеров. Основное внимание, однако, уделено энергетическим характеристикам выходного излучения.

1. Лазеры с разрядом в полом катоде. Поиск активных сред для лазеров на парах металлов сопровождался непрерывным поиском наиболее эффективного для каждого металла способа создания необходимого давления его паров. В табл. 1 для каждого металла, на ионных переходах которого наблюдалась генерация в лазерах с РПК, приведена температура, соответствующая давлению насыщающих паров 0,1 тор, оптимальному для большинства лазеров с поперечными типами разряда [1].

Для таких веществ, как Hg, Cd, Zn, I, Se, As, Tl и т. д., в большинстве экспериментов использовался наиболее простой метод — испарение (вполпка) вещества при его нагреве [3, 4, 6—32]. Для Cu, Ag, Au, Al, Ni, Sn, рабочие температуры которых превышают 1100°С, а также для Pb наиболее простым оказалось изготовление катода из рабочего вещества лазера и применение катодного распыления [5, 6, 33—47]. Снижение рабочей температуры достигалось также подбором химического соединения, в состав которого входят атомы данного металла и имеющего меньшую температуру испарения, с последующей диссоциацией этого соединения в разряде [26, 48].

В табл. 2 для лазеров с РПК приведены диапазон длин волн и число ионных линий генерации различных металлов. Отметим, что генерация в РПК наблюдалась также на ионных переходах аргона, криптона и ксенона [1], но ее характеристики (удельная мощность излучения, ненасыщенный коэффициент усиления и другие) значительно уступают характеристикам лучших лазеров на парах металлов. Генерация, за исключением четырех переходов в кадмии и цинке, происходит только в смеси буферный инертный газ — пары металла. Это связано с тем, что буферный газ выполняет несколько функций. Во-первых, возбуждение подавляющего большинства переходов осуществляется в процессе передачи энергии и заряда атомам металла от ионов газа, т. е. путем так называемой перезонансной перезарядки. Остальные же переходы — 325

Таблица 1

Температура (°С), соответствующая давлению паров 0,1 тор

Металл	Hg	Cd	Zn	I	Se	As	Tl	Ga	Be	Ca	Sr	Cu	Ag	Au	Al	Ni	Sn	Pb
Температура	82	220	408	12	287	317	706	1180	1360	690	620	1419	1163	1574	1293	1255	1412	837

CW Laser Action in Atomic Fluorine

J. J. ROCCA, J. D. MEYER, B. G. PIHLSTROM, AND G. J. COLLINS

Abstract—**We have obtained CW laser action on four transitions in the doublet system of atomic fluorine for the first time. All previously reported laser action was on a pulsed basis only. CW laser radiation was obtained when F_2 or AgF was used as a fluorine donor in an electron beam pumped helium plasma. A multiline output power of 200 mW was obtained.**

SEVERAL authors [1]-[6] have previously reported pulsed laser action in atomic fluorine. Kovacs and Ultree [1] obtained 1-2 μs laser pulses on the 7037.5, 7127.9, and 7202.4 Å lines of atomic fluorine in either CF_4, SF_6, or C_2F_6 and helium mixtures. The lower laser levels ($3s^2P$) are relatively depopulated via allowed resonant transitions and they concluded that radiation trapping of the lower level via reabsorption of the 955 and 956 Å resonant radiation limited the laser pulse length. Jeffers and Wiswall [2] obtained quasi-CW laser pulses, 20 μs long, in a He-HF discharge. They reported that the trapping of the resonant radiation was not a limiting factor in their experiment due to the existence of a second lower laser level de-excitation process involving the atomic H produced in the dissociation of HF via the reaction $F(3s^2P) + H(n = 1) \rightarrow F(2p^5\ ^2P^o) + H(n = 5) + \Delta E$. However, their laser operated in the afterglow of the discharge pulse, precluding CW operation. More recently, Crane and Verdeyen [3] reported 80 μs long laser pulses using a hollow cathode discharge. In this case the premature termination of the laser pulse with respect to the excitation pulse was suggested to be due to the depletion of the fluorine donor.

We report CW laser action on the 7037.5, 7127.9, 7202.4, and 7800.2 Å laser transitions of atomic fluorine using a dc electron beam to excite either He-F_2 or He-AgF gas mixtures. The laser setup empolyed in this experiment was similar to the

Manuscript received November 21, 1983, revised February 9, 1984. This work was supported by the National Science Foundation and is part of a joint project between Colorado State University and Spectra Physics, Mountain View, CA.

The authors are with the Department of Electrical Engineering, Colorado State University, Fort Collins, CO 80523.

0018-9197/84/0600-0625$01.00

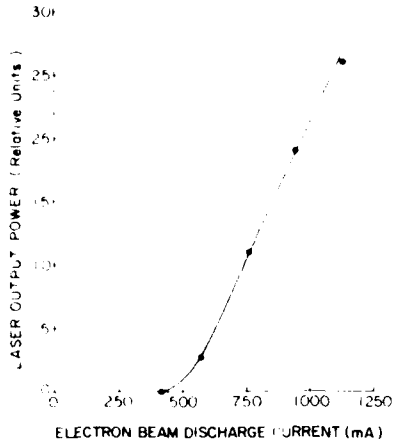

Fig. 1. Multiline laser output power of the red atomic fluorine laser transitions as a function of electron beam discharge current. He and F_2 partial pressures 1.9 torr and 35 mtorr, respectively. Axial magnetic field 3.2 kG.

one we previously used to obtain CW laser action in several singly ionized species, and has been described in previous publications [7]. A multiline CW output power of 200 mW was obtained in a He-F_2 gas mixture at partial pressures of 1.9 torr and 35 mtorr, respectively. This maximum output power was obtained at an electron beam discharge current of 1.2 A, an electron beam energy of 2 keV, and with an axial magnetic field of 3.2 kG. The magnetic field was used to help confine the electron beam in the active region. Fig. 1 shows the variation of the laser output power with electron beam discharge current in a He-F_2 mixture. CW laser action was also obtained using AgF as a fluorine donor, when a reservoir containing AgF connected to the plasma tube was heated above 500°C. Laser action was obtained when helium was used as a buffer gas, as it was in all the cases in which pulsed laser action was previously reported [1]-[6]. When neon was used as a buffer gas, laser action was not obtained. However, the addition of only 50 mtorr of He to a 0.3 torr Ne buffer gas discharge resulted in CW fluorine laser oscillation. This indicates that helium plays an important role in the excitation mechanism of the upper laser levels.

Observation of the laser output with a 0.5 m spectrometer showed that oscillation can occur at two frequencies displaced with respect to the line center of the atomic spontaneous emission. Fig. 2 shows the spectrum of the 7127.9 Å laser line for three partial pressures of F_2. This splitting of the laser lines is attributed to very different velocity distributions of the atomic fluorine in the upper ($3p^2P$) and lower ($3s^2P$) levels. The velocity distribution of the upper laser levels can be substantially broadened if these levels are excited by a process with an energy surplus, in which the energy difference is balanced by a gain in the kinetic energy of the atoms involved. The velocity distribution of the atoms in the lower laser levels is narrower as a result of the imprisonment of resonant radiation and subsequent lengthening of the effective lifetime. When the pressure of F_2 is reduced, the density of atomic fluorine in the ground state decreases and the trapping of the resonant radiation becomes less severe, increasing the gain at line center,

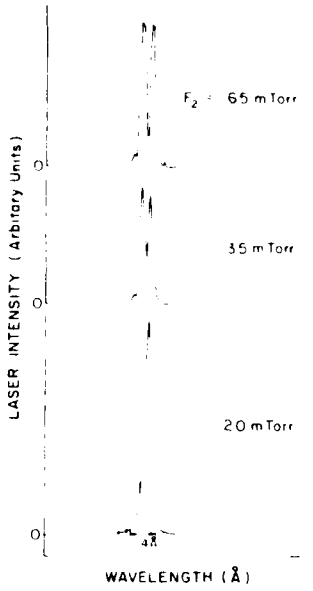

Fig. 2. Spectrum of the 7127.9 Å laser output for three F_2 partial pressures. Helium balance to a total average pressure of 1.9 torr.

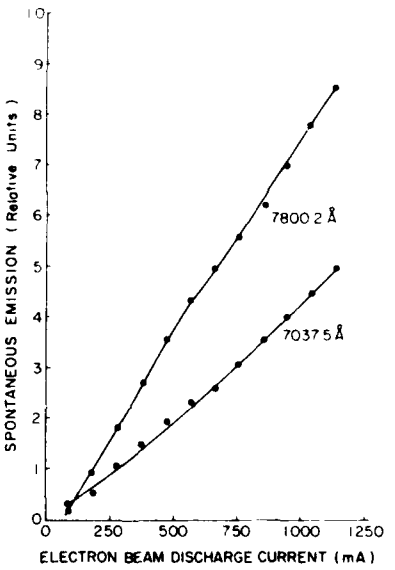

Fig. 3. Variation of the spontaneous emission of the 7037.5 and 7800.2 Å atomic fluorine laser transitions as a function of electron beam discharge current. He and F_2 partial pressures 1.9 torr and 35 mtorr, respectively.

in agreement with Fig. 2. This characteristic of the spectral distribution of the laser light has been previously observed in the 8446 Å Ar-O_2 laser [8]-[10]. In this laser, the velocity distribution of the atoms in the $3p^3P^o_{1,2}$ levels is broadened due to excitation involving collisions of the second kind between O_2 and Ar* which have surplus energy. The gain profile is also split as a consequence of radiation trapping which occurs at line center on the strong resonant line at 1300 Å connecting the lower laser level with O I ground state.

Fig. 3 shows the variation of the spontaneous emission of two laser transitions as a function of the electron beam discharge current. The spontaneous emission shows a linear

dependence on the current as does the laser output power, indicating an excitation mechanism requiring a single electron collision. The dissociative excitation processes indicated in reactions (1) and (2), in which the helium metastable is assumed to be pumped by direct electron impact (3), are "single step" mechanisms

$$He(2^3S) + F_2 \rightarrow F^* + F + He(1s) + \Delta E \quad (1)$$

$$He(2^3S) + AgF \rightarrow F^* + Ag + He(1s) + \Delta E \quad (2)$$

$$e^- + He(1s) \rightarrow He(2^3S) + e^- \quad (3)$$

Reactions (1) and (2) have a surplus energy ΔE of 3.7 and 1.6 eV, respectively. Notice that in dissociative excitation a close energetic resonance discrepancy is not required for efficient transfer [11]. For example, the energy discrepancy in the dissociative collision of Ar* and O_2 in the atomic oxygen laser operating at 8446 Å is 2 eV [12], [13]. This excess energy must, however, be carried off as kinetic energy by the products of the reaction. This super thermal velocity distribution is consistent with the split line profile of the laser lines observed experimentally. The helium excited state is indicated as the 2^3S state because this is the most abundantly populated level in an electron beam excited negative glow helium discharge [14]. The $He(2^1S)$ metastable is efficiently destroyed by superelastic collisions with electrons and is converted to the $He(2^3S)$ metastable. However, this and other excited states of helium can also contribute to (1) and (2). Notice that the metastable atoms of Ne do not have enough energy to satisfy (2). This also consistent with our experimental observation that no laser action is obtained with Ne as a buffer gas.

Another possible excitation mechanism involving helium metastable levels is

$$He(2^3S) + F_2 \rightarrow F^+ + F + He(1s) + e^- \quad (4)$$

followed by three-body electron recombination

$$F^+ + 2e^- \rightarrow F^* + e^- \quad (5)$$

This mechanism, however, would not cause a difference in the velocity distribution of the laser levels since in (4) most of the excess energy would be taken by the resulting electron.

Other possible mechanisms exciting the upper laser levels are two-body ion–ion recombination reactions such as

$$He^+ + F^- \rightarrow F^* + He + \Delta E \quad (6)$$

$$He^+ + F^- \rightarrow F^+ + He + e^- + \Delta E \quad (7)$$

$$He^+ + F_2^- \rightarrow F^+ + He + e^- + \Delta E \quad (8)$$

where (7) and (8) are followed by three-body electron recombination. Miller and Morgner [11] predict large cross sections for (6) and (7). Notice, however, that this process requires at least two electrons to create the reactant ions since one electron is required in the dissociative attachment (or attachment) process and another in ionizing He. Consequently, it is not consistent with our observation of a linear increase in the spontaneous emission with current. Reactions of negative fluorine ions with Ne ions would also be allowed from an energetic point of view.

Reaction (1) seems to be the most likely excitation mechanism of the He–F_2 laser. The production rate of metastable atoms in our electron beam discharge has been calculated to be sufficient to provide the needed pumping rate, through (1), for the measured 0.2 W laser output power. However, when Ar was added to the plasma with a 2 torr He–F_2 mixture in an Ar:F_2 proportion of up to 4:1, with the purpose of quenching the helium metastables, the electron beam current necessary to achieve the threshold for laser action increased by only 20 percent. This is not sufficient, however, to rule out (1) as the major excitation mechanism since the cross section for quenching helium metastables by F_2, which is not available in the literature, could be several times larger than the one corresponding to He*–Ar collisions, which is 5.3 Å^2 [15]. For example, the cross section for quenching $He(2^3S)$ by SF_6 was measured to be 20.6 Å^2 [15]. Clearly, a more detailed study is necessary to determine the dominant excitation mechanisms of the CW electron beam pumped fluorine laser.

Finally, we observed CW laser action on the 8446 Å line of atomic oxygen exciting a He–O_2 mixture with a dc electron beam in the same experimental setup. CW laser action was also obtained when the electron beam was used to excite pure oxygen gas. The output power on this transition was, however, only 1 mW using totally reflecting mirrors.

Summarizing, we have obtained CW laser action on the red lines of atomic fluorine for the first time. This was obtained using F_2 or AgF as a fluorine donor in an electron beam excited helium plasma. A collisional excitation reaction with an energy surplus populates the upper laser level, causing a difference in the velocity distribution of the atoms in the upper and lower laser levels. This avoids the self-termination of the laser output caused by trapping of the lower state resonant radiation observed in previous studies. Direct current electron beams are thereby demonstrated to be a suitable method to excite CW atomic lasers.

References

[1] M. A. Kovacs and C. J. Ultee "Visible laser action in fluorine I," *Appl. Phys. Lett.*, vol. 17, pp. 39–40, 1970.

[2] W. Q. Jeffers and C. L. Wiswall, "Laser action in atomic fluorine based on collisional dissociation of HF," *Appl. Phys. Lett.*, vol. 17, pp. 444–447, 1970.

[3] J. K. Crane and J. T. Verdeyen, "The hollow cathode helium fluorine laser," *J. Appl. Phys.*, vol. 51, pp. 123–129, 1980.

[4] L. J. Bigio and R. T. Begley, "High-power visible laser action in neutral atomic fluorine," *Appl. Phys. Lett.*, vol. 28, pp. 263–264, 1976.

[5] T. R. Loree and R. C. Sze, "The atomic fluorine laser: Spectral pressure dependence," *Opt. Commun.*, vol. 21, pp. 255–257, 1977.

[6] J. L. Lawler, J. W. Parker, L. W. Anderson, and W. A. Fitzsimmons, "Experimental investigation of the atomic fluorine laser," *IEEE J. Quantum Electron.*, vol. QE-15, pp. 609–613, 1979.

[7] J. J. Rocca, J. D. Meyer, and G. J. Collins, "1-W Zn ion laser," *Appl. Phys. Lett.*, vol. 43, pp. 37–39, 1983; see also and J. J. Rocca, J. D. Meyer, G. Letzer, Z. Yu, and G. J. Collins, Conf. Lasers Electro-Optics, Baltimore, MD, May 1983.

[8] S. G. Rautian and P. L. Rubin, "On some features of gas lasers containing mixtures of oxygen and rare gas," *Opt. Spectrosc.*, vol. 18, pp. 180–181, 1965.

[9] L. N. Tunitskii and E. M. Cherkasov, "Pulse mode generation in an argon-oxygen laser," *Opt. Spectrosc.*, vol. 26, pp. 344–346, 1969.

[10] [illegible], "The mechanism of laser action in oxygen-inert gas mixtures," *Opt. Spectrosc.*, vol. 18, pp. 154–157, 1967.

[11] W. A. Miller and H. Morgner, "A unified treatment in penning ionization and excitation transfer," *J. Chem. Phys.*, vol. 67, pp. 4923–4930, 1977.

[12] C. Wilett, *Introduction to Gas Lasers. Population Inversion Mechanisms.* Oxford, England: Pergamon, 1974.

[13] W. R. Bennett, W. L. Faust, R. A. McFarlane, and C. K. N. Patel, "Dissociative excitation transfer and optical laser oscillation in Ne-O_2 and Ar-O_2 rf discharges," *Phys. Rev. Lett.*, vol. 8, pp. 470–473, 1962.

[14] J. J. Rocca, "Electron beam pumping of cw ion lasers," Ph.D dissertation, Colorado State University, Fort Collins, CO, 1983; see also J. R. McNeil, "New sputtered metal vapor laser systems," Ph.D. dissertation, Colorado State University, Fort Collins, CO, 1977.

[15] A. L. Schmeltekopf and F. C. Fehsenfeld, "De-excitation rate constants for helium metastable atoms with several atoms and molecules," *J. Chem. Phys.*, vol. 53, pp. 3173–3177, 1970.

Glow-discharge-created electron beams: Cathode materials, electron gun designs, and technological applications

J. J. Rocca, J. D. Meyer, M. R. Farrell, and G. J. Collins
Department of Electrical Engineering, Colorado State University, Fort Collins, Colorado 80523

(Received 21 July 1983; accepted for publication 4 October 1983)

The operating characteristics of glow-discharge-created electron beams are discussed. Ten different cathode materials are compared with regard to maximum electron beam current achieved and the beam generation efficiency as measured calorimetrically. Specific electron gun designs are presented for a variety of applications that include: cw ion laser excitation; electron beam assisted chemical vapor deposition of microelectronic films; and wide area annealing of ion-implantation damage to silicon substrates. The use of sintered metal-ceramic (e.g., Mo-Al_2O_3) cathodes to generate multikilowatt electron beams in a pure noble gas discharge is reported. Cathode materials with high secondary electron emission coefficients by ion bombardment allow for electron beam production in glow discharges at 50%–80% generation efficiency values.

I. INTRODUCTION

The most common way of producing high voltage direct current electron beams involves thermionic electron emission and subsequent acceleration at background pressures below 10^{-4} Torr. Consequently, the use of complex differential pumping systems is usually required in any attempt to inject this vacuum generated electron beam into an experimental chamber containing gases at pressures in excess of 1 Torr.

This paper summarizes our work in direct plasma generation of kilovolt electron beams in a 10^{-1} to 3.0-Torr ambient using a glow discharge and secondary electron emission from a cold cathode. In the past, glow discharge electron beams have been used in material processing, welding, melting, and heat treatment. This previous work was discussed by Dugdale[1] and Boring[2] as well as by Hurley.[3] More recently, new technologies such as the excitation[4–8] of cw ion lasers, the deposition of thin microelectronic films,[9] and electron beam annealing of ion-implantation damage[10] have also required direct current electron beams operating in ambient pressures of 1 Torr. In this paper we present glow discharge electron guns designed especially for these three new purposes as well as electron beam discharge *I-V* characteristics as a function of pressure and electron beam generation efficiency. Different cathode materials are compared and the use of sintered refractory metal-ceramic oxide cathode materials is reported. Finally, we briefly discuss new applications of glow discharge electron beams.

II. GLOW DISCHARGE ELECTRON GUNS AND THEIR OPERATION

Glow discharge electron guns can be divided into two groups: "hollow cathode" or internal plasma electron generation types and "front face emission" or secondary electron emission types. Figure 1(a) shows a hollow cathode glow discharge electron gun which we have designed for the excitation of cw lasers.[11] In this type of electron gun, the plasma that develops inside the hollow cathode acts as a source of electrons for the electron beam. Electrons emitted by the internal walls of the cathode (following bombardment by ions, fast neutrals, and photons) are accelerated through an internal voltage drop of several hundred volts. These electrons are electrostatically trapped inside the hollow cathode and lose most of their energy in exciting and ionizing collisions that sustain the internal plasma. The majority of the discharge voltage drop, however, occurs in the external cathode dark space region shown in Fig. 1(a). This external dark space presents a voltage drop of several kilovolts to the electrons which emerge from the hollow cathode plasma, thereby forming the electron beam. Hollow cathode electron guns have two modes of operation. One mode is a high impedance one in which the electron beam is produced, and the other is a low impedance mode where no electron beam is produced. Operation in the beam mode occurs over a limited range of current and pressure.[11,12] When these two parameters are

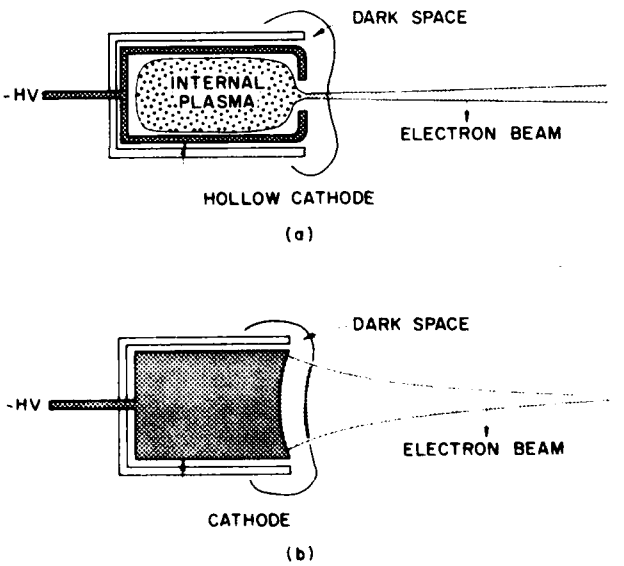

FIG. 1. Schematic repesentation of glow discharge electron guns. (a) Hollow cathode electron gun. (b) Front face secondary emission cold cathode electron gun.

 0021-8979/84/150790-08$02.40

not properly chosen the extenal dark space vanishes, production of the electron beam ceases, and the discharge then operates in the low impedance mode. In this mode the cathode operates as a regular hollow cathode,[13] where the voltage drop is a few hundred volts and a positive column occupies the distance between electrodes. This low impedance mode of operation prevents electron beam production. Instabilities in the discharge can switch the discharge from the electron beam mode to the low impedance mode, and this is undesirable for stable operation of the electron gun. We briefly discuss below hollow cathode electron guns operating in the 10^{-2}- to 1-Torr pressure region.

The pressure P, at which a hollow cathode electron gun will operate in the high impedance, electron beam mode, is determined by the internal cathode diameter D. Consequently, the scaling gas discharge law $PD = C$ can be used to guide the design of these electron guns,[12] where C is a constant dependent upon both the nature of the gas and the cathode surface. Using a 4.7-mm cathode hole diameter, we were able to operate hollow cathode electron guns in the beam mode at pressures up to 1.4 Torr in helium and 0.4 Torr in argon. We obtained electron beam generation at the 1-kW power level at beam currents up to 0.1 A.[11] We also obtained "sheet electron beams" 20-cm long and several millimeters wide by operating a transverse hollow cathode electron gun.[12] Beam generation efficiencies of 50%–70% are typical for solid wall hollow cathode guns.[11] It is noteworthy that perforated wall hollow cathode guns have also been successfully operated.[14,15] The cathode wall in this latter case is constructed of metallic mesh. These mesh electron guns are very simple; however, their operating efficiency is considerably lower, typically 20% to 30%. We will emphasize in the remainder of this paper "front face secondary emission" electron guns. Such devices can operate at higher pressures and provide larger electron beam currents with higher operating efficiency. For a more complete discussion of hollow cathode electron guns, see Refs. 2, 11, and 12.

Figure 1(b) shows a "front face secondary emission" type of electron gun. In this case, electron emission from the cathode wall is produced following bombardment of the cathode surface both by ions and by fast neutrals created by resonant charge transfer in the cathode sheath. The secondary electrons produced at the cathode surface are accelerated along the electric field lines through the cathode dark space to form a well-collimated electron beam. This is clearly shown in Fig. 2 where the electron-beam-created plasma is visible. The cathode face was made concave to focus the electron beam electrostatically. To confine the emission to the cathode front face, all other cathode surfaces were shielded. In contrast with hollow cathode electron guns, secondary emission electron guns present only one mode of operation and, hence, represent a considerable practical advantage for stable electron beam production. Secondary emission electron guns can operate at slightly higher pressures (0.1–3 Torr) than the hollow cathode guns. Operation at even higher pressures is also possible, however, the electron beam becomes poorly collimated as the gas density increases.

A cathode material with a high secondary electron emission coefficient by ion bombardment γ is required for efficient electron production using cold cathodes. Cathodes with a low sputtering yield are also required for prolonged cathode lifetime. In the next section we compare the results of beam generation using various cathode materials. The best cathode materials possess both a high secondary emision coefficient and a low sputtering yield.

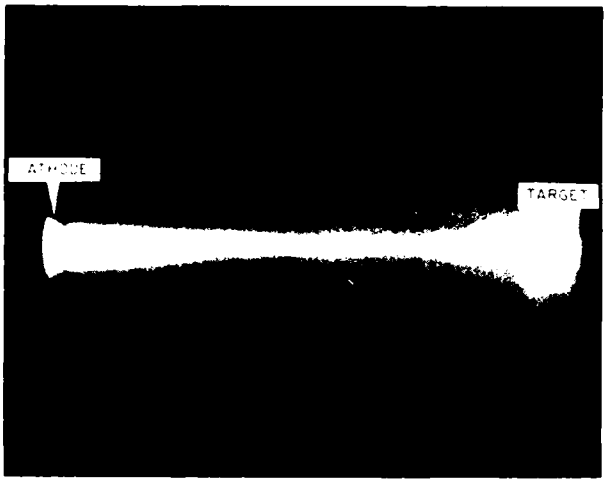

FIG. 2. Electron beam plasma formed by a front face secondary emission electron gun.

III. EFFECT OF CATHODE MATERIALS ON BEAM GENERATION

We constructed cathodes of 10 different materials. Each cathode was 3.1 cm in diameter with a 6-cm radius of curvature concave front face. The cathodes were surrounded by an insulating ceramic tube to confine the emission solely to the cathode front face. The distance between the cathode shield and the cathode was approximately 1 mm.

Table I lists the cathode materials tested, the maximum electron beam discharge current obtained, and the relative sputtering erosion of that cathode material. Cathode sputtering was evaluated only qualitatively by comparing the state of the cathode surface before and after a discharge and by observing the spontaneous emission from cathode material species in the glow discharge just in front of the cathode. In the case of materials with a high sputtering yield, the characteristic spectral lies of the cathode materials are strong in the emission spectrum while low sputtering yield cathode materials had weak spectra. The first five materials listed in Table I are both good sources of secondary electrons and at the same time have a low sputtering yield. Consequently, they are judged to be good cathode materials. Well-collimated multikilowatt dc electron beams have been obtained with all five of these cathodes. Graphite has the lowest sputtering yield but a low secondary electron emission coefficient, γ, and can be used when small (0.1 A) electron beam discharge currents are sufficient. The last five materials listed in Table I are considered poor glow discharge cathode materials. For example, copper beryllium has a high secondary electron emission coefficient by ion bombardment ($\gamma = 2$ for 3-keV ions),[16] but unfortunately a high sputtering rate of cathode materials is observed. Thus, while it is possi-

TABLE I. Characteristics of glow discharge electron gun cathode materials.

Cathode material	Composition	Maximum current (A) (3.1-cm-diam cathode)	Sputtering
1. Aluminum	coated with a thin oxide layer	1.2	low
2. Magnesium	coated with a thin oxide layer	1.2	low
3. Lanthanum hexaborate		0.8	acceptable
4. Sintered Molybdenum-Al_2O_3	50-50% by weight	1.0	acceptable
5. Sintered Molybdenum-MgO	50-50% by weight	0.6	acceptable
6. Graphite		0.1	low
7. Copper		0.05	very high
8. Copper-beryllium	98-2%	0.05	very high
9. Stainless steel		0.05	high
10. Molybdenum		0.05	high

ble to increase the current of the glow discharge, the rapid destruction of the cathode is enhanced by sputtering. Even at small discharge currents, a green cloud is visually observed in the vicinity of the cathode. Current values below 0.05 A for the maximum discharge current in Table I have little significance because a well-defined electron beam is not observed. Similar behavior is observed when stainless steel and molybdenum are used as cathode materials. These materials are also poor electron emitters following ion bombardment. Again, in both cases it is possible to observe with the eye a distinctive colored emission characteristic of the sputtered cathode material.

Next, we will discuss in more detail the characteristics of electron beam production with the five cathode materials considered practical. These will be discussed in three groups: aluminum and magnesium; lanthanum hexaborate; and sintered ceramic-metal composites.

A. Aluminum and magnesium cathodes with oxide coatings

Both aluminum and magnesium have strongly adherent native oxide layers. When covered by a thin oxide layer these cathode materials are excellent emitters of secondary electrons by ion bombardment, possessing a secondary emission coefficient nearly 10 times greater than that of the pure metals. These oxide coatings are also highly resistant to sputtering. However, when operated in a pure noble gas atmosphere at high current densities (100 mA/cm^2), energetic ions and neutral atoms which impinge on the cathode surface soon sputter off the native oxide layer. When this coating is removed, the secondary electron emissivity of the cathode drops nearly an order of magnitude and the material of the cathode itself starts to rapidly sputter into the discharge. This transition can be seen by the eye as a change of color in the light emitted from the discharge region close to the cathode. It is possible, however, to maintain a stable oxide layer by adding a few millitorr of O_2 into the discharge. In this way, the cathode oxide layer is continuously restored via plasma-induced oxidation and we observed no change in the emission characteristics after 10 h of operation at high (100 mA/cm^2) current densities. The I-V characteristics of the electron beam glow discharge with an aluminum cathode 3.1 cm in diameter covered by a thin Al_2O_3 film are shown in Fig. 3(a) with He pressure as a parameter. This figure shows generation of electron beam discharge currents over 1 A (cathode current density >0.15 A/cm^2) and that discharge powers up to 5 kW have been obtained. This figure also shows that the impedance of the electron beam glow discharge is significantly reduced when an axial magnetic field (1–4 kG) is applied in the electron beam drift region. The magnetic field increases the plasma density, and subsequently, the ion flux to the cathode, thereby enhancing secondary electron emission from the cathode and lowering the discharge impedance.

We performed calorimetric measurements to determine the efficiency at which the electron beam is generated. A copper calorimeter was situated 13 cm from the cathode emitting surface. The calorimeter was supported only by a thin wall stainless-steel tube of poor heat conductance to ensure good thermal insulation. The temperature of the calorimeter was continuously measured with a thermocouple and its variation with time plotted with an x-t chart recorder. The discharge current I and voltage V of the glow discharge were also monitored and recorded. The efficiency E_f, with which beam electrons are generated by the electron gun was then calculated as

$$E_f = \frac{\frac{dT}{dt} MC(T)}{IV},$$

where M is the mass of the calorimeter and $C(T)$ is the specific heat of copper. The results of these measurements for an electron gun with an aluminum cathode in a He ambient (with 20 mTorr of O_2) are shown in Fig. 3(b). The electron

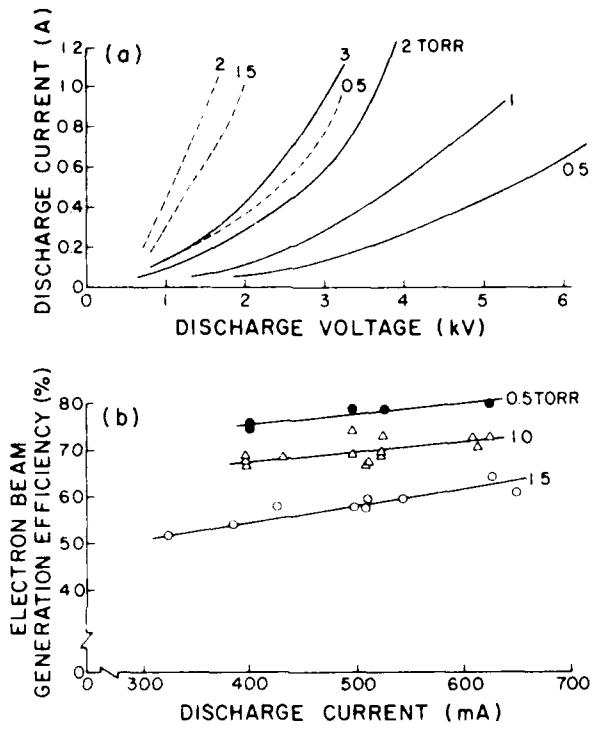

FIG. 3. (a) V-I characteristics of the aluminum cathode electron-beam discharge in helium with 20 mTorr of oxygen added to the discharge chamber. Solid line: without magnetic field. Dashed line: operating the electron gun 1.3 cm from a solenoid producing a magnetic field of 3.2 kG. Fringing field at the cathode front face 40 G. (b) Electron-beam generation efficiency as a function of discharge current for an aluminum cathode. The He pressure in Torr is shown. 20 mTorr of oxygen was also added to the discharge chamber.

beam generation efficiency is observed to increase as the total pressure decreases and as the cathode current increases. This is attributed to the increase of the secondary emission coefficient as a function of the energy of the impinging ions.[17] The energy of these ions and associated fast neutrals, created by charge transfer, increases with the discharge voltage.[18] A maximum electron beam generation efficiency of 80% was measured at 0.5 Torr of helium and a beam current of 0.65 A.

Magnesium covered with a thin oxide layer is also an excellent emitter of secondary electrons following ion bombardment. As in the case of aluminum, the oxide has a low sputtering yield. Again, if the cathode is to be continuously operated in pure noble gas environments at a high current density (0.1 A/cm^2), then a few millitorr of O_2 is needed to compensate for erosion of the cathode oxide layer. We discovered that electron guns with magnesium cathodes create glow discharges with lower impedance than the ones obtained with aluminum cathodes of the same geometry. We have obtained electron beam discharge currents of 1.2 A at an energy of 1.5 keV by operating a Mg electron gun with a 3.1-cm-diam cathode in 1 Torr of helium with 10 mTorr of oxygen.

We have previously measured the energy spectrum of the transmitted electron beam, created by a magnesium cathode coated with a thin oxide layer, using an electrostatic energy analyzer.[19] Electron beam energy distributions were measured at pressures between 0.15 and 0.8 Torr, currents between 60 and 700 mA, and discharge voltages between 1 and 2.5 kV. The glow-discharge-generated electron beams have an energy width at half-maximum of 100–300 eV.[19] The energy width was observed to decrease for all pressures as the current was incremented. Also, at certain pressure-current conditions the electron beam energy profile was observed to degrade abruptly into a broad distribution. This change was coincident with the sudden appearance of a plasma region with a very intense luminosity and with the emission of intense microwave radiation. This phenomena was attributed to the generation of plasma oscillations driven by the electron beam and is treated in more detail elsewhere.[19]

B. Lathanum hexaborate

LaB_6 has been used in the past as a thermionic emitter.[20] We have used LaB_6 as a cold cathode in glow discharge electron guns. We observed that after exposure to the ambient atmosphere lathanum hexaborate is a good electron emitter by ion bombardment alone. However, after operation in a pure noble gas atmophere, an increasing voltage was needed to maintain a constant current. When a small amount of O_2 (20 mTorr) was introduced into the discharge the cathode rapidly recovered its electron emission. A thin oxide coating is, as in the case of Al and Mg cathodes previously discussed, apparently of fundamental importance in providing a high secondary electron emission coefficient, γ. The I-V characteristics of a 3.1-cm-diam LaB_6 cathode operating in a helium atmosphere with 20 mTorr of O_2 are shown in Fig. 4(a). Well-collimated electron beam glow discharges with discharge currents up to 0.8 A have been obtained. Calorimetric measurements of the electron beam production efficiency are shown in Fig. 4(b). They indicate that electron beam generation efficiencies up to 70% are obtainable with LaB_6 cathodes in a helium atmosphere with a 20-mTorr partial pressure of oxygen.

C. Sintered ceramic-metal cathodes

The need for O_2 in the plasma to achieve prolonged operation of Al, Mg, and LaB_6 cathodes can be undesirable in some applications. For example, if the electron guns are to be used for laser excitation, the presence of oxygen in the laser active medium can in some cases interfere with the laser excitation mechanisms. We have therefore developed cathode materials which can operate in a pure noble gas atmosphere without the need of a partial pressure of oxygen.

The materials are obtained by hot press sinterization of molybdenum and aluminum oxide or molybdenum and magnesium oxide particles 10 μm in diameter. This ceramic-metal composite has unique cathode properties. The oxide particles have a high secondary electron emission coefficient while the molybdenum particles make the material a good conductor of electricity enabling dc operation of the electron beam. We experimented with several different ratios by weight of Mo to oxide particles to find the optimum proportions for beam generation. We found that in the case of Mo-MgO, equal portions by weight worked well. This is equiva-

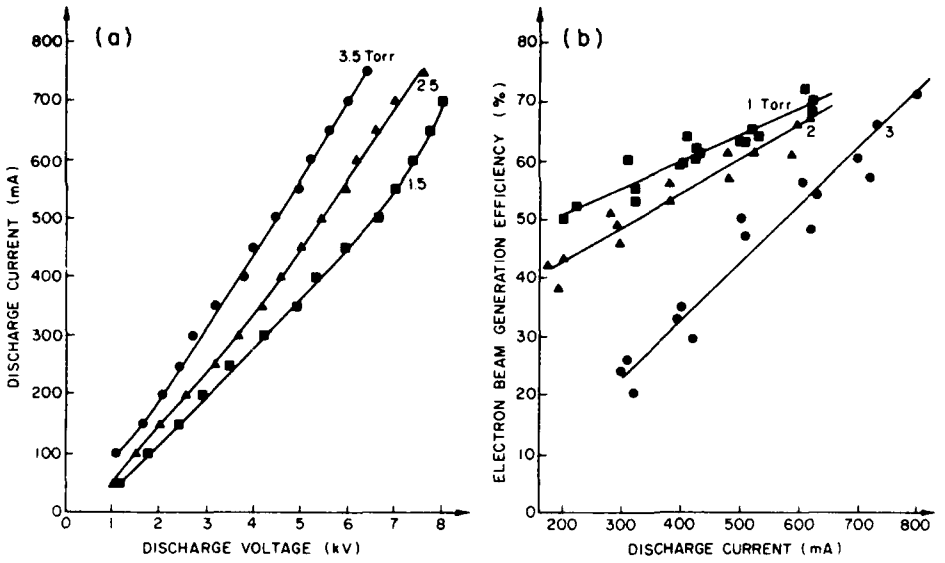

FIG. 4. (a) *V-I* characteristics of the helium glow discharge obtained using a 3.1-cm-diam, 6-cm-radius-of-curvature lanthanum hexaborate cathode. 20 mTorr of oxygen was added to the discharge chamber. (b) Electron-beam generation efficiency as a function of discharge current for the lanthanum hexaborate electron gun. The He pressure is in Torr. 20 mTorr of oxygen was added to the discharge.

lent to approximately 74% MgO and 26% Mo by volume. Consequently, the ions bombarding the cathode surface mostly impinge on the oxide particles, allowing for efficienct electron beam production. Increasing the amount of MgO results in an undesirable decrease of the electrical conductivity of the cathode preventing dc operation. In the Mo–Al_2O_3 sintered mixtures, equal portions by weight of 10-μm-diam particles give good results as cathode material. Figures 5(a) and 5(b) show the *V-I* characteristics and electron beam production efficiency of a glow discharge using a 3.1-cm-diam Mo–MgO cathode operating in helium. These figures show that electron beam discharge powers of 3 kW and discharge currents up to 0.6 A have been obtained with these electron guns at efficiencies up to 75%. Figure 6(a) shows the *V-I* characteristics of a discharge using Mo–Al_2O_3 cathode, also 3.1 cm in diameter. In this case the maximum discharge current obtained was 1 A. The electron beam generation efficiencies as a function of current with helium pressure as parameter are shown in Fig. 6(b). Beam generation efficiencies up to 75% were demonstrated.

In summary, both sintered ceramic-metal mixtures constitute good cathode materials, producing multikilowatt elecron beams in a pure helium atmosphere at efficiencies up to 75%. The MgO–Mo cathode fractured after a 0.6-A discharge, probably due to a poor thermal shock resistance. This prohibited tests at higher currents and explains why the maximum current obtained with the MgO–Mo cathode was smaller than with the Al_2O_3–Mo cathode.

IV. GLOW DISCHARGE ELECTRON GUN GEOMETRIES

Electron beams of tailored geometries can be realized with front face secondary emission glow discharge electron guns. The geometry of the cathode face largely determines the shape of the resulting electron beam. However, as discussed previously, the cathode material needs to have a high secondary electron emission coefficient by ion bombardment for efficient electron beam generation and a low sputtering yield for prolonged lifetime. If a multikilowatt dc electron beam is desired on a continuous basis, the cathode must be water cooled. Usually we make the water-cooled body of the cathode out of copper, and press fit the selected cathode material into this cooled section. This two-piece construction allows for efficient cooling of the porous cathodes made of sintered materials. The entire cathode is completely surrounded by an insulating shield that confines the secondary emission to the unshielded cathode surface. The distance between the insulating shield and the cathode is approximately 1 mm and is always less than an electron collision mean free path. A grounded metallic shield has also been used.

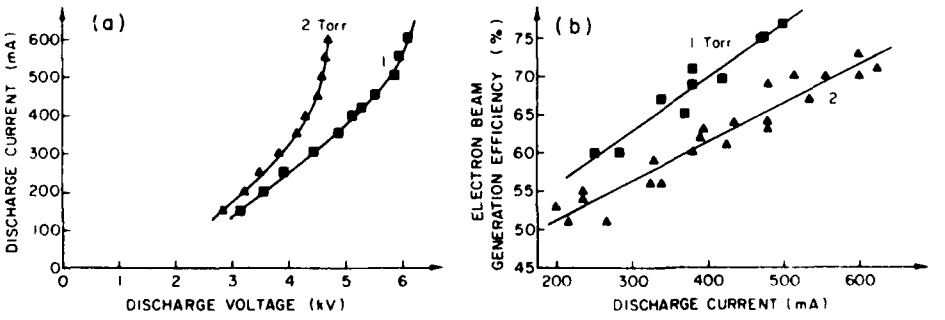

FIG. 5. (a) *V-I* characteristics of the helium glow discharge obtained using a sintered MgO (50% by weight)—Mo concave cathode 3.1 cm in diameter and with a 6-cm radius of curvature. (b) Electron beam generation efficiency as a function of discharge current for the sintered MgO–Mo electron gun

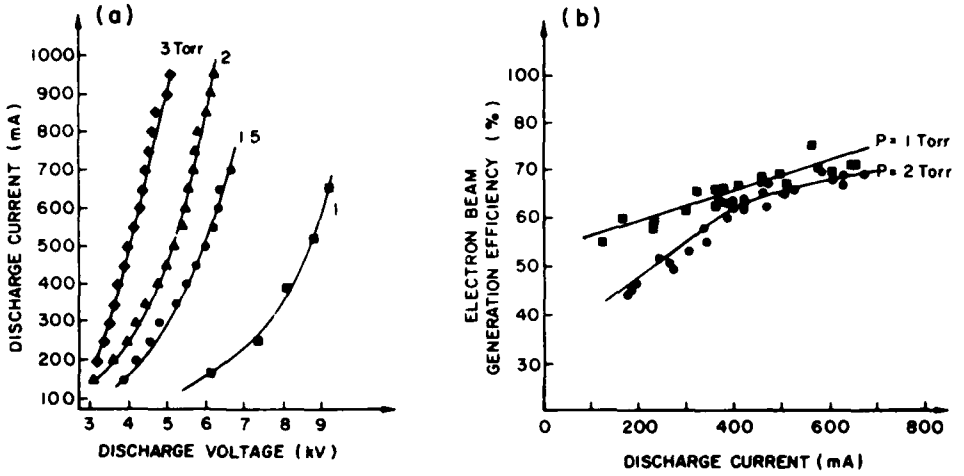

FIG. 6. (a) *V-I* characteristics of the helium glow discharge obtained using a sintered Al_2O_3 (50% by weight)—Mo concave cathode 3.1 cm in diameter with a 6-cm radius of curvature. (b) Electron beam generation efficiency as a function of discharge current for the sintered Al_2O_3—Mo electron gun.

The primary application of glow discharge electron guns in our work has been in the excitation of cw ion lasers. Figure 7 shows the structure of an electron gun developed for this purpose. The electron gun geometry (doughnut-like) provides a clear 0.5-cm-diam optical path throughout the axis. This permits one to easily match the electron-beam-created plasma volume with the volume of an optical resonator. To confine the emission to the cathode front face only, the rest of the cathode walls are shielded. Specifically, a ceramic tube (99.8% Al_2O_3) covers the external cathode walls and a quartz tube shields the inner cathode walls. The cathode was made of aluminum 3.1 cm in diameter and was operated in a helium atmosphere which contained approximately 20 mTorr of O_2. The rest of the cathode was made of copper and was water cooled for adequate heat dissipation at multikilowatt dc operating conditions. The cathode front face was made concave to focus the electron beam as shown in Fig. 1(b). We have used both 6 and 9 cm as a radius of curvature. Similar electron guns with cathodes made of sintered metal-ceramic materials described in Sec. III were also successfully used to excite cw ion lasers. The position of the anode is not important so we usually use the stainless-steel vacuum chamber in which the electron gun operates as the anode. The use of this electron gun design in exciting cw lasers is discussed further in Sec. V of this paper.

Figure 8 shows a broad area (7.5 cm in diameter) electron gun constructed for the purpose of electron beam annealing of ion-implanted silicon wafers. The cathode was made of a sintered Mo–MgO mixture of equal portions by weight. The cathode was supported by an aluminum piece which was not water cooled in this case as only short electron beam operating times (60 sec) were required for this application. The broad area cathode was surrounded by a quartz shield which confined the emission to the front face. Discharge currents up to 700 mA and discharge powers of 3 kW (70 W/cm^2) were easily obtained. The *I-V* characteristics of this electron gun operating in helium are shown in Ref. 10.

Figure 9 shows the structure of an electron gun designed to produce a line source 5-cm long and approximately 2-mm wide at the focal plane. This electron gun has been used for both annealing silicon wafers as well as recrystallizing polysilicon films. The geometry of this electron gun is similar to the transverse hollow cathode electron gun for plasma excitation described in Ref. 12; the main difference being that the cathode shown in Fig. 9 is slotless. Notice that the operation of this electron gun is similar to the electron guns previously described, except for the geometry, and consequently does not need further discussion.

V. APPLICATIONS OF GLOW DISCHARGE ELECTRON GUNS

A. Excitation of cw ion lasers

We have used the electron guns described in Sec. II and IV to excite helium-metal-vapor gas mixtures and obtain cw

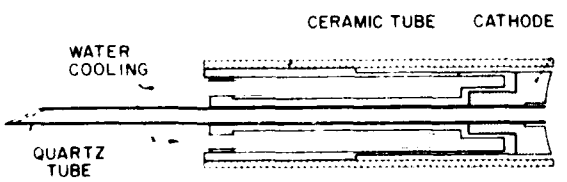

FIG. 7. Structure of the glow discharge electron gun for longitudinal laser excitation.

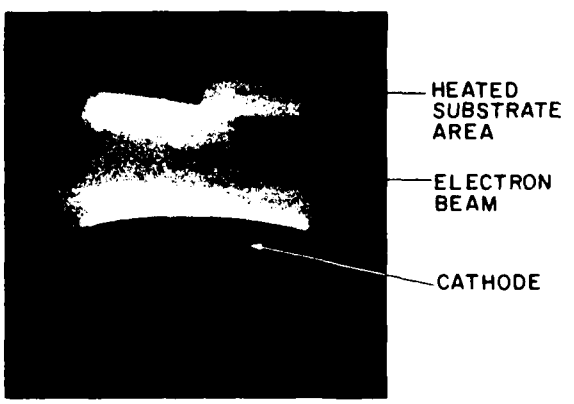

FIG. 8. Experimental setup used to anneal *n*-type silicon wafers implanted with 30-keV boron ions to a total dose of 5×10^{15} ions/cm^2.

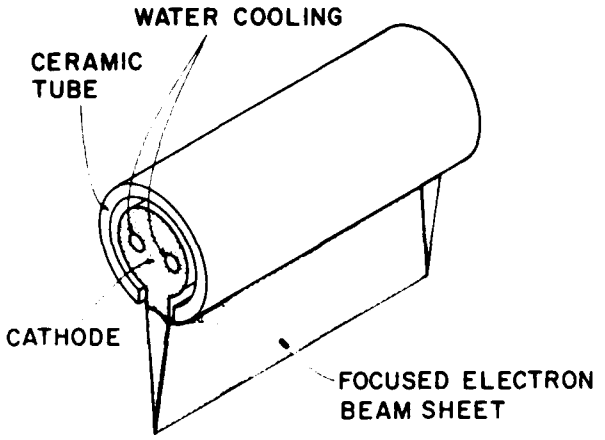

Fig. 9. Structure of an electron gun designed to produce an electron sheath 5-cm long and approximately 2-mm wide at the focal plane. This sheath geometry is used for annealing silicon wafers and recrystallizing polysilicon wafers.

laser action in seven different singly ionized metallic species.[4–8] We successfully used both, oxide-coated aluminum cathodes[21] and sintered metal-ceramic cathodes. In the first case we introduced 10–20 mTorr of oxygen into the gas mixture, to allow stable electron emission over prolonged periods of time. In all seven laser media, the presence of the oxygen impurity did not affect the laser output power in a measurable way. The axial path of the electron guns allows for an easy overlap of the electron-beam-created plasma with the volume of the optical resonator as show in Fig. 10. The excitation scheme shown in this figure uses two electron guns that produce two counter propagating electron beams. The electron beams are kept collimated along the 1-m-long plasma tube by use of an axial magnetic field of 1–4 kG. Using this electron beam excitation scheme we have obtained cw laser radiation on more than 40 ion transitions.[22] A cw laser power output of 1.2 W, for example, was obtained on the 4911.6 and 4924.0-Å transitions of Zn II. This repesents an order of magnitude increase in the laser output power and efficiency previously obtained for these metal vapor transitions using hollow cathode discharges.[23]

In summary, electron beam pumping is a new way to excite ion lasers that has the potential of increasing both the operating efficiency of these devices as well as the output power.[23]

B. Large area glow discharge electron beam annealing of ion-implantation damage

We have thermally annealed ion-implant damage in silicon wafers using a broad area (7.5 cm in diameter) glow discharge electron gun. This allowed for irradiation of an entire 3-in. (7.5-cm) wafer without beam or wafer scanning as did previous investigators.[24] An electron beam power of up to 3 kW at a current of 0.7 A was created using a magnesium oxide-molybdenum cathode. The electron beam was produced in helium at a pressure between 0.1 and 2 Torr. The experimental setup shown in Fig. 8 was used to anneal *n*-type silicon wafers implanted with 30-keV boron ions to a total dose of 5×10^{15} ions/cm^2. Samples were isochronally annealed for 15 sec at different electron beam power densities and the change in sheet resistivity was measured. The reduction of sheet resistivity exhibited a threshold of 160 J/cm^2 and reached 10% of the initial value at a total energy of 725 J/cm^2. Annealing of doped polysilicon and silicide films was also achieved.

In summary, broad area glow discharge electron guns provide enough power density to allow processing of large area wafers in a few seconds without requiring focusing and/or scanning of the electron beam.

C. Electron-beam-assisted chemical vapor deposition

We have used glow discharge electron beams to deposit SiO_2 and Si_3N_4 films on silicon wafers at low substrate temperatures (200° to 400°C). The need for low temperautre semiconductor processing becomes increasingly important as semiconductor device structures move to submicron dimensions. Low temperature processes reduce dopant redistribution, wafer warpage, and crystalline defect generation each of which are induced by high temperature processing. We used electron beam dissociation of the reactants as a new CVD technique compared to conventional rf plasma assisted CVD. In contrast with radio frequency CVD, where the reaction volume fills almost all of the chamber, in the electron beam scheme the reaction is confined to the volume determined by the electron-beam-created plasma. In this way, the amount of reactants lost to the walls is largely reduced as is the undesired sputtering from chamber walls. We used both aluminum and sintered cathodes to produce rectangular electron beam sheets (2×30 mm) located parallel to the wafer surface. The beam electrons collide with the reactant gas molecules dissociating and creating free radial species that include excited atoms and molecules, as well as positive and negative ions. These species diffuse across a boundary layer to the heated substrate. Nucleation and film growth occurs at absorption sites leading to the formation of islands. The process continues with coalescence of these islands to form a continuous film. The experimental setup we used to obtain electron beam induced CVD of SiO_2 and Si_3N_4 is shown in Fig. 11. We expect the electron beam CVD technique to be

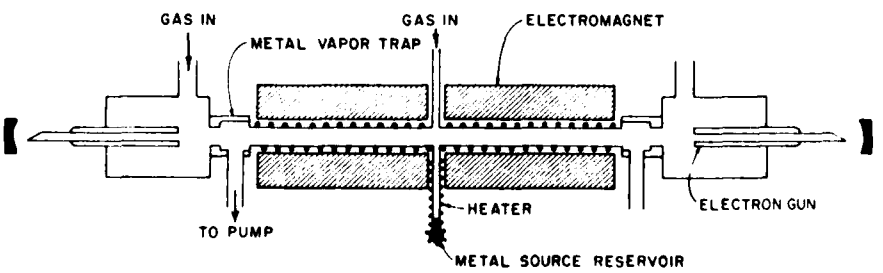

FIG. 10. Setup used for electron beam pumping of cw ion lasers utilizing two electron guns that produce two counter propagating electron beams. Electromagnet keeps the two beams well collimated.

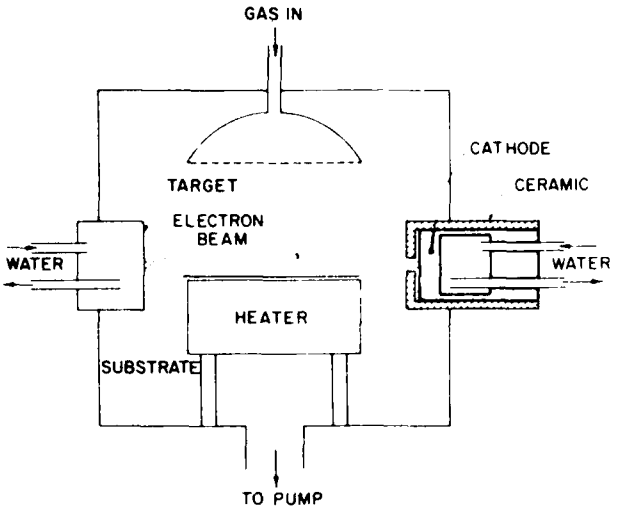

FIG. 11. Experimental setup for electron beam CVD of SiO_2 and Si_3N_4. The wafer is located on the substrate heater.

useful as a means to deposit a large variety of insulating, metallic, as well as semiconducting, films over large areas.

D. Other suggested applications of glow-discharge-created electron beams

Glow discharge electron guns can find other applications in experimental situations in which an electron beam is needed at pressures between 10^{-2} and 3 Torr; since, they can operate at these pressures without differential pumping. Glow discharge electron beams of 1 keV, for example, can be used to simulate heavier particles which ionize and excite the laser medium as in the case of a nuclear-pumped laser plasma.[25] Another application is the generation of x rays for preionizing gas laser discharges or for x-ray photolithography. Glow discharge electron guns could also be used as the ionization source in broad area ion sources. Unique advantages would be both the broad area of the source as well as the abundance of multiple ionized species. Finally, electron-beam-assisted unidirectional etching of microelectronic thin films and substrates is possible using the electron beam to enhance surface etching rates without the surface texturing or crystal damage that ion beams cause.

VII. SUMMARY

Ten different electron gun cathode materials have been compared for the production of glow discharge electron beams in helium at pressures between 0.1 and 3 Torr. Aluminum and magnesium, when covered by a thin oxide layer can produce electron beams with discharge currents up to 1.2 A at measured beam generation efficiencies of up to 80%. However, a small amount of oxygen (5 to 20 mTorr) must be present in the discharge to allow for the regrowth and maintenance of the oxide layer which is continually sputtered away by the bombardment of the cathode surface by ions and fast neutrals. A similar need for an oxide layer was observed for LaB_6 cathodes. The use of sintered refractory metal-ceramic cathode materials such as Mo–Al_2O_3 allowed us to produce multikilowatt electron beams at an efficiency of up to 75% in a pure noble gas atmosphere without the need for a partial pressure of oxygen. Glow discharge electron guns have been successfully used in the excitation of cw ion lasers, chemical vapor deposition of thin microelectronic films, and for the rapid thermal annealing of ion-implanted damage in silicon wafers. Other applications are suggested.

ACKNOWLEDGMENTS

The authors wish to thank the experimental assistance of Zeng-qi Yu (Fudan University), Lisa Happel, Jim McGinn, Allan Brown, Angus McCamant, Cameron Moore, and Lance Thompson. We also thank Don Jennings of NBS-Boulder for the loan of a power supply and Dr. W. K. Schuebel for helpful technical discussions. This work was supported by the National Science Foundation and AFOSR.

[1] R. A. Dugdale, J. Mater. Sci. **10**, 896 (1975).
[2] K. L. Boring and L. A. Stauffer, Proc. Nat. Electron. Conf. **19**, 535 (1963).
[3] R. E. Hurley and J. H. Holliday, Vacuum **28**, 453 (1978).
[4] J. J. Rocca, J. D. Meyer, and G. J. Collins, Appl. Phys. Lett. **40**, 300 (1982).
[5] J. D. Meyer, J. J. Rocca, Z. Yu, and G. J. Collins, IEEE J. Quantum Electron. **QE-18**, 326 (1982).
[6] J. J. Rocca, J. D. Meyer, and G. J. Collins, Phys. Lett. A **90**, 358 (1982).
[7] J. J. Rocca, J. D. Meyer, and G. J. Collins, Opt. Commun. **42**, 125 (1982).
[8] J. J. Rocca, J. D. Meyer, and G. J. Collins, IEEE J. Quantum Electron. **QE-18**, 1052 (1982).
[9] L. Thompson, J. J. Rocca, K. Emery, P. Boyer, and G. Collins, Appl. Phys. Lett. **43**, 777 (1983).
[10] C. A. Moore, J. J. Rocca, T. Johnson, G. J. Collins, and P. E. Russell, Appl. Phys Lett. **43**, 290 (1983).
[11] J. J. Rocca, J. D. Meyer, and G. J. Collins, Phys. Lett. A **87**, 237 (1982).
[12] Z. Yu, J. J. Rocca, J. D.Meyer, and G. J. Collins, J. Appl. Phys. **53**, 4704 (1982).
[13] C. W. Willet, *Introduction to Gas Lasers: Population Inversion Mechamisms* (Pergamon, Oxford, 1974).
[14] H. L. Van Passen, E. C. Muly, and R. J. Allen, Proc. Nat. Electron. Conf. **18**, 597 (1962).
[15] G. S. Ward, Vacuum **18**, 507 (1968).
[16] M. J. Higatsberger, H. L. Demorest, and A. O. Nier, J. Appl. Phys. **25**, 883 (1954).
[17] G. Carter and J. S. Colligon, *Ion Bombardment of Solids* (Elsevier, New York, 1968).
[18] W. Davis and T. A. Vanderslice, Phys. Rev. **131** 219 (1963).
[19] Z. Yu, J. J. Rocca, and G. J. Collins, J. Appl. Phys. **54**, 131 (1983).
[20] A. N. Broers, J. Appl. Phys. **38**, 1991 (1967).
[21] J. J. Rocca, J. D. Meyer, Z. Yu, M. Farrell, and G. J. Collins, Appl. Phys. Lett. **41**, 811 (1982).
[22] J. J. Rocca, J. D. Meyer, Z. Yu, and G. J. Collins, Appl. Phys. B **28**, 239 (1981).
[23] J. J. Rocca, J. D. Meyer, and G. J. Collins, Appl. Phys. Lett. **43**, 37 (1983).
[24] N. J. Ianno, J. T. Verdeyen, S. S. Chan, and B. S. Streetman, Appl. Phys. Lett. **39**, 622 (1981).
[25] A. M. Pointu, Laboratoire de Physique des Gas et Plasmas, Universite de Paris-Sud (private communication).

END

FILMED

5-85

DTIC